DISSERTATION

DEVELOPMENT OF AN *EX VIVO* PULSATILE HEART MODEL OF FUNCTIONAL MITRAL REGURGITATION TO FACILITATE POSTERIOR PAPILLARY MUSCLE GEOMETRIC STUDIES AND SUBVALVULAR SURGICAL STRATEGY

Submitted by

Krishaporn Kradangnga

Department of Clinical Sciences

In partial fulfillment of the requirements

For the Degree of Doctor of Philosophy

Colorado State University

Fort Collins, Colorado

Spring 2018

Doctoral Committee:

Advisor: Eric Monnet

Christopher Orton
Pedro Boscan
Lakshmi P. Dasi

ABSTRACT

DEVELOPMENT OF AN *EX VIVO* PULSATILE HEART MODEL OF FUNCTIONAL MITRAL REGURGITATION TO FACILITATE POSTERIOR PAPILLARY MUSCLE GEOMETRIC STUDIES AND SUBVALVULAR SURGICAL STRATEGY

Surgical method of choice for functional ischemic mitral regurgitation (FIMR) is debatable, since recurrence of FIMR post-annuloplasty has been reported in significant number of cases. Developing an *ex vivo* pulsatile functional mitral regurgitation (FMR) heart model by left ventricular (LV) dilatation can be a favorable option for usage in the primary stages of developing new surgical techniques that adjunctively targets the posterior papillary muscle (PPM) geometry. Posterior papillary muscle of *ex vivo* ovine hearts was displaced by 3 different sizes of patches to induce LV dilatation and FMR. Mitral regurgitation (MR) flow, LV and annular geometry were measured from the dynamic pulsatile flow system before and after patch placement. Applying the large patch produced the highest proportion of FMR heart models (87.5%, P=0.031). In conclusion, the large patch *ex vivo* pulsatile heart model demonstrated outward displacement of the PPM and significantly produced MR flow. This *ex vivo* pulsatile heart model can be used to facilitate surgical techniques that targets the PPM displacement in FMR patients.

The following phase of our research was aimed to utilize this *ex vivo* pulsatile heart model for PPM geometric studies in FMR with PPM displacement despite normal mitral annulus. This scenario mimics post-annuloplasty cases when the annular dilatation was corrected

by ring annuloplasty but the underlying LV remodeling was not treated. Sonomicrometry was used to evaluate the three-dimensional tethered distances and tethered angles of the PPM due to regional LV dilatation. The findings of this study implied that although annular dilatation was normalized, the increased PPM displacement outside and away from the mitral ring could deteriorate mitral leaflet tethering. The decreased tethering angle of the PPM from the annular fibrosa, reflecting the overall anterior mitral leaflet (AML) tethering and AML bending, could be used for MR prediction.

Lastly, the *ex vivo* pulsatile heart model with PPM lateral displacement and septo-lateral annular dilatation was used to facilitate additional subvalvular surgical strategy. Reduction annuloplasty was used as the standard FIMR treatment but showed suboptimal results with recurrent MR. Post-annuloplasty progression of LV remodeling and papillary muscles displacement could increase leaflet tethering. Annuloplasty alone did not correct submitral problems, therefore, adjunct procedures should be used to address the LV remodeling, prevent recurrent FIMR and insure durability of the balanced mitral complex mechanisms after surgery.

In addition to septo-lateral mitral annular reduction, the PPM repositioning was done by using the epicardial apparatus to baso-medially relocate the PPM base toward the mitral fibrosa. The concept of this technique was to reduce the tethering distance of the PPM from the mitral annulus and the interpapillary muscle distance. In conclusion, this study demonstrates the feasibility of an epicardial correction to study geometric changes after mitral annular reduction alone compared to PPM repositioning adjunct with mitral annulus reduction in a pulsatile *ex vivo* heart model of FMR. This study was aimed to fulfill the gap of the complex FIMR mechanisms and provides preliminary data of the mitral geometry from PPM repositioning outside the LV chamber.

ACKNOWLEDGEMENTS

I am very blessed and honored to receive this prestigious scholarship from the Anandamahidol foundation for the opportunity to pursue my Doctorate degree at Colorado State University. Thank you Dr. Eric Monnet for the strength and knowledge to complete this program. You are the best advisor that I could possibly have and words cannot describe how grateful I am to be your advisee. You have been my role model in both veterinary profession and life. Thank you Maud Monnet for your kindness and joyful moments together. Thank you my committee members, Dr. Christopher Orton, Dr. Pedro Boscan and Dr. Lakshmi P. Dasi, for the valuable comments throughout my program. I would like to acknowledge Kimberly Lebsock for helping me with sample collections. Thank you all my formal mentors in Thailand without you I would not have been able to see further and come this far. I am grateful for my colleagues and friends, especially Marissak Kalpravidh, Onsiri Cheunsuang, Sudson Sirivaidyapong, Pasakorn Brishavana, who have encouraged me to take this path and pursue my dream.

My life would not be complete without all the good friends and family who have shared laughter and tears together. To all the good old friends and all the new friends that I have made along the way, especially Nadhapat Bunnag, who have made this PhD journey more fun and meaningful. Sorry that I could not mention all of you but you know who you are. You will always have a place in my heart.

Finally, I would like to honor my parents, Prasarn and Orawan; my brother, Teerapat; and my close relatives. Thank you for all your support in every way, believing in me and the unconditional love that a daughter/niece/granddaughter could ever ask for.

DEDICATION

In remembrance of His Majesty King Bhumibol Adulyadej.

ธ สถิตในดวงใจตราบนิรันดร์

TABLE OF CONTENTS

LIST OF TABLES

LIST OF FIGURES

1. INTRODUCTION

Functional ischemic mitral regurgitation is associated with complications and poor prognosis after cardiac surgery. The risk of heart failure and mortality significantly worsen with increased MR severity. Regarding to normal mitral leaflet structures, FIMR is related to dilatation of the mitral annulus and restriction of the mitral leaflets mobility during systole due to papillary muscles (PMs) displacement. FIMR patients have restricted leaflet closure from the tethering force influenced by the apically displaced PMs and concurrent dilated annulus.

Mitral valve repair has been a favorable option for many decades. Mitral annular dilatation has been hypothesized as the main predictor for FIMR, therefore, reduction mitral ring annuloplasty has been used as the treatment of choice for FIMR. However, significant recurrent MR as high as 20-30 percent could be found post-annuloplasty and the outcomes varied among patients. Ring annuloplasty alone incompletely addresses the subvalvular components contributing to MR. Recently, clinical researches have been focusing on patients with moderate to severe FIMR requiring an adequate surgical strategy addressing the subvalvular apparatus to improve the long-term durability of the repair and prevent reoperation from recurrent MR.

Experimental and clinical studies increased interest in surgical techniques targeting the subvalvular area. More studies and technical development are needed, since there is no best treatment at present.

There have been few heart models developed to test mitral valve function in an *ex vivo* state due to the technical difficulties. Developing a pulsatile heart model mimicking clinical findings in FIMR patients could be a favorable option for usage in the primary stages of the study. Therefore, the first goal of this dissertation was to develop an *ex vivo* pulsatile heart model

to help facilitate FIMR studies and use for further studies on FIMR mechanisms and designing optimal treatment strategies. Our second goal of the study was to utilize the pulsatile *ex vivo* heart model to evaluate geometric changes of the mitral apparatus in PPM displacement despite normal annular size. We would like to study the parameters that have not been reported including the tethered angle of the PMs referred to the annulus.

Reduction annuloplasty with adjunct procedures were combined to address the remodeled LV and prevent recurrence of FIMR after annuloplasty. Subvalvular surgical techniques that focused on correcting the PMs displacement by repositioning the PPM affect both mitral leaflets, since both leaflets were suspended by PMs. Studies have shown cut-offs and predictive values for tethered angles and distances of the mitral leaflet but few have focused directly on the PMs itself. This study can help us know how to manipulate the PPM to achieve balanced leaflet closure which could we assessed by MR reduction. The final goal was to demonstrate how additional subvalvular repositioning of the PPM by adjusting the epicardial surface could affect MR volume and other geometric parameters. Many subvalvular techniques required extended aortic clamping and cardiopulmonary bypass (CPB) time which is not ideal to lower post-operative complications. Developing additional subvalvular techniques that required less or does not require CPB time is more favorable. The knowledge that we gained from this research study should provide more depth in FIMR mechanism, moreover; it showed the preliminary data on how repositioning the PPM from outside the LV chamber could be done to lower MR.

2. LITERATURE REVIEWS

Mitral regurgitation is a retrograde flow from the left ventricle into the left atrium during systolic phase when normal mitral valve tends to close. The causes can be from an ischemic and non-ischemic event. MR is usually classified into 3 types by the functional characteristics of the leaflets;[18]

Type I – normal leaflet motion with mitral annular dilatation and/or leaflet perforation

Type II – excessive leaflet motion; such as papillary muscle rupture

Type III – restricted leaflet movement

Type IIIa- restriction during diastole; such as rheumatic disease

Type IIIb- restriction during systole; such as functional disease and cardiomyopathy

In this dissertation, we will focus on secondary ischemic MR, or aka functional ischemic mitral regurgitation, which is one of the major cause of MR in western countries and the standard treatment strategies are still uncertain.[23] Ischemic heart disease is the leading cause of cardiovascular (CVS) deaths in the United States and worldwide.[15] Approximately 1 million people in the United States are diagnosed with ischemic heart disease annually.[15] Within this numbers, 20-30 %,[10,11,17,61,64] or as high as 59% will encounter FIMR.[36] FIMR occurs despite structurally normal mitral leaflets and is characterized by most commonly type IIIb and occasionally Carpentier type I functional classification. It is a common complication found after myocardial ischemia and is often overlooked in coronary artery disease patients.[79] FIMR is associated with complications and poor prognosis after cardiac surgery.[7,57] Even with mild MR,

the risk of heart failure and mortality significantly increases. Outcomes are worse with increased severity of FIMR.[11,30,31,60,70]

2.1 Mitral apparatus

We have to understand the anatomy of the mitral apparatus to better understand the mechanisms and apply on how to efficiently treat FIMR. The mitral apparatus consisted of 6 components including the left atrial wall, mitral annulus, mitral leaflets, chordae tendineae, PMs and the LV wall.[89] The balanced function of the mitral apparatus ensures normal leaflets closure.

2.1.1. Left atrial wall

The left atrial wall has continuity with the mitral annulus and mitral leaflets. Therefore, enlargement of the left atrium can contribute to MR by directly displacing the posterior mitral leaflet. The anterior mitral leaflet is not mainly affected since its base is connected to a more stationary structure (atrioventricular septal area).[65] Although the left atrial wall contraction and relaxation seems to associate with mitral leaflets coaptation. Human study has shown that MR was not noticeable in the absence of left atrial contraction.[111]

2.1.2. Mitral annulus

The mitral annulus is mainly collagenous tissue that separates the left atrium and the left ventricle. It is the basal attachment of the mitral leaflets. The mitral annular area reduces 25-50% and has a saddle shape during systole both in human and in animal models.[3,46,50,97] The annular size and saddle shape are associated with complete leaflet coaptation.[37]

2.1.3. Mitral leaflets and chordae tendineae

There are 2 main mitral leaflets, the anterior (septal) and posterior (lateral) mitral leaflets. The anterior mitral leaflet (AML) has a semicircular shape with no scallop and spans between the commissures of the mitral annulus in the fibrous trigone region. The base of the AML is connected with the aortic annulus. The posterior mitral leaflet (PML) consisted of 3 scallops and spans 2/3 of the lateral annular circumference in adjunct with the atrioventricular groove **(Figure 2.1)**. These individual scallops are believed to help leaflet opening during diastole. The height of the normal PML is less than half of the AML; however, each mitral leaflet takes up 50% of the mitral orifice area during leaflet closure. The rough zone or coaptation zone is the free margin area at the atrial side of the leaflets. This represents the coaptation surface of the valve. The non-coaptation surfaces of the leaflets are called the smooth zone.

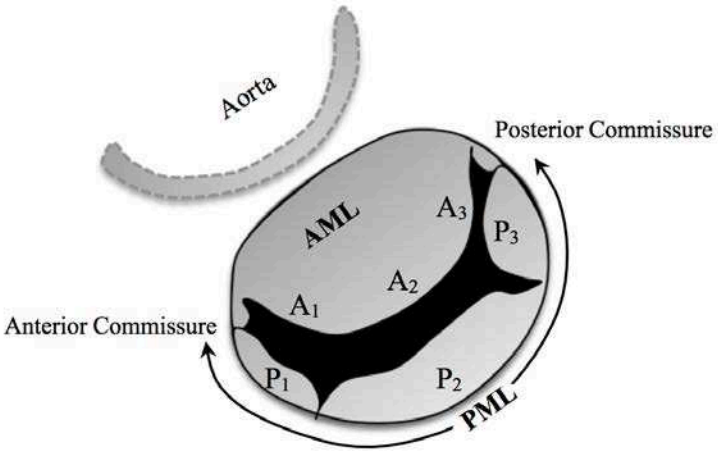

Figure 2.1. Mitral leaflets nomenclature. AML, Anterior mitral leaflet; PML, posterior mitral leaflet. The PML has 3 scallops, P_1-P_3. The AML is divided into three coaptation segments (A_1-A_3) that oppose the PML scallops.

The chordae tendineae connect mitral leaflets to the PMs and LV wall. They act as the leaflet suspension system which maintain the position and tension on the leaflet throughout the cardiac cycle. They are divided into 3 groups depending on the attachment sites of the mitral leaflets. The marginal or "primary" chordae attach to the free margin of the leaflets. They prevent prolapse of the leaflet when the left ventricular pressure (LVP) increases during systole. Strut or "secondary" chordae attach to the ventricular surface of the leaflets rough zone and smooth zone. They contribute to ventricular-valve continuity and optimize systolic function. The strut chordae that attach the PML are called "intermediate" chordae. Basal or "tertiary" chordae connect the PML at the base near mitral annulus to the LV wall.

2.1.4. Papillary muscles and left ventricular wall

The PMs and the LV wall are the muscular portions of the mitral apparatus. There are two PMs; the anterior papillary muscle (APM) and the posterior papillary muscle (PPM). Each papillary muscle has chordae tendineae connecting both AML and PML. A geometric study in ovine hearts revealed that the interpapillary muscle tip distance was 2.1 cm and the distance between the PPM tip and the annular fibrosa was 2.6-2.8 cm.[51]

The LV is supplied by 3 major arteries; left anterior descending artery, right coronary artery and left circumflex artery. LV remodeling after myocardial infarction in human commonly associated with asymmetrical LV remodeling of the inferior wall (PPM region) of the heart since 63% of the cases are mainly perfused by a single blood supply from either the posterior descending branch of a dominant right coronary artery or by the third obtuse marginal branch. On the contrary, 71% of the cases have dual blood supplying the APM, the first obtuse marginal,

originating from the left circumflex artery, and the first diagonal branch, originating from the left anterior descending, which makes it less vulnerable to infarction and rupture.[113]

Each mitral component plays an important part for mitral leaflet competence. The synchrony of the mitral apparatus working as a whole unit prevents MR during isovolumetric contraction and ejection phase in the cardiac cycle. Disruption of this synchronized function or abnormality of mitral apparatus after myocardial ischemia can result in FIMR.

2.2. Mechanisms of FIMR

Mitral valve competence consisted of complex mechanisms contributing to the process of systolic leaflet cooptation. Therefore, any alterations in one or more of mitral structures could contribute to regurgitation. Regarding to normally mitral leaflet structures, patients that developed MR after myocardial infarction had more dilated annulus compared to normal patients.[39,57,103] Tibayan and colleagues[103] used chronic ovine FIMR models to demonstrate that FIMR was associated with greater septo-lateral annular dilatation compared to non-FIMR animals. Asymmetrical annular dilatation usually occurs at the lateral annulus, which is bordered with the free wall of the LV. Where else the septal portion, which is adjacent to the interventricular septal area, obtained lesser geometric changes.[59] This event is secondary from LV dilatation and remodeling after cardiac ischemic events. In FIMR patients, the mitral annulus dilates, looses its saddle shape and becomes more flatten as asymmetrical septo-lateral dilatation progresses.[37,53,63,97] The mitral annular dynamic contraction is also reduced.[63,97]

Although annular dilatation is a common finding in FIMR and mitral annular area was a strong predictor of MR,[101] it is uncertain whether it is the major determinant of FIMR or not,

since annular dilatation alone did not produce significant MR.[88] Moreover, persistent and recurrent FIMR could be found after reduction mitral annuloplasty.[43,57,71] This shifts the knowledge of FIMR to a more ventricular problem. The current knowledge of FIMR mechanisms is shown in **Figure 2.2**. Historically, PMs function was suggested as a determinant of FIMR, a study in FIMR patients showed that PMs longitudinal systolic strain did not affect MR severity.[105] Left ventricular remodeling occurs typically after posterior-lateral (inferior) myocardial infarction.[57] This mainly causes asymmetrical PMs displacement at the level of the LV wall where ischemia occurs.[48,82] In a ovine model of FIMR, the PPM was displaced laterally, apically and posteriorly.[103] The interpapillary muscles distance increased significantly in FIMR patients[55] and was the only independent predictor for FIMR severity.[48] Uemura and colleagues have showed that increased PPM tethering distance from the annular fibrosa was the only independent risk factor MR severity in FIMR patients.[105] Papillary muscles displacement after LV remodeling induced systolic tenting of mitral leaflets away from the annulus causing incomplete leaflets closure.

FIMR patients have restricted leaflet closure due to tethering force influenced by the displaced PMs and concurrent dilated annulus. Echocardiography is an essential tool used to investigate leaflet configurations. Preoperative tethering angles of both AML and PML were major determinants for FIMR.[114] The tethering angle is measured as the angle between the mitral annulus and the AML or PML. Tenting area, coaptation depth, annular dilatation, and left atrial size were all associated with baseline MR severity. Many studies have found that leaflet tethering angles, AML bending angle and coaptation heights were related to recurrent MR after reduction annuloplasty. Preoperative predictors for recurrent FIMR and cut-offs are shown in **Table 2.1**.

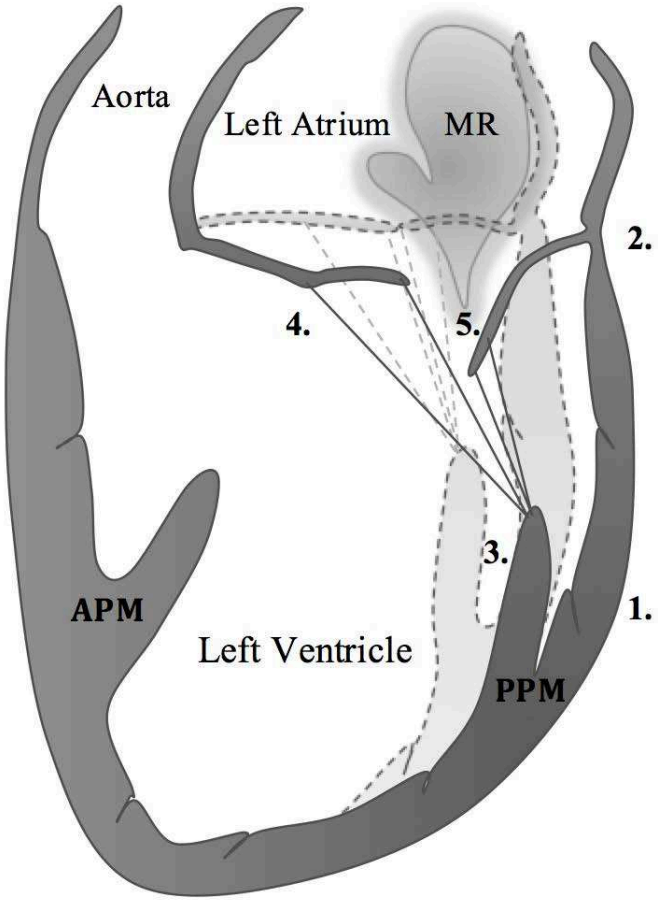

Figure 2.2. This schematic features the mechanisms of FIMR. After myocardial infarction, (1) the LV remodeled along with (2) mitral annular septo-lateral dilatation occurred. (3) The PPM displaced apically and laterally pulling the (4, 5) leaflets down toward the LV apex which restricted the leaflets from complete coaptation.

Table 2.1. Predictive parameters for recurrent FIMR after ring annuloplasty.

Authors	**Pre-operative predictor**
Calafiore *et al.*, 2014 [13]	Coaptation depth >10mm, AML bending angle >145°
Magne *et al.*, 2007 [69]	PML tethering angle ≥ 45 degrees
Troubil *et al.*, 2012 [104]	AML tethering angle ≥27 degrees
van Garsse *et al.*, 2012 [112]	Anterior/posterior tethering angle ratio >0.76
Gelsomino *et al.*, 2008 [33]	LVESV ≥145mL LV systolic sphericity index ≥0.7 LV myocardial performance index <0.9 LV wall motion score index <1.5
Roshanali *et al.*, 2007 [95]	Interpapillary muscle distance of 20mm (base to base measurement at end systole)
Bouma *et al.*, 2016 [9]	P3 tethering angle >29.9 degrees
Kuwahara *et al.*, 2006 [58]	PML tethering angle
Gelsomino *et al.*, 2008 [33] van Garsse *et al.*, 2012 [112]	AML tethering angle ≥39.5 degrees

Modified from Jensen et al. 2015. Surgical treatment of functional ischemic mitral regurgitation. Dan Med J 65(3): B4993.[47]

2.3. Surgical treatments

Surgical treatments were aimed to eliminate MR and restore LV function. Coronary artery bypass grafting (CABG) was used to treat ischemic myocardiopathy and mitral valve surgery was added to treat the dilated annulus. Mitral valve repair had more benefits than mitral valve replacement in moderate FIMR.[35] Mitral valve repair at the time of CABG significantly reduced MR grade and increased LV ejection fraction.[27] A sub-analysis of the STICH (Surgical Treatment for Ischemic Heart Failure) trial supported that adding mitral annuloplasty to CABG

improved moderate to severe MR and survival rate compared with CABG alone or medical therapy alone.[23]

2.3.1. Ring annuloplasty

In addition to CABG, mitral valve repair by ring annuloplasty were used as FIMR treatment for many decades.[8,40,110] Lillehei and colleagues first introduced the concept of annuloplasty for mitral insufficiency correction in 1957.[67] In 1961, the annuloplasty ring was first invented and used by Carpentier.[18] Today, there are many types and sizes of mitral annuloplasty rings used for FIMR treatment.[50,71,99] Reduction annuloplasty gain popularity after Bolling and Bach reported the efficacy of using reduction annuloplasty for MR patients.[6] Reduction (or *restricted or undersizing)* mitral annuloplasty was done by using an annuloplasty ring 1–2 sizes smaller than the normal ring size based on the AML height and annular intertrigonal distance. This procedure had high successful rate in short-term studies[22,87] and is the current treatment of choice for FIMR.[87] To minimized cardiopulmonary bypass (CPB) time and complication, the transcatheter mitral annular techniques were developed.[60,90,100] Although this idea reduced high-risk complications, most techniques had limitations such as limited septo-lateral annular dimensional reduction from the anatomical position of the coronary sinus, dislodging, unequal tension on the left atrium and mitral annulus.[20]

Surgical leaders have used reduction annuloplasty techniques to treat FIMR patients for many decades. This approach solely addressed the annular dilatation; however, it did not address the LV remodeling, PMs displacement and leaflet tethering. Despite early satisfactory outcomes of mitral annuloplasty, late recurrence of FIMR has been observed in a significant number of cases.[12,35,47,71] Approximately 10-20 percent of the patients after 5 years of ring annuloplasty had

recurrent FIMR and progression of LV remodeling.[31] Jensen and colleagues has summarized 35 studies published between 2001-2012 on adding ring annuloplasty to CABG in patients with moderate to severe FIMR. This study revealed 20-30% post-operative recurrence of FIMR after 2-4 years follow-up, despite half of the studies have used aggressive reduction ring annuloplasty.[47] High recurrent rate might be due to restricted leaflet mobility, augmentation of the posterior leaflets causing tethering of the leaflets, ongoing LV remodeling, PMs displacement outside of the mitral annulus, or combinations of the following events.

The concept of ring annuloplasty is to bring the annular dimension closer together so that the mitral leaflets can completely form coaptation. Although the annuloplasty ring shifts the lateral annulus closer to the septal annulus, reduction annuloplasty alone could worsen PML restriction by increasing the distance between the already lateral displaced PPM and the lateral portion of the annulus **(Figure 2.3.A)**.[39,43,58,114] Green and colleagues[39] reported that restricted PML was associated with persistent and early post-annuloplasty recurrent MR. Therefore, ring annuloplasty could exacerbate leaflet tethering when the reduction of annular dimension exceeded the LV remodeling.[43,114]

Continued LV remodeling was presented in patients after reduction annuloplasty and could further worsen the imbalanced LV-mitral ring ratio **(Figure 2.3.B)**. Hung and colleague[43] have reported that recurrent MR after ring annuloplasty was associated with continued LV remodeling. Capoulade and colleague[16] showed that the LV-mitral ring mismatch ratio after 1 year post-operative ring annuloplasty was significantly associated with recurrent moderate or greater MR in the Cardiothoracic Surgical Trials Network (CTSN) randomized trials.

Reduction annuloplasty did not address the LV complex mechanism of FIMR. Therefore adjunct procedures were needed to address the PMs displacements from the remodeled LV,

relieve the tethered leaflets and prevent recurrent FIMR after annuloplasty. Many studies have looked at subvalvular treatments to help correct the LV problem. Annuloplasty combined with adjunct subvalvular techniques (e.g. chordal cutting, direct papillary muscle relocation and PMs approximation) have been studied and have shown promising results for moderate to severe FIMR.[26,76-78,86,101,106,108]

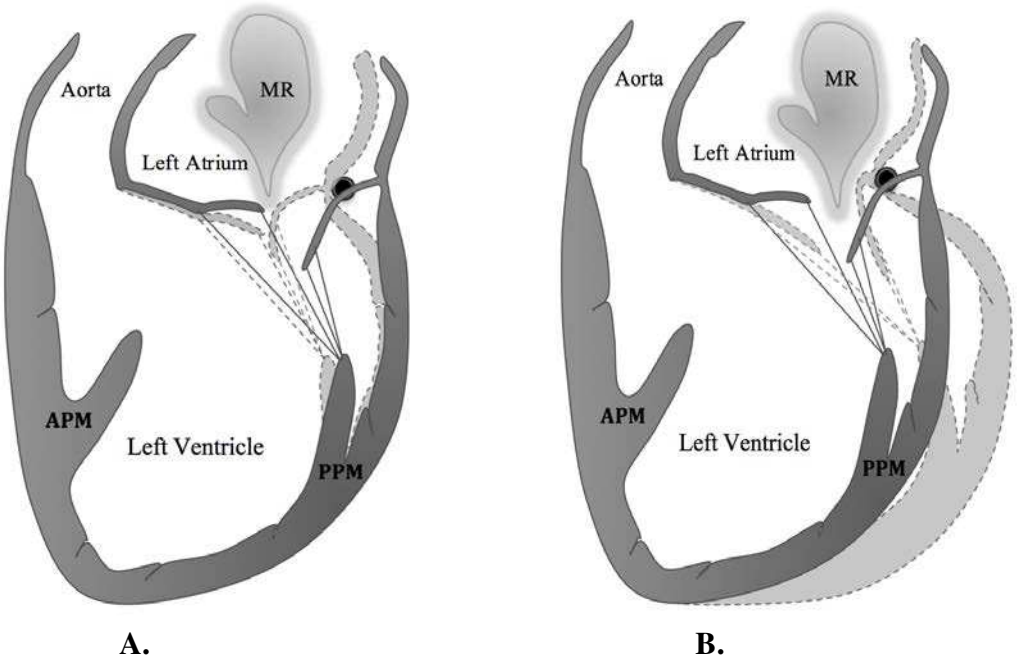

Figure 2.3. Schematics of (A) persistent and (B) recurrent MR after ring annuloplasty.

2.3.2. Chordal cutting

In 2001, Messas and colleagues[74] developed chordal cutting by severing 2 strut chordae which restricted the AML in a rigid open position bend in the basal anterior leaflet ("seagull sign"). Chordal cutting did not impair LV function.[73-75] It increased AML mobility without

leaflet prolapse in animal studies. Eventually, polytetrafluoroethylene chordal suspension sutures could be done if leaflet prolapse occurs. This procedure relied on the AML to act as a unileaflet since the PML remained vertically rigid due to relatively lateral PPM displacement from reduction annuloplasty. Therefore, the AML needs to have adequate tissue length to maintain complete closure. The indication for strut chordal cutting is when the AML bending angle is <145° and the coaptation depth ≤10mm.[14,34]

Szymanski and colleagues compared isolated reduction annuloplasty versus isolated bileaflet chordal cutting versus the combined therapy in ovine models with mild to moderate FIMR. After surgical treatments, MR in the combined treatment group was reduced to trace and the LV end-systolic volume in the combined treatment was significantly lesser than each intervention alone (P<0.01).[101]

2.3.3. Papillary muscle relocation (Kron's technique)

In 2002, Kron and colleagues[56] were the first to clinically use PMs relocation by using suture material to anchor the PPM tip to the lateral annulus. The concept of this procedure was to lower the distance between the PMs and the mitral annulus which believed to reduced leaflet tethering. The original technique used pledgetted suture to anchor the PPM tip toward the mitral annulus near the posterior fibrous trigone prior to reduction annuloplasty in chronic FIMR patients. In this study, no patients had recurrent MR 2 months postoperatively. This technique could be easily reproduced and decreased early and late mortality.[56] PPM relocation alone reduced MR in ovine models of acute FIMR. (Langer 2005) Modification of this technique was done by adding APM relocation to the original technique in a porcine experimental model. Results showed reduced PPM-anterior annular distance and lateral leaflet tethering compared to

isolated reduction annuloplasty.[49] Recently, Fattouch and colleagues[28] reported a midterm follow-up that PPM relocation adjunct to non-reduction ring annuloplasty decreased recurrent MR and improved reversal in LV remodeling than isolated reduction ring annuloplasty in patients.[28,29] In addition to ring annuloplasty, Langer and colleagues[58] modified the Kron's technique to allow adjustment of the PPM relocation under partially loaded beating heart. This technique is called the 'RING+STRING'. They have reported less MR residual when applying this technique in moderate to severe FIMR patients undergoing CABG and reduction annuloplasty.[62]

2.3.4. Papillary muscle approximation

Papillary muscles relocation or the RING+STRING techniques correct tethering at the subvalvular level. However, relocating the PMs could not reduce apical, posterior and outward tethering since the PMs were suspended toward the mitral annulus. Therefore, these procedures were not ideal for patients with severe LV remodeling when the PMs were displaced far apart. Papillary muscle approximation is a procedure that was developed to correct mitral leaflets tethering, especially in the outward and posterior directions, by directly reducing the displaced PMs. The concept of PMs approximation was to correct tethering by decreasing the interpapillary muscles distance due to LV remodeling. The PMs could completely be approximated (complete PMs approximation) through an LV incision or partially at the level of the PMs tips to the mid portion (incomplete PMs approximation) through the mitral or aortic orifice.[92]

Papillary muscle approximation in combination with reduction annuloplasty reduced recurrent MR and improved reversal of LV remodeling when compared to reduction

annuloplasty alone in a randomized clinical trial (Papillary Muscle Approximation trial) of severe FIMR patients.[86] Similarly, results from a 5-year randomized controlled clinical trial comparing patients who either had PMs approximation in combination with reduction annuloplasty or reduction annuloplasty alone showed that the mortality rate after 2-year follow-up was significantly higher in the isolated reduction annuloplasty group. The combined treatment had better LV reverse remodeling at 5-year follow-up. At the last follow-up, patients with reduction annuloplasty had 55.9% moderate or severe regurgitation compared to 27% in the combined group.[84,85] Wakasa and colleagues[107] compared outcomes between complete and incomplete PMs approximation. They found that the complete group was associated with lower mortality and a lower moderate or greater recurrent MR. The 4-year survival rate and rate of freedom from moderate or greater recurrent MR were 83% and 85% for those with complete PMs approximation, respectively.[107]

These subvalvular techniques directly helped correct PMs displacement and reduced the tethering force on the leaflets. Nevertheless, the combination of CABG procedure, mitral repair and additional subvalvular techniques required additional aortic cross-clamping and surgical assisted-CPB time or placement of synthetic sutures or prostheses inside the LV chamber.[26,42,44,56] CPB for cardiac surgery is related to morbidity and mortality.[83] Multivariate analyses done by Salis and colleague have revealed that 30-minute increment of CPB time is an independent risk factor for postoperative death.[98] The common postoperative complications in cardiac surgery assisted with CPB are systemic inflammation responses, acute renal injury and pulmonary complications.[66,81,102] Seven percent of the patients undergoing assisted-CPB cardiac surgery will develop postoperative acute renal injury, where else pulmonary complications in cardiac valvular surgery range from 5-7 percent and 3-16 percent in CABG.[96,98,109] This

influenced researchers to focus on interventions that do not require CPB by using extra-mural devices placed over or insert through the epicardium. In 1999, Power and colleague[88] have proven that a passive LV constraint mesh placed around both ventricles known as "Acorn device" can lower functional MR by indirectly decreasing PMs displacement.[1,2,91] Coapsys, a trans-ventricular device that reduces LV dilatation between the PMs, has shown promising results compared to ring annuloplasty, but further studies were terminated from discontinued of funding.[19,45] Newer studies of epicardial devices are being tested and validated such as the "Basal Annuloplasty of the Cardia Externally (BACE) device", which is a silicone band placed apically to the atrioventricular groove.[93] This device is mainly for treatment of annular dilatation with or without PMs displacement in FIMR patients. It can be inflated to modify the ventricular component and correct MR.[93]

As mentioned earlier, mitral valve surgery gave suboptimal results and late recurrent MR was found in significant number of cases. Patients that did not required CABG would rarely receive mitral valve surgery. Therefore, minimally invasive transcatheter mitral valve repair strategies were used as an alternative MR treatment. These strategies were developed to mimic standard surgical approaches including annuloplasty, edge-to-edge repair, chordal plication and LV remodeling.[20] At present, the MitraClip system is Food and Drug Administration (FDA) approved for primary MR and used widely compared to other transcatheter mitral valve repair. There are ongoing treatment studies for FIMR.[5] MitraClip used the same concept as the edge-to-edge repair, based on the surgical Alfieri technique,[4] by grasping and clipping a free margin of the AML and PML together. The prospective multicenter single-arm study to evaluate the feasibility, safety, and efficacy of the MitraClip system (EVEREST I) showed that freedom from death and freedom from surgery were 94% and 76.3% after 3 years, respectively.[32]

All techniques as mentioned above, have their own advantages and disadvantages and no studies have definite comparison of these procedures. As mentioned earlier, the complete mechanisms of FIMR is unclear which makes it harder to develop a surgical treatment of choice. More studies in this area are needed to optimize and improve new strategies for FIMR treatment. Developing new surgical tools and techniques for FMR treatment requires excessive testing and validation. Animal trials are normally used for standard testing but requires time and expenses. Utilizing *ex vivo* heart models could be a favorable option in the primary stages of the testing and validating new surgical strategies, since it is more cost efficient, required less time, reduced complexity, lessened the need of laboratory animal usage and sacrifice. In 1997, He and colleagues[41] developed an *in vitro* model of FMR. The model was used for studying the independent variation of PMs position, annular size, and trans-mitral pressure. The mitral valve and the attached PMs were dissected and fixed to an annulus board mounted in a pressurized chamber. Many studies have adopted this idea and used it for studying FMR, chordal rupture and other mitral apparatus abnormalities.[25,52] The downside was that it did not have physiological mitral opening and continuity LV as in intact heart. An *in situ* heart model was developed by isolating and maintaining the beating heart for several hours.[21] This model was ideal for *ex vivo* studies, since it mimics physiological cardiac function. However, it required complex preparation and did not eliminate the use of additional laboratory animals as recipients for heart transplantation. In 2009, an intact heart model with pulsatile pressurization was developed by Richard and colleagues.[94] They aimed to facilitate surgical correction of annular dilation and chordal rupture. In 2013, Monnet and colleague published a study of an *ex vivo* heart model of FMR which was done by using static continuous flow through the heart.[80]

REFERENCES

1. Acker MA, Bolling S, Shemin R, et al. 2006. Mitral valve surgery in heart failure: Insights from the Acorn Clinical Trial. *J Thorac Cardiovasc Surg* 132:568-577. https://doi.org/10.1016/j.jtcvs.2006.02.062
2. Acker MA, Jessup M, Bolling SF, et al. 2011. Mitral valve repair in heart failure: Five-year follow-up from the mitral valve replacement stratum of the Acorn randomized trial. *J Thorac Cardiovasc Surg* 142:569-574. https://doi.org/10.1016/j.jtcvs.2010.10.051
3. Ahmad RM, Gillinov AM, McCarthy PM, et al. 2004. Annular geometry and motion in human ischemic mitral regurgitation: Novel assessment with three-dimensional echocardiography and computer reconstruction. *Ann Thorac Surg* 78:2063-8.
4. Alfieri O, Maisano F, De Bonis M, et al. 2001. The double-orifice technique in mitral valve repair: A simple solution for complex problems. *J Thorac Cardiovasc Surg* 122:674–681. https://doi.org/10.1067/mtc.2001.117277
5. Asgar AW, Mack MJ, Stone GW. 2015. Secondary mitral regurgitation in heart failure: pathophysiology, prognosis, and therapeutic considerations. *J Am Coll Cardiol* 65:1231–1248. https://doi.org/10.1016/j.jacc.2015.02.009
6. Bach DS, Bolling SF. 1995. Early improvement in congestive heart failure after correction of secondary mitral regurgitation in end-stage cardiomyopathy. *Am Heart J* 129:1165–1170.
7. Badiwala MV, Verma S, Rao V. 2009. Surgical Management of Ischemic Mitral Regurgitation. *Circulation* 120:1287–1293. https://doi.org/10.1161/CIRCULATIONAHA.108.836627
8. Bonow RO, Carabello BA, Chatterjee K, et al. 2008. Focused update incorporated into the ACC/AHA 2006 guidelines for the management of patients with valvular heart disease a report of the American College of Cardiology/American Heart Association task force on practice guidelines (Writing committee to revise the 1998 guidelines for the management of patients with valvular heart disease): Endorsed by the Society of Cardiovascular Anesthesiologists, Society for Cardiovascular Angiography and Interventions, and Society of Thoracic Surgeons. *Circulation* 118:e523–e661. https://doi.org/10.1161/CIRCULATIONAHA.108.190748
9. Bouma W, Lai EK, Levack MM, et al. 2016. Preoperative three-dimensional valve analysis predicts recurrent ischemic mitral regurgitation after mitral annuloplasty. *Ann Thorac Surg* 101:567–575. https://doi.org/10.1016/j.athoracsur.2015.09.076
10. Bursi F, Enriquez-Sarano M, Jacobsen SJ, Roger VL. 2006. Mitral regurgitation after myocardial infarction: A review. *Am J Med* 119:103–112. https://doi.org/10.1016/j.amjmed.2005.08.025

11. Bursi F, Enriquez-Sarano M, Nkomo VT, et al. 2005. Heart failure and death after myocardial infarction in the community the emerging role of mitral regurgitation. *Circulation* 111:295–301. https://doi.org/10.1161/01.CIR.0000151097.30779.04
12. Calafiore AM, Gallina S, Di Mauro M, et al. 2001. Mitral valve procedure in dilated cardiomyopathy: repair or replacement? *Ann Thorac Surg* 71:1146–1152. https://doi.org/10.1016/S0003-4975(00)02650-3
13. Calafiore AM, Refaie R, Iacò AL, et al. 2014. Chordal cutting in ischemic mitral regurgitation: A propensity-matched study. *J Thorac Cardiovasc Surg* 148:41–46. https://doi.org/10.1016/j.jtcvs.2013.07.036
14. Calafiore AM, Refaie R, Iacò AL, et al. 2014. Chordal cutting in ischemic mitral regurgitation: A propensity-matched study. *J Thorac Cardiovasc Surg* 148:41–46. https://doi.org/10.1016/j.jtcvs.2013.07.036
15. Cannon B, 2013. Cardiovascular disease: Biochemistry to behaviour. *Nature* 493:S2–S3. https://doi.org/10.1038/493S2a
16. Capoulade R, Zeng X, Overbey JR, et al. 2016. Impact of left ventricular to mitral valve ring mismatch on recurrent ischemic mitral regurgitation after ring annuloplasty. *Circulation* 134: 1247–1256. https://doi.org/10.1161/CIRCULATIONAHA.115.021014
17. Carabello, B.A., 2008. The Current Therapy for Mitral Regurgitation. *J Am Coll Cardiol* 52: 319–326. https://doi.org/10.1016/j.jacc.2008.02.084
18. Carpentier A. 1983. Cardiac valve surgery: the "French correction." *J Thorac Cardiovasc Surg* 86:323–37.
19. Carrick R, Ge L, Lee LC, et al. 2012. Patient-specific finite element based analysis of ventricular myofiber stress after Coapsys: Importance of residual stress. *Ann Thorac Surg* 93: 1964–1971. https://doi.org/10.1016/j.athoracsur.2012.03.001
20. Chiam PTL, Ruiz CE. 2011. Percutaneous transcatheter mitral valve repair: a classification of the technology. *JACC Cardiovasc Interv* 4:1–13. https://doi.org/10.1016/j.jcin.2010.09.023
21. Chinchoy E, Soule CL, Houlton AJ, et al. 2000. Isolated four-chamber working swine heart model. *Ann Thorac Surg* 70:1607–1614. https://doi.org/10.1016/S0003-4975(00)01977-9
22. Daneshmand MA, Milano CA, Rankin JS, et al. 2009. Mitral valve repair for degenerative disease: a 20-year experience. *Ann Thorac Surg* 88:1828–1837. https://doi.org/10.1016/j.athoracsur.2009.08.008
23. Deja MA, Grayburn PA, Sun B, et al. 2012. Influence of mitral regurgitation repair on survival in the surgical treatment for ischemic heart failure trial. *Circulation* 125(20):2639-2648. https://doi.org/10.1161/CIRCULATIONAHA.111.072256
24. Enriquez-Sarano M, Akins CW, Vahanian A. 2009. Mitral regurgitation. The Lancet 373:1382–1394. https://doi.org/10.1016/S0140-6736(09)60692-9
25. Espino DM, Hukins DWL, Shepherd DET, Watson MA, Buchan K. 2006. Determination of the pressure required to cause mitral valve failure. *Med Eng Phys* 28:36–41. https://doi.org/10.1016/j.medengphy.2005.04.011

26. Fattouch K, Castrovinci S, Murana G, et al. 2014. Papillary muscle relocation and mitral annuloplasty in ischemic mitral valve regurgitation: Midterm results. *J Thorac Cardiovasc Surg* 148:1947–1950. https://doi.org/10.1016/j.jtcvs.2014.02.047
27. Fattouch K, Guccione F, Sampognaro R, et al. 2009. POINT: Efficacy of adding mitral valve restrictive annuloplasty to coronary artery bypass grafting in patients with moderate ischemic mitral valve regurgitation: A randomized trial. *J Thorac Cardiovasc Surg* 138:278–285. https://doi.org/10.1016/j.jtcvs.2008.11.010
28. Fattouch K, Lancellotti P, Castrovinci S, et al. 2012. Papillary muscle relocation in conjunction with valve annuloplasty improve repair results in severe ischemic mitral regurgitation. *J Thorac Cardiovasc Surg* 143:1352–1355. https://doi.org/10.1016/j.jtcvs.2011.09.062
29. Fattouch K, Murana G, Castrovinci S, Nasso G, Speziale G, 2012. The role of papillary muscle relocation in ischemic mitral valve regurgitation. *Semin Thorac Cardiovasc Surg* 24:246–253. https://doi.org/10.1053/j.semtcvs.2012.12.002
30. Fattouch K, Sampognaro R, Speziale G, et al. 2010. Impact of moderate ischemic mitral regurgitation after isolated coronary artery bypass grafting. *Ann Thorac Surg* 90:1187–1194. https://doi.org/10.1016/j.athoracsur.2010.03.103
31. Feinberg MS, Schwammenthal E, Shlizerman L, et al. 2000. Prognostic significance of mild mitral regurgitation by color Doppler echocardiography in acute myocardial infarction. *Am J Cardiol* 86:903–907. https://doi.org/10.1016/S0002-9149(00)01119-X
32. Feldman T, Kar S, Rinaldi M, et al. 2009. Percutaneous mitral repair with the mitraclip system: safety and midterm durability in the initial EVEREST (Endovascular Valve Edge-to-Edge REpair Study) Cohort. *J Am Coll Cardiol* 54:686–694. https://doi.org/10.1016/j.jacc.2009.03.077
33. Gelsomino S, Lorusso R, Caciolli S, et al. 2008. Insights on left ventricular and valvular mechanisms of recurrent ischemic mitral regurgitation after restrictive annuloplasty and coronary artery bypass grafting. *J Thorac Cardiovasc Surg* 136:507–518. https://doi.org/10.1016/j.jtcvs.2008.03.027
34. Gelsomino S, Lorusso R, Caciolli S, et al. 2008. Insights on left ventricular and valvular mechanisms of recurrent ischemic mitral regurgitation after restrictive annuloplasty and coronary artery bypass grafting. *J Thorac Cardiovasc Surg* 136:507–518. https://doi.org/10.1016/j.jtcvs.2008.03.027
35. Gillinov AM, Wierup PN, Blackstone EH, et al. 2001. Is repair preferable to replacement for ischemic mitral regurgitation? *J Thorac Cardiovasc Surg* 122:1125–1141. https://doi.org/10.1067/mtc.2001.116557
36. Golia G, Anselmi M, Rossi A, et al. 2001. Relationship between mitral regurgitation and myocardial viability after acute myocardial infarction: Their impact on prognosis. *Int J Cardiol* 78:81–90. https://doi.org/10.1016/S0167-5273(00)00476-9

37. Gorman III, JH, Jackson BM, Enomoto Y, Gorman RC. 2004. The effect of regional ischemia on mitral valve annular saddle shape. *Ann Thorac Surg* 77:544–548. https://doi.org/10.1016/S0003-4975(03)01354-7
38. Green GR, Dagum P, Glasson JR, et al. 1999. Mitral annular dilatation and papillary muscle dislocation without mitral regurgitation in sheep. *Circulation* 100:II–95–II–102. https://doi.org/10.1161/01.CIR.100.suppl_2.II-95
39. Green GR, Dagum P, Glasson JR, et al. 1999. Restricted posterior leaflet motion after mitral ring annuloplasty. *Ann Thorac Surg* 68:2100–2106. https://doi.org/10.1016/S0003-4975(99)01175-3
40. Hillis LD, Smith PK, Anderson JL, et al. 2011. ACCF/AHA Guideline for coronary artery bypass graft surgery a report of the American College of Cardiology Foundation/American Heart Association task force on practice guidelines. *Circulation* 124:e652–e735. https://doi.org/10.1161/CIR.0b013e31823c074e
41. He S, Fontaine AA, Schwammenthal E, Yoganathan AP, Levine RA, 1997. Integrated mechanism for functional mitral regurgitation: Leaflet restriction versus coapting force: In vitro studies. *Circulation* 96:1826–1834. https://doi.org/10.1161/01.CIR.96.6.1826
42. Hung J, Chaput M, Guerrero JL, et al. 2007. Persistent reduction of ischemic mitral regurgitation by papillary muscle repositioning structural stabilization of the papillary muscle–ventricular wall complex. *Circulation* 116:I–259–I–263. https://doi.org/10.1161/CIRCULATIONAHA.106.679951
43. Hung J, Papakostas L, Tahta SA, et al. 2004. Mechanism of recurrent ischemic mitral regurgitation after annuloplasty continued lv remodeling as a moving target. *Circulation* 110:II–85–II–90. https://doi.org/10.1161/01.CIR.0000138192.65015.45
44. Hvass U, Tapia M, Baron F, Pouzet B, Shafy A, 2003. Papillary muscle sling: a new functional approach to mitral repair in patients with ischemic left ventricular dysfunction and functional mitral regurgitation. *Ann Thorac Surg* 75:809–811. https://doi.org/10.1016/S0003-4975(02)04678-7
45. Inoue M, McCarthy PM, Popović ZB, et al. 2004. The Coapsys device to treat functional mitral regurgitation: in vivo long-term canine study. *J Thorac Cardiovasc Surg* 127:1068–1077. https://doi.org/10.1016/j.jtcvs.2003.12.005
46. Jassar AS, Vergnat M, Jackson BM, et al. 2014. Regional annular geometry in patients with mitral regurgitation: Implications for annuloplasty ring selection. *Ann Thorac Surg* 97:64–70. https://doi.org/10.1016/j.athoracsur.2013.07.048
47. Jensen H, Jensen MO, Nielsen SL 2015. Surgical treatment of functional ischemic mitral regurgitation. *J Heart Valve Dis* 24:30–42.
48. Jensen H, Jensen MO, Smerup MH, et al. 2010. Three-dimensional assessment of papillary muscle displacement in a porcine model of ischemic mitral regurgitation. *J Thorac Cardiovasc Surg* 140:1312–1318. https://doi.org/10.1016/j.jtcvs.2009.12.042

49. Jensen H, Jensen MO, Smerup MH, et al. 2009. Impact of papillary muscle relocation as adjunct procedure to mitral ring annuloplasty in functional ischemic mitral regurgitation. *Circulation* 120:S92–S98. https://doi.org/10.1161/CIRCULATIONAHA.108.817833
50. Jensen MO, Jensen H, Levine RA, et al. 2011. Saddle-shaped mitral valve annuloplasty rings improve leaflet coaptation geometry. *J Thorac Cardiovasc Surg* 142:697–703. https://doi.org/10.1016/j.jtcvs.2011.01.022
51. Kalyanasundaram A, Qureshi A, Nassef LA, Shirani J. 2010. Functional anatomy of normal mitral valve-left ventricular complex by real-time, three dimensional echocardiography. *J Heart Valve Dis* 19(1):28-34.
52. Katoh T, Ikeda N, Nishi K, et al. 1999. A newly designed adapter for testing an ex vivo mitral valve apparatus. *Artificial Organs* 23:920–923. https://doi.org/10.1046/j.1525-1594.1999.06293.x
53. Khabbaz KR, Mahmood F, Shakil O, et al. 2013. Dynamic 3-dimensional echocardiographic assessment of mitral annular geometry in patients with functional mitral regurgitation. *Ann Thorac Surg* 95:105–110. https://doi.org/10.1016/j.athoracsur.2012.08.078
54. Kim JH, Kocaturk O, Ozturk C, et al. 2009. Mitral cerclage annuloplasty, a novel transcatheter treatment for secondary mitral valve regurgitation: initial results in swine. *J Am Coll Cardiol* 54:638–651. https://doi.org/10.1016/j.jacc.2009.03.071
55. Kim K, Kaji S, An Y, et al. 2014. Interpapillary muscle distance independently affects severity of functional mitral regurgitation in patients with systolic left ventricular dysfunction. *J Thorac Cardiovasc Surg* 148:434–440.e1. https://doi.org/10.1016/j.jtcvs.2013.09.029
56. Kron IL, Green GR, Cope JT. 2002. Surgical relocation of the posterior papillary muscle in chronic ischemic mitral regurgitation. *Ann Thorac Surg* 74:600–601. https://doi.org/10.1016/S0003-4975(02)03749-9
57. Kumanohoso T, Otsuji Y, Yoshifuku S, et al. 2003. Mechanism of higher incidence of ischemic mitral regurgitation in patients with inferior myocardial infarction: Quantitative analysis of left ventricular and mitral valve geometry in 103 patients with prior myocardial infarction. *J Thorac Cardiovasc Surg* 125:135–143. https://doi.org/10.1067/mtc.2003.78
58. Kuwahara E, Otsuji Y, Iguro Y, et al. 2006. Mechanism of recurrent/persistent ischemic/functional mitral regurgitation in the chronic phase after surgical annuloplasty importance of augmented posterior leaflet tethering. *Circulation* 114:I–529–I–534. https://doi.org/10.1161/CIRCULATIONAHA.105.000729
59. Kwan J, Shiota T, Agler DA, et al. 2003. Geometric differences of the mitral apparatus between ischemic and dilated cardiomyopathy with significant mitral regurgitation real-time three-dimensional echocardiography study. *Circulation* 107:1135–1140. https://doi.org/10.1161/01.CIR.0000053558.55471.2D

60. Lam BK, Gillinov AM, Blackstone EH, et al. 2005. Importance of moderate ischemic mitral regurgitation. *Ann Thorac Surg* 79:462–470. https://doi.org/10.1016/j.athoracsur.2004.07.040
61. Lamas GA, Mitchell GF, Flaker GC, et al. 1997. Clinical significance of mitral regurgitation after acute myocardial infarction. *Circulation* 96:827–833. https://doi.org/10.1161/01.CIR.96.3.827
62. Langer F, Kunihara T, Hell K, et al. 2009. RING+STRING: Successful repair technique for ischemic mitral regurgitation with severe leaflet tethering. *Circulation* 120:S85-91.
63. Levack MM, Jassar AS, Shang EK, et al. 2012. 3D-echocardiographic analysis of mitral annular dynamics: implication for annuloplasty selection. *Circulation* 126:S183–S188. https://doi.org/10.1161/CIRCULATIONAHA.111.084483
64. Levine RA, Schwammenthal E, 2005. Ischemic mitral regurgitation on the threshold of a solution from paradoxes to unifying concepts. *Circulation* 112:745–758. https://doi.org/10.1161/CIRCULATIONAHA.104.486720
65. Levy MJ, Edwards JE. 1962. Anatomy of mitral insufficiency. *Prog Cardiovasc Dis* 5:119.
66. Levy JH, Tanaka KA. 2003. Inflammatory response to cardiopulmonary bypass. *Ann Thorac Surg* 75:S715–720.
67. Lillehei CW, Gott VL, Dewall RA, Varco RL. 1957. Surgical correction of pure mitral insufficiency by annuloplasty under direct vision. *Lancet* 77:446–449.
68. Lopez-Perez A, Sebastian R, Ferrero JM, 2015. Three-dimensional cardiac computational modelling: methods, features and applications. *Biomed Eng OnLine* 14:35. https://doi.org/10.1186/s12938-015-0033-5
69. Magne J, Pibarot P, Dagenais F, Hachicha Z, Dumesnil JG, Sénéchal M, 2007. Preoperative posterior leaflet angle accurately predicts outcome after restrictive mitral valve annuloplasty for ischemic mitral regurgitation. *Circulation* 115:782–791. https://doi.org/10.1161/CIRCULATIONAHA.106.649236
70. Mallidi HR, Pelletier MP, Lamb J, et al. 2004. Late outcomes in patients with uncorrected mild to moderate mitral regurgitation at the time of isolated coronary artery bypass grafting. *J Thorac Cardiovasc Surg* 127:636–644. https://doi.org/10.1016/j.jtcvs.2003.09.010
71. McGee Jr EC, Gillinov AM, Blackstone EH, et al. 2004. Recurrent mitral regurgitation after annuloplasty for functional ischemic mitral regurgitation. *J Thorac Cardiovasc Surg* 128:916–924. https://doi.org/10.1016/j.jtcvs.2004.07.037
72. Melvin DB. 1992. Ventricular radius reduction without resection: a computational analysis. *Asaio J Am Soc Artif Intern Organs* 45:160–165.
73. Messas E, Bel A, Szymanski C, et al. 2010. Relief of mitral leaflet tethering following chronic myocardial infarction by chordal cutting diminishes left ventricular remodeling. *Circ Cardiovasc Imaging* 3:679–686. https://doi.org/10.1161/CIRCIMAGING.109.931840

74. Messas E, Guerrero JL, Handschumacher MD, et al. 2001. Chordal cutting a new therapeutic approach for ischemic mitral regurgitation. *Circulation* 104:1958–1963. https://doi.org/10.1161/hc4201.097135
75. Messas E, Yosefy C, Chaput M, et al. 2006. Chordal cutting does not adversely affect left ventricle contractile function. *Circulation* 114:I–524–I–528. https://doi.org/10.1161/CIRCULATIONAHA.105.000612
76. Mihos CG, Larrauri-Reyes M, Santana O, 2016. A meta-analysis of ring annuloplasty versus combined ring annuloplasty and subvalvular repair for moderate-to-severe functional mitral regurgitation. *J Card Surg* 31:31–37. https://doi.org/10.1111/jocs.12662
77. Mihos CG, Santana O, 2016. Is an adjunctive subvalvular repair during mitral annuloplasty for secondary mitral regurgitation effective in preventing recurrent regurgitation? *Interact Cardiovasc Thorac Surg* 22:216–221. https://doi.org/10.1093/icvts/ivv328
78. Mihos CG, Xydas S, Yucel E, et al. 2017. Mitral valve repair and subvalvular intervention for secondary mitral regurgitation: a systematic review and meta-analysis of randomized controlled and propensity matched studies. *J Thorac Dis* 9:S582–S594. https://doi.org/10.21037/jtd.2017.05.56
79. Miller DC. 2001. Ischemic mitral regurgitation redux—To repair or to replace? *J Thorac Cardiovasc Surg* 122:1059–1062. https://doi.org/10.1067/mtc.2001.120341
80. Monnet E, Pouching K. 2013. An ex vivo model of left ventricular dilation and functional mitral regurgitation to facilitate the development of surgical techniques. *Heart Surg Forum* 16:329–335.
81. Murphy GJ, Angelini GD, 2004. Side effects of cardiopulmonary bypass. *J Card Surg* 19:481–488. https://doi.org/10.1111/j.0886-0440.2004.04101.x
82. Nakai H, Kaku K, Takeuchi M, et al. 2012. Different influences of left ventricular remodeling on anterior and posterior mitral leaflet tethering. *Circ J Off J Jpn Circ Soc* 76:2481–2487.
83. Nakasuji M, Matsushita M, Asada A, 2005. Risk factors for prolonged ICU stay in patients following coronary artery bypass grafting with a long duration of cardiopulmonary bypass. *J Anesth* 19:118–123. https://doi.org/10.1007/s00540-005-0301-9
84. Nappi F, Spadaccio C, Chello M, Mihos CG, 2017. Papillary muscle approximation in mitral valve repair for secondary MR. *J Thorac Dis* 9:S635–S639. https://doi.org/10.21037/jtd.2017.06.98
85. Nappi F, Lusini M, Spadaccio C, et al. 2016. Papillary muscle approximation versus restrictive annuloplasty alone for severe ischemic mitral regurgitation. *J Am Coll Cardiol* 67:2334-46.

86. Nappi F, Spadaccio C, Nenna A, et al. 2017. Is subvalvular repair worthwhile in severe ischemic mitral regurgitation? Subanalysis of the Papillary Muscle Approximation trial. *J Thorac Cardiovasc Surg* 153:286–295.e2. https://doi.org/10.1016/j.jtcvs.2016.09.050
87. Nishimura RA, Otto CM, Bonow RO, et al. 2017. AHA/ACC focused update of the 2014 AHA/ACC guideline for the management of patients with valvular heart disease: A report of the American College of Cardiology/American Heart Association task force on clinical practice guidelines. *Circulation* CIR.0000000000000503. https://doi.org/10.1161/CIR.0000000000000503
88. Otsuji Y, Kumanohoso T, Yoshifuku S, et al. 2002. Isolated annular dilation does not usually cause important functional mitral regurgitation: Comparison between patients with lone atrial fibrillation and those with idiopathic or ischemic cardiomyopathy. *J Am Coll Cardiol* 39:1651–1656. https://doi.org/10.1016/S0735-1097(02)01838-7
89. Perloff JK, Roberts WC, 1972. The mitral apparatus functional anatomy of mitral regurgitation. *Circulation* 46:227–239. https://doi.org/10.1161/01.CIR.46.2.227
90. Piazza N, Asgar A, Ibrahim R, Bonan R, 2009. Transcatheter mitral and pulmonary valve therapy. *J Am Coll Cardiol* 53:1837–1851. https://doi.org/10.1016/j.jacc.2008.12.067
91. Power JM, Raman J, Dornom A, et al. 1999. Passive ventricular constraint amends the course of heart failure: a study in an ovine model of dilated cardiomyopathy. *Cardiovasc Res* 44:549–555. https://doi.org/10.1016/S0008-6363(99)00255-2
92. Rama A, Praschker L, Barreda E, et al. 2007. Papillary muscle approximation for functional ischemic mitral regurgitation. *Ann Thorac Surg* 84:2130–2131.
93. Raman J, Jagannathan R, Chandrashekar P, Sugeng L, 2011. Can we repair the mitral valve from outside the heart? A novel extra-cardiac approach to functional mitral regurgitation. *Heart Lung Circ* 20:157–162. https://doi.org/10.1016/j.hlc.2010.12.001
94. Richards AL, Cook RC, Bolotin G, Buckner GD, 2009. A dynamic heart system to facilitate the development of mitral valve repair techniques. *Ann Biomed Eng* 37:651–660. https://doi.org/10.1007/s10439-009-9653-x
95. Roshanali F, Mandegar MH, Yousefnia MA, et al. 2007. A prospective study of predicting factors in ischemic mitral regurgitation recurrence after ring annuloplasty. *Ann Thorac Surg* 84(3):745-9.
96. Sachdev G, Napolitano LM, 2012. Postoperative pulmonary complications: Pneumonia and acute respiratory failure. *Surg Clin North Am* 92:321–344. https://doi.org/10.1016/j.suc.2012.01.013

97. Salgo IS, Gorman JH, Gorman RC, et al. 2002. Effect of annular shape on leaflet curvature in reducing mitral leaflet stress. *Circulation* 106:711–717.
98. Salis S, Mazzanti VV, Merli G, et al. 2008. Cardiopulmonary bypass duration is an independent predictor of morbidity and mortality after cardiac surgery. *J Cardiothorac Vasc Anesth* 22:814–822.
https://doi.org/10.1053/j.jvca.2008.08.004
99. Smith PK, Puskas JD, Ascheim DD, et al. 2014. Surgical treatment of moderate ischemic mitral regurgitation. *N Engl J Med* 371:2178–2188.
https://doi.org/10.1056/NEJMoa1410490
100. Stone GW, Vahanian AS, Adams DH, et al. 2015. Clinical trial design principles and endpoint definitions for transcatheter mitral valve repair and replacement: Part 1: Clinical trial design principles: A consensus document from the mitral valve academic research consortium. *J Am Coll Cardiol* 66:278–307.
https://doi.org/10.1016/j.jacc.2015.05.046
101. Szymanski C, Bel A, Cohen I, et al. 2012. Comprehensive annular and subvalvular repair of chronic ischemic mitral regurgitation improves long-term results with the least ventricular remodeling. *Circulation* 126:2720–2727.
https://doi.org/10.1161/CIRCULATIONAHA.111.033472
102. Taylor KM, 1996. SIRS—The systemic inflammatory response syndrome after cardiac operations. *Ann Thorac Surg* 61:1607–1608.
https://doi.org/10.1016/0003-4975(96)00225-1
103. Tibayan FA, Rodriguez F, Zasio MK, et al. 2003. Geometric distortions of the mitral valvular-ventricular complex in chronic ischemic mitral regurgitation. *Circulation* 108:II–116–II–121.
https://doi.org/10.1161/01.cir.0000087940.17524.8a
104. Troubil M, Marcian P, Gwozdziewicz M, et al. 2012. Predictors of failure following restrictive annuloplasty for chronic ischemic mitral regurgitation. *J Cardiac Surg* 27(1):6-12.
105. Uemura T, Otsuji Y, Nakashiki K, et al. 2005. Papillary muscle dysfunction attenuates ischemic mitral regurgitation in patients with localized basal inferior left ventricular remodeling: Insights from tissue Doppler strain imaging. *J Am Coll Cardiol* 46:113–119.
https://doi.org/10.1016/j.jacc.2005.03.049
106. Wagner CE, Kron IL. 2014. Subvalvular techniques to optimize surgical repair of ischemic mitral regurgitation. *Curr Opin Cardiol* 29:140–144.
https://doi.org/10.1097/HCO.0000000000000042
107. Wakasa S, Kubota S, Shingu Y, Ooka T, Tachibana T, Matsui Y. 2014. The extent of papillary muscle approximation affects mortality and durability of mitral valve repair for ischemic mitral regurgitation. *J Cardiothorac Surg* 9:98.
https://doi.org/10.1186/1749-8090-9-98

108. Wakasa S, Shingu Y, Ooka T, Katoh H, Tachibana T, 2015. Surgical strategy for ischemic mitral regurgitation adopting subvalvular and ventricular procedures. *Ann Thorac Cardiovasc Surg* 21:370–377. https://doi.org/10.5761/atcs.oa.14-00204
109. Weissman C, 2004. Pulmonary complications after cardiac surgery. *Semin Cardiothorac Vasc Anesth* 8:185–211. https://doi.org/10.1177/108925320400800303
110. Vahanian A, Alfieri O, Andreotti F, et al. 2012. Guidelines on the management of valvular heart disease (version 2012). *Eur Heart J* 33:2451–2496. https://doi.org/10.1093/eurheartj/ehs109
111. Vanderberg RA, Williams JCP, Strum RE, Wood EH. 1971. Effect of varying ventricular function by extra systolic potentiation on closure of the mitral valve. *Amer J Cardiol* 28:43.
112. Van Garsse L, Gelsomino S, Luca F, et al. 2012. Importance of anterior leaflet tethering in predicting recurrence of ischemic mitral regurgitation after restrictive annuloplasty. *J Thorac Cardiovasc Surg* 143(4):S54-9.
113. Voci P, Bilotta F, Caretta Q, Mercanti C, Marino B. Papillary muscle perfusion pattern. A hypothesis for ischemic papillary muscle dysfunction. *Circulation.* 1995;91:1714–1718
114. Zhu F, Otsuji Y, Yotsumoto G, et al. 2005. Mechanism of persistent ischemic mitral regurgitation after annuloplasty importance of augmented posterior mitral leaflet tethering. *Circulation* 112:I–396–I–401. https://doi.org/10.1161/CIRCULATIONAHA.104.524561

3. HYPOTHESES AND AIMS

The hypotheses of this dissertation are as follow:

Hypothesis 1: It is assumed that MR can be induced in an *ex vivo* pulsatile heart model by sufficient displacement of the PPM despite normal mitral annulus. Determination of the effectiveness of the heart model and quantifying the MR severity were conducted by measuring MR flow and the geometry of the mitral apparatus when different degrees of PPM displacement was applied to the *ex vivo* heart model. The aims to accomplish the hypothesis are as follow:

Aim 1.1: To examine the chances of producing MR flow in heart models with different degrees of PPM displacement.

Aim 1.2: To examine the geometric changes of the PPM compared to baseline in different degrees of PPM displacement by using sonomicrometric measurements.

Hypothesis 2: We hypothesized that the tethered distances and tethered angles of the PPM increases from baseline in the *ex vivo* heart models that developed MR compared to heart models that did not developed MR. Evaluation of the geometric tethered distances and tethered angles of the PPM compared to baseline should give additional information on the mechanisms of FMR despite normal mitral annulus. The aims to accomplish the hypothesis are as follow:

Aim 2.1: The 3D tethered distances and tethered angles of the PPM after inducing left ventricular dilatation and PPM displacement were compared to baseline.

Aim 2.2: To identify the geometric determinants that were associated with MR volume despite normal mitral annulus.

Hypothesis 3: Additional subvalvular PPM repositioning by using epicardial apparatus lowers MR compared to isolated septo-lateral annular reduction. The aims to accomplish the hypothesis are as follow:

Aim 3.1: We assessed the results of isolated septo-lateral annular reduction and additional PPM repositioning. The *ex vivo* pulsatile heart model was used to determine the physical changes of the annulus and PMs before and after epicardial contouring apparatus. Reducing the septo-lateral mitral annular dimension adjunct with reversing the PMs displacement in the baso-septal position can reduce greater MR.

Aim 3.2: Piezo-electric crystals were used for tethered distance measurements and the three dimensional (3D) geometry of the mitral apparatus. Differences of the mitral annular area (MAA), annular septo-lateral dimension and geometry of the PMs tips from the heart model were assumed to have an effect on the MR volume through different degrees of the LV epicardial apparatus adjustments. We aimed to show how septo-lateral mitral annular reduction, overall papillary muscle tethering distances, 3D PPM geometry, papillary muscle tethering angle and different methods of treatment influenced MR reduction.

4. LEFT VENTRICULAR DILATATION AND POSTERIOR PAPILLARY MUSCLE DISPLACEMENT IN AN EX VIVO PULSATILE MODEL OF FUNCTIONAL MITRAL REGURGITATION

Functional mitral regurgitation is defined as regurgitation due to dysfunction of the mitral apparatus with normally structural mitral leaflets causing incomplete closure of the mitral orifice. Remodeling of the LV wall after cardiac ischemic event altered ventricular geometry inducing papillary muscles displacement.[12] Displacement of the papillary muscles exerts traction of the leaflets through the chordae causing the leaflets to tether and restricting it from normal coaptation. Other factors proposed to cause FMR are asymmetrical dilatation of mitral annulus and increased LV sphericity.[3,11,17,19]

Patient with heart failure carries a worse prognosis in the long term when FMR developed.[12] Mitral annular dilation and the displacement of the PPM are main components for imbalanced forces causing leaflets mal-coaptation. Understanding and assessing the geometry of these components and the limitation of standard ischemic FMR repairs can improve and provide better treatment strategies.[1] One way to determine the mechanism of imbalance forces on the leaflets leading to FMR is by using *ex vivo* heart models. Furthermore, heart models can be use in initial studies of surgical strategies for FMR treatments to lessen the cost and time compared to animal models and clinical studies.

Effective *ex vivo* heart model that mimics FMR have been reported, [10,18,20] but none are suitable for studying LV remodeling and PPM displacement. Monnet and colleague[15] developed an *ex vivo* model that has the continuity of the LV wall. Annular dilatation, posterior papillary

muscles repositioning or both were used for induction of LV dilatation and FMR. However, the model was built with a static continuous retrograde flow through the aorta.

The purpose of this study is to develop a pulsatile *ex vivo* model of FMR with a forward flow through the apex of the LV. Determination of the effectiveness of the model and quantifying the MR severity were conducted by measuring MR flow and the geometry of the mitral apparatus when different degrees of PPM displacement were applied to the *ex vivo* heart model.

4.1 Material and methods

4.1.1. Heart preparation

Fresh ovine hearts were collected from 36 adult Dorsett sheep 70±5 kg euthanized for reason not related to this study, stored at 4°C. They were prepared for the experiment within 24 hours of euthanasia. Excessive tissue and the pericardium were trimmed out leaving the aorta and pulmonary veins intact. The aorta and LV apex were cannulated with a 3/8" cannula. A valve was placed on the cannula coming out of the aorta to control resistance of the output flow. The largest pulmonary vein was cannulated with a 1/4" cannula and the rest of the vessels were secured with sutures. The cannula that was placed into the pulmonary vein that had an orifice 15 cm above the mitral annulus. This was used for measurement of MR flow at 15 cm of water pressure (11 mmHg). The cannulated aorta and the LV apex were connected to the pulsatile pump system **(Figure 4.1)**. The pulsatile pump infused the heart with water at room temperature at a rate of 40 cycles per minute with an average flow of 4 L/min. A pressure transducer (Millar, Houston, Texas, USA) was inserted through the aorta into the LV to measure the left ventricular

pressure (LVP). Maximum LVP for each cycle was maintained above 70 mmHg throughout the experiment by adjusting the flow of the pump or resistance in the cannula in the aorta. The pulsatile pump generated a pulsatile flow traveling in a forward flow from the LV apex to the aorta.

To allow displacement of the PPM, a full thickness incision was made in the wall of the LV around the PPM without damaging the chordae. The PPM remains attached to the apex of the LV with a 2 cm strip of myocardium and to the mitral valve leaflets with the chordae. The left atrium was incised to expose the mitral annulus and leaflets. Under direct visualization, 2 mm piezo-electric crystals (2 mm round Piezo-electric crystals, Sonometrics, London, Canada) were carefully tunneled into the endocardium based on prior studies on papillary muscles geometry.[4,5,15] Six 2 mm piezo-electric crystals (2 mm round Piezo-electric crystals, Sonometrics, London, Canada) were placed to determine geometry of the annulus and the displacement of the PPM **(Figure 4.2)**. Patches of diaphragm were sutured around the PPM muscle and the remaining LV wall to reestablish the integrity of the LV. Patches of different sizes were used to induce different degrees of displacement of the PPM. The transducers were connected to a data acquisition system (Sonosoft, Sonometrics, London, Canada).

The hearts were randomly assigned into 3 different sizes of diaphragmatic patches: Small patch (SP) group, Medium patch (MP) group, and Large patch (LP) group. The patch was 1, 2 and 3 cm at the widest point for the SP, MP, and LP group respectively **(Figure 4.3)**. It was sutured with 4-0 suture materials with continuous suture pattern as described by Monnet et al.[15] Distances between each pair of transducers were measured at maximum LVP of each cycle at baseline and after placement of the patch. The MR flow was measured in milliliter per minute (ml/min). Displacement of the PPM and mitral annular geometry were evaluated at maximum

LVP. Heart with maximum LVP lesser than 70 mmHg, abnormalities of the mitral apparatus such as rupture and tear, severe leakage after patch placement and dislocation of the piezo-electric crystals transducers were excluded from the study.

4.1.2. Statistical analysis

Data from MR flow and dimension between transducer pairs were expressed as median and interquartile range (IQR) at maximum LVP of the cardiac cycle both at baseline and after patch placement. Comparison of the paired continuous variables in each treatment group from its baseline was performed by Wilcoxon Signed-rank test. A Kruskal-Wallis Test was used for comparing continuous variables between treatment groups and comparison of unpaired continuous variables was done by Wilcoxon rank sum test. Categorical variables comparison was assessed by Fisher's exact test. Significance of the data was considered when $P<0.05$.

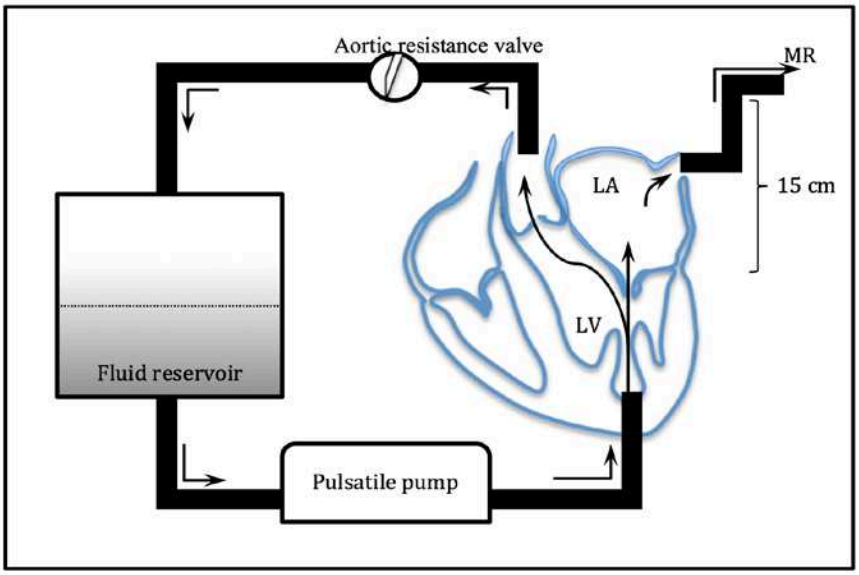

Figure 4.1. Dynamic pressurization system that generates pulsatile forward flow (indicate as black arrows) through the left ventricle. Mitral regurgitation flow was collected at 15 cm above the mitral annulus; LA, left atrium; LV, left ventricle; MR, mitral regurgitation.

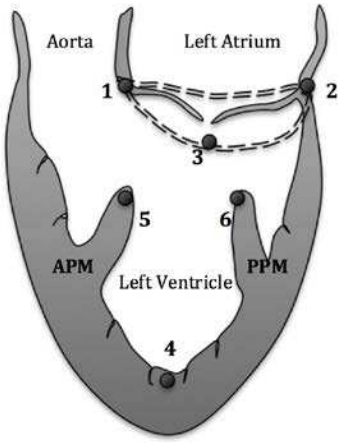

Figure 4.2. Location of the piezo-electric crystals placement. Piezo-electric crystal #1 was placed at the level of the septo-lateral (fibrosa) part of the mitral annulus and piezo-electric crystal #2 was placed opposite side of piezo-electric crystal #1 on the mid-lateral part of mitral annulus. Piezo-electric crystal #3 was placed at the anterior commissure of the mitral annulus and piezo-electric crystal #4 at the apex. Piezo-electric crystals #5 and #6 were placed on the tip of anterior papillary muscle (APM) and posterior papillary muscle (PPM).

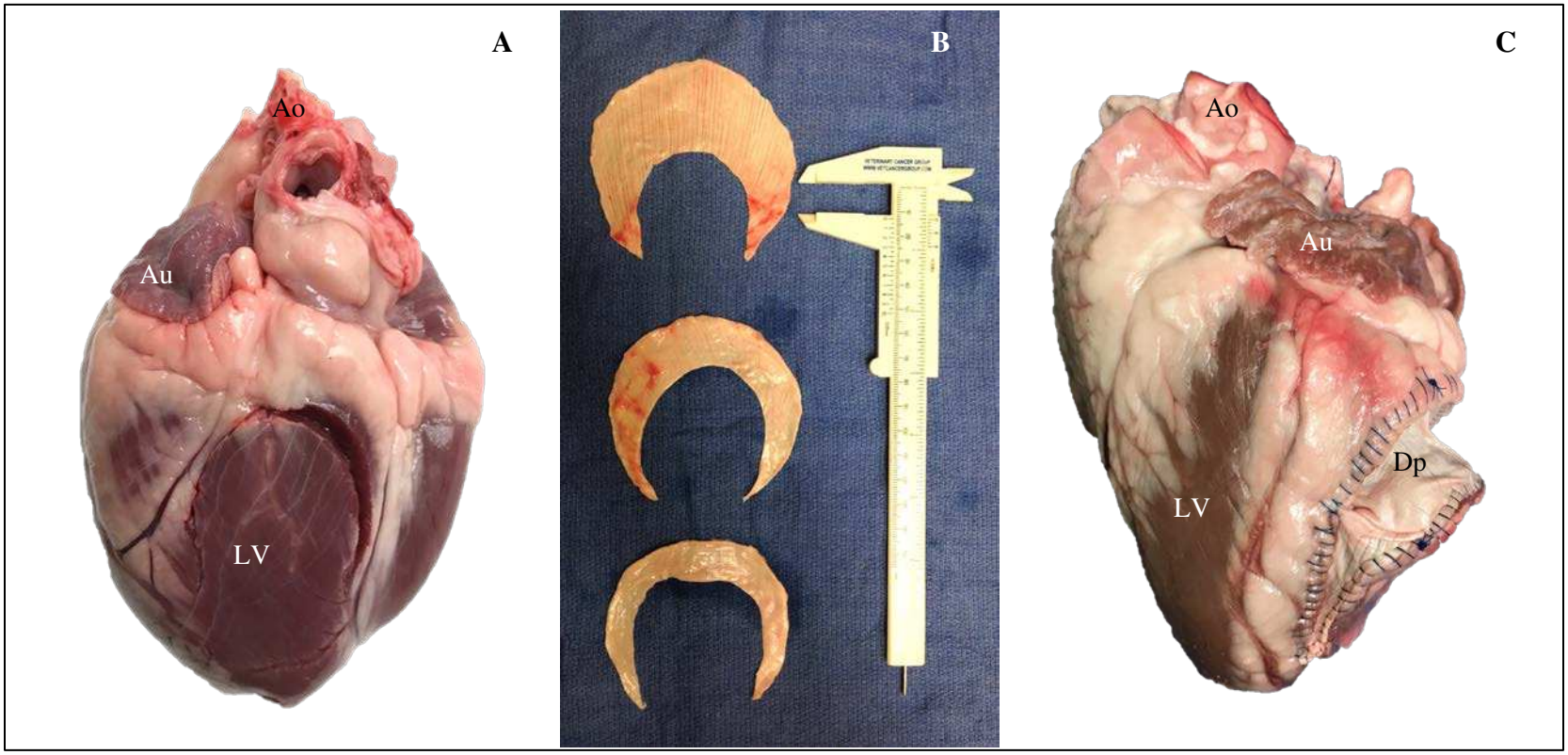

Figure 4.3. Illustrates the (A) "U"-shaped incision made around the PPM, (B) three sizes of crescent-shaped diaphragmatic patches and (C) after application of the diaphragmatic patch; Ao, Aorta; Au; Right auricle; Dp, diaphragmatic patch; LV, Left ventricle.

4.2. Results

Thirty-six hearts were used in the study. After placement of the diaphragmatic patches, 22 hearts were included in the final analysis of this study. Fourteen hearts were excluded from the study due to failure to maintain LVP from leakage at suture line (10 hearts), dislodging of the ultrasound transducer (1 heart) and torn left atrium (3 hearts). Seven hearts were in the SP and MP groups and eight in the LP group. Eleven hearts produced mitral regurgitation: 2 in each of the SP and MP group; 7 in the LP group.

Left ventricular pressure measured at baseline and after patch placement are reported in **Table 4.1.** At baseline and after patch placement, maximum and minimum pressure were not significantly different when compared between the 3 treatment groups (P>0.05). After patch placement, maximum and minimum pressure were not significantly different compared respectively to baseline (P>0.05). The maximum LVP for each treatment group was significantly higher than the minimum LVP (P=0.0156, 0.0156 and 0.0078 for SP, MP and LP groups respectively). The pressure-time relationships before and after applying the patch generated by the pulsatile pressurization system are illustrated in **Figure 4.4**.

Measured MR flow was reported in **Table 4.2.** Mitral regurgitation flow increased significantly after applying the large patch from 0 ml/min at baseline to 554 ml/min (IQR: 185-1,919.3 ml/min, P=0.0156). There were no significant changes in the MR flow from baseline in the SP and MP groups (P>0.05). In the LP group, 87.5% of the heart had mitral regurgitation while 28.6% of the heart in the SP and MP groups developed mitral regurgitation (P=0.034). There was no significant difference between the number of hearts that developed mitral regurgitation between the SP and MP groups (P>0.05). Boxplot representing the median and interquartile range of MR flow by patch sizes are shown in Figure 4.5. The measured MR flow

increased significantly after applying the large patch from 0 ml/min at baseline to 554 (185-1,919.3) ml/min (P=0.0156). However, there were no significant changes in the MR flow from baseline in both small and medium patch groups (P>0.05). Large patch placement produced 3.06 times higher MR heart models than the small and medium patches. 87.5% of the large patch heart models have MR. The small and medium patch group each produced 28.6% heart models with MR. Applying a Fisher's exact test, the proportion of heart models that produce MR flow is significantly higher in the large diaphragmatic patch compared to small and medium patches (P=0.034 and P=0.034, respectively). Significant differences in the proportion of having MR heart models where not found between the small and medium patch (P>0.05).

Table 4.1. Left ventricular pressure after patch placement versus baseline in heart models at maximum and minimum pressure. Data is presented as median (IQR).

Patch size	**Minimum Pressure (mmHg)**		**Maximum Pressure (mmHg)**	
	Baseline	**After Patch**	**Baseline**	**After Patch**
Small *(n=7)*	49.7 [a] (30.9-51.6)	59.2 [a] (48.9-64.5)	102.5 [b] (90.66-118.4)	89.3 [b] (76.7-100.1)
Medium *(n=7)*	62 [a] (54.7-79.5)	53.9 [a] (47.6-79.5)	100.7 [b] (96-113.2)	97.9 [b] (79.3-100.2)
Large *(n=8)*	55.5 [a] (40.5-68.8)	48.55 [a] (20.5-70.85)	108.6 [b] (95.5-116.05)	101.05 [b] (79.35-106)

Minimum and maximum values similar superscripts were not significant difference (P-value > 0.05).

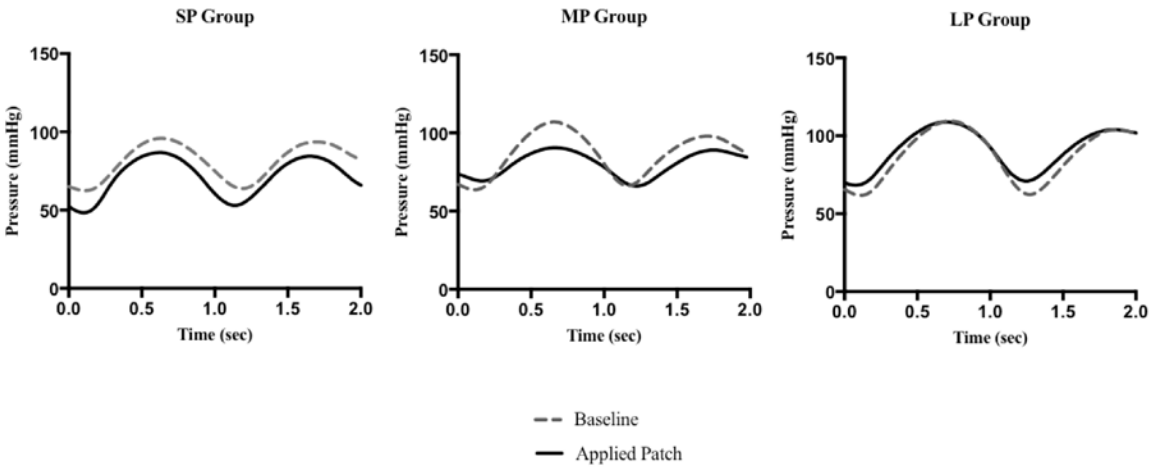

Figure 4.4. Left ventricular Pressure-Time graph during one cycle at baseline and after patch application. SP: Small patch; MP; Medium patch; LP; Large patch.

Table 4.2. Mitral regurgitation flow by patch sizes. Values are shown as median (IQR)

Patch size	**Mitral Regurgitation Flow Rate (ml/min)**		**Number of Hearts with regurgitation**	
	Baseline	**After Patch**	**Baseline**	**After Patch**
Small *(n=7)*	0	0 (0-2,520)	0	2
Medium *(n=7)*	0	0 (0-260)	0	2
Large *(n=8)*	0	554* (185-1,919.3)	0	7*

* Indicates significant difference from baseline (*P-value* < 0.05)

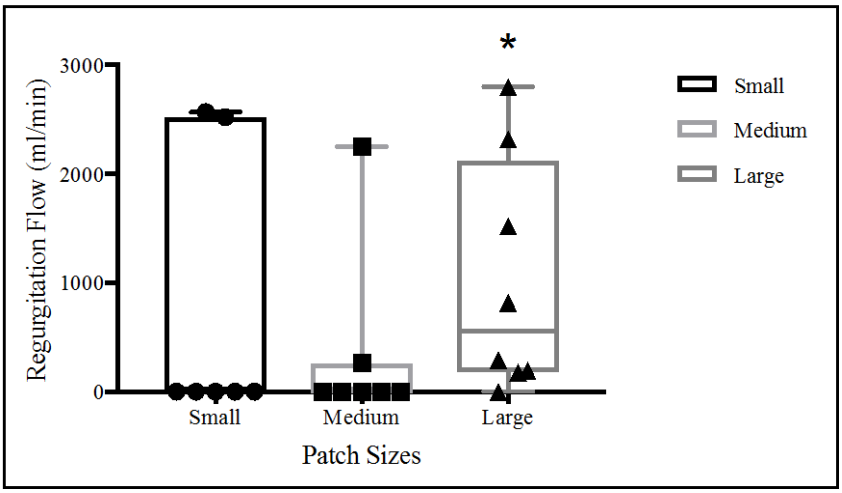

Figure 4.5. Boxplot comparison of median mitral regurgitation flow by patch sizes; * Indicates significant difference from baseline (P<0.05)

Geometric measurements of the mitral annulus and LV at maximum LVP in the three groups are reported in Table 4.3. The commissure to commissure annular dimension and mitral annular area were not significantly different after patch placement when compared to baseline in the three groups. In the SP group, after placement of the patch, the distance from fibrosa to PPM (P=0.016) and interpapillary length (P=0.016) increased significantly from baseline. In the MP group, after placement of the patch, the distance from the fibrosa to PPM (P=0.031), distance from mid-lateral annular to PPM (P=0.031) and interpapillary length (P=0.031) increased significantly from baseline. In the LP group, after placement of the patch, interpapillary length was significantly increased from baseline (P=0.008). Differences of all the dimensions between the three patch sizes were not significant (P>0.05). In the LP group, volume of the LV significantly increased from 18.5 ml (IQR: 15.0-26.0 ml) at baseline to 27.5 ml (IQR: 19.5-42.5

ml) after applying the large patch (P=0.031). The LVV did not increase significantly from baseline in the SP and MP groups (P>0.05).

Table 4.3. Geometric measurements of the annulus and lv chamber after patch placement versus baseline in heart models at maximum pressure. Values are shown as median (IQR)

	Small Patch		**Medium Patch**		**Large Patch**	
	Baseline ***(n = 7)***	**Patch** ***(n = 7)***	**Baseline** ***(n = 7)***	**Patch** ***(n = 7)***	**Baseline** ***(n = 8)***	**Patch** ***(n = 8)***
Mitral annulus						
SL (mm)	28.14 (21.19-34.14)	32.12 (20.78-47.19)	25.5 (20.61-28.8)	27.93 (22.01-29.93)	26.3 (24.05-35.48)	24.21 (21.42-31.00)
CC (mm)	39.58 (32.84-47.24)	39.00 (32.52-56.13)	41.19 (35.11-46.98)	45.99 (38.81-55.7)	51.6 (36.59-61.55)	46.98 (37.7-55.49)
MAA (cm^2)	8.75 (5.96-15.03)	11.42 (5.54-21.66)	9.15 (5.87-11.08)	9.45 (8.62-11.71)	8.64 (7.12-16.66)	10.33 (6.31-17.74)
LV Chamber						
LVV (ml)	21.01 (16.75-35.73)	22.57 (19.69-29.51)	20.08 (16.0-31.14)	28.31 (17.37-34.14)	18.53 (15.01-26.03)	27.5* (19.45-42.46)
Fibrosa-PPM (mm)	46.6 (44.5-55.91)	57.0* (46.3-65.9)	49.3 (47.48-50.7)	55.92* (53.77-56.8)	52.0 (48.2-55.72)	57.0 (50.20-58.66)
LA-PPM (mm)	32.59 (27.98-38.0)	33.3 (27.45-37.4)	33.36 (32.12-45.32)	33.9* (31.4-40.91)	36.5 (33.7-43.8)	35.8 (32.8-40.29)
Interpapillary (mm)	19.62 (18.7-23.7)	24.9* (23.0-31.01)	19.38 (14.32-22.95)	23.34* (20.5-35.9)	19.65 (14.65-23.65)	23.35* (20.9-29.415)

SL: Septo-lateral; CC: Commissure to commissure; LVV: Left Ventricular volume; PPM: Posterior papillary muscle; LA: Lateral annular;
* Denotes *P-value* <0.05 versus Baseline.

4.3. Discussions

Application of a patch around the PPM induced LV dilatation and outward displacement of the PPM. Mitral regurgitation resulted from displacement of the PPM without mitral annular dilatation. This *ex vivo* model is using a pulsatile forward flow from the apex of the LV toward the aorta.

Left ventricular pressure was maintained during the experiment. Monnet et al.[15] used a large patch sutured around the PPM to induce FMR in a static model of LV remodeling. In this study after suturing a patch around the PPM a pulsatile flow was used to generate a pressure wave in the LV. The pressure wave was similar before and after placing the patch. A maximum LVP of 100 mm Hg was used. The minimum and maximum pressures generated in the LV were not affected by the size of the patch sutured around the PPM. The flow was also maintained in a forward direction from the apex of the LV toward the aorta, which is more physiologic than the direction of the flow used in another study with a continuous flow.[15]

Myocardial infarction is commonly associated with asymmetrical LV remodeling with outward displacement of the PPM.[21] The distance between the fibrosa and the PPM increased as well as distance between the papillary muscles. Therefore, this model reproduces the outward displacement of the PPM reported in several clinical studies.[6,21,22] This was achieved by suturing a patch only around the PPM. The outward displacement does not seem to correlate with the size of the patch since the distances measured in this experiment were not significantly different between the three different sizes of patches. Left ventricular dilatation was only significant with the large patch. In clinical cases the dilation is the result of an aneurysmal dilation of the infarcted wall around the PPM.[6] Only the larger patch resulted in significant MR and LV dilatation. In clinical cases, FMR patients had more dilated annulus and LV compared to normal

patients.[3,12,13] Stretching of the mitral valve annulus is possible.[15,18] Annular dilation was not induced in this experiment because we wanted to reproduce a model reproducing only tethering of the papillary muscle. We wanted a model that would reproduce the LV dilation that is occurring after undersized annuloplasty. [7,14]

Despite claiming reduction annuloplasty as the standard treatment for FIMR, recurrence of moderate to severe MR can be found 28% post-operatively.[14] Balanced forces on the leaflets are being explored especially the PPM displacement and the impeding force from the annulus being shifted away from the PPM post-annuloplasty.[2,8,9] Also having a model reproducing only the outward rotation of the PPM would be more valuable for the evaluation of procedures targeting specifically modification of the geometry of the LV for treatment of FMR.

Mitral valve regurgitation developed mostly with the large patch. The amount of mitral regurgitation was significantly larger with the large patch because the geometry of the LV and the tethering of the PPM on the mitral valve leaflets were more important than with other patches used. The LVV was only significantly affected with the large size patch. The interpapillary muscle distance during LVP_{max} increased after application of patches. In vivo studies on FMR have showed similar results.[8,9] Animal models and clinical cases have shown that ischemic FMR was associated with the displacement of the PPM from the septal annulus[5,21] similar measurements were found in the small and medium patch sizes. Variation of the patch sizes was proposed to affect the severity of MR. Although the PPM displacement distances after patch placement were not different between the 3 patch size groups, the large patch group produced the highest rate of MR and MR volume. This study suggested that using the large patch application for the proposed pulsatile *ex vivo* model of FMR was more appropriate. Larger patch sizes have been used in previous studies and have resulted in larger volume of MR[15] with a patch of 5 cm at

its widest point. The MR was 1383 ml/min which was higher than the flow recorded in this present study. Monnet and colleague[15] stretched first the mitral annulus contributing to the flow of MR.

4.4. Limitations

The *ex vivo* heart used in the pulsatile system were non-vital tissue; therefore the effect of contractility during physiologic cardiac cycle could not be evaluated. To minimize further effects from non-vital tissue, the experiment must be done within 24 hours after the animals were euthanized. Clinical studies from Otsuji and colleagues[16] reported that papillary muscles dysfunction or annular dilatation alone were not associate with ischemic MR. This implied that the pulsatile *ex vivo* model in this study despite the absence of contraction could be used for assessing other factors associated with the MR severity

In this experiment lot of *ex vivo* constructs were rejected for several technical reasons. However, the *ex vivo* constructs were mostly rejected at the beginning when we learn how to suture the patches on the myocardium. Also, we noticed that each constructs could only be used for a limited amount of experiments because the patches started to tear from the myocardium. A maximum LVP of 120 mm Hg was used because when the pressure was increased the myocardium was tearing even more frequently. This limitation on the pressure limited the variation of the LVV during each cycle.

Interpreting the results need to be carefully taken into consideration since the mitral valve in physiological state closes during isovolumetric contraction phase when LVP rises and the LV contraction occurs. If mitral leaflet mal-coaptation occurs, MR will be noticeable during early

and late phase of isovolumetric contraction. MR was less seen during mid-phase when LVP reaches its maximum (counter acting the tethered force on the leaflets).[6] In the pulsatile system, the pump generated maximum LVP forcing the mitral leaflet to close and the LVV increased from fluid pressurization. Leaflets closed at the same pressurization phase as in physiological heart except for in vivo the LVV decreased from LV contraction.

Patch application mimics LV remodeling which occurs in a 3 dimensional fashion. Our study, however, only evaluate the PPM displacement in 2 dimensions. This may be the explanation for no significant differences of the PPM displacement distances between the patch groups. Studies have shown significant 3 dimensional geometric displacements of the PPM and tethered angle of the leaflets.[8,13,21] Three-dimensional PPM geometry needs to be assessed to give a better idea of how the PPM displacement associates MR severity.

In conclusion, FMR can be induced in a pulsatile ex-vivo model of LV dilatation and PPM displacement. Our model generated LVP waveforms and PPM geometry similar to in vivo studies without disrupting the mitral leaflets and chordae while the LV wall remained intact. Surgical treatments for FMR that involves annuloplasty, LV wall reshaping and PPM repositioning can be applied to this model prior to *in vivo* studies

REFERENCES

1. Braun J, Klautz RJM. 2012. Mitral valve surgery in low ejection fraction, severe ischemic mitral regurgitation patients: should we repair them all? *Curr Opin Cardiol* 27:111-–7.
2. Capoulade R, Zeng X, Overbey JR, et al. 2016. Impact of left ventricular to mitral valve ring mismatch on recurrent ischemic mitral regurgitation after ring annuloplasty. *Circulation* 134:1247-56. http://circ.ahajournals.org/content/134/17/1247
3. Enriquez-Sarano M, Akins CW, Vahanian A. 2009. Mitral regurgitation. *The Lancet* 373:1382–94. http://www.sciencedirect.com/science/article/pii/S0140673609606929
4. Green GR, Dagum P, Glasson JR, et al. 1999. Mitral annular dilatation and papillary muscle dislocation without mitral regurgitation in sheep. *Circulation* 100:II95–II102.
5. Gorman III M, Gorman RC, Jackson BM, et al. 1997. Distortions of the mitral valve in acute ischemic mitral regurgitation. *Ann Thorac Surg* 64:1026–1031. http://www.sciencedirect.com/science/article/pii/S0003497597008503
6. He S, Fontaine AA, Schwammenthal E, Yoganathan AP, Levine RA. 1997. Integrated mechanism for functional mitral regurgitation. *Circulation* 96:1826-1834 http://circ.ahajournals.org/content/96/6/1826
7. Hung J, Solis J, Handschumacher MD, et al. 2012. Persistence of mitral regurgitation following ring annuloplasty: is the papillary muscle outside or inside the ring? *J Heart Valve Dis* 21(2):218-24. http://www.ncbi.nlm.nih.gov/pmc/articles/PMC3509931
8. Jensen H, Jensen MO, Smerup MH, et al. 2010. Three-dimensional assessment of papillary muscle displacement in a porcine model of ischemic mitral regurgitation. *J Thorac Cardiovasc Surg* 140:1312-8. http://www.sciencedirect.com/science/article/pii/S002252231000036X
9. Kalra K, Wang Q, McIver BV, et al. 2014. Temporal changes in interpapillary muscle dynamics as an active indicator of mitral valve and left ventricular interaction in ischemic mitral regurgitation. *J Am Coll Cardiol* 64(18):1867-79.
10. Katoh T, Ikeda N, Nishi K, et al. 1999. A newly designed adapter for testing an ex vivo mitral valve apparatus. *Artificial Organs* 23:920–3.
11. Kono T, Sabbah HN, Rosman H, Alam M, Jafri S, Goldstein S. 1992. Left ventricular shape is the primary determinant of functional mitral regurgitation in heart failure. *J Am Coll Cardiol* 20:1594–1598. http://www.sciencedirect.com/science/article/pii/073510979290455V
12. Kumanohoso T, Otsuji Y, Yoshifuku S, et al. 2003. Mechanism of higher incidence of ischemic mitral regurgitation in patients with inferior myocardial infarction: quantitative analysis of left ventricular and mitral valve geometry in 103 patients with prior myocardial infarction. *J Thorac Cardiovasc Surg* 125:135–43. http://www.jtcvsonline.org/article/S0022522302733254/abstract

13. Kwan J, Shiota T, Agler DA, et al. 2003. Geometric differences of the mitral apparatus between ischemic and dilated cardiomyopathy with significant mitral regurgitation real-time three-dimensional echocardiography study. *Circulation* 107:1135–40. http://circ.ahajournals.org/content/107/8/1135
14. McGee J, Edwin C, Gillinov AM, et al. 2004. Recurrent mitral regurgitation after annuloplasty for functional ischemic mitral regurgitation. *J Thorac Cardiovasc Surg* 128:916–24. http://www.sciencedirect.com/science/article/pii/S0022522304011432
15. Monnet E and Pouching K. 2013. An ex vivo model of left ventricular dilation and functional mitral regurgitation to facilitate the development of surgical techniques. *The Heart Surgery Forum* 16(6): 332-38.
16. Otsuji Y, Levine RA, Takeuchi M, Sakata R, Tei C. 2008. Mechanism of ischemic mitral regurgitation. *J Cardiol* 51:145–156. http://www.sciencedirect.com/science/article/pii/S0914508708000877
17. Perloff JK, Roberts WC. 1972. The mitral apparatus functional anatomy of mitral regurgitation. *Circulation* 46:227–239. http://circ.ahajournals.org/content/46/2/227
18. Richards AL, Cook RC, Bolotin G, Buckner GD. 2009. A Dynamic Heart System to Facilitate the Development of Mitral Valve Repair Techniques. *Ann Biomed Eng* 37:651–60.
19. Sabbah HN, Kono T, Rosman H, Jafri S, Stein PD, Goldstein S. 1992. Left ventricular shape: A factor in the etiology of functional mitral regurgitation in heart failure. *Am Heart J* 123:961–966. http://www.sciencedirect.com/science/article/pii/000287039290703X
20. Siefert AW, Rabbah JPM, Koomalsingh KJ, Touchton SA Jr, Saikrishnan N, McGarvey JR. 2013. In vitro mitral valve simulator mimics systolic valvular function of chronic ischemic mitral regurgitation ovine model. *Ann Thorac Surg* 95:825–30. http://www.sciencedirect.com/science/article/pii/S0003497512026045
21. Tibayan FA, Rodriguez F, Zasio MK, et al. 2003. Geometric distortions of the mitral valvular-ventricular complex in chronic ischemic mitral regurgitation. *Circulation* 108:II–116–II–121. http://circ.ahajournals.org/content/108/10_suppl_1/II-116
22. Uemura T, Otsuji Y, Nakashiki K, et al. 2005. Papillary muscle dysfunction attenuates ischemic mitral regurgitation in patients with localized basal inferior left ventricular remodeling: insights from tissue Doppler strain imaging. *J Am Coll Cardiol* 46:113-9. http://www.sciencedirect.com/science/article/pii/S0735109705007692

5. EVALUATION OF THE EFFECT OF THE THREE-DIMENSIONAL GEOMETRY OF THE LEFT VENTRICLE ON THE SEVERITY OF MITRAL REGURGITATION VOLUME IN AN *EX VIVO* PULSATILE MODEL OF LEFT VENTRICULAR DILATATION WITH POSTERIOR PAPILLARY MUSCLE DISPLACEMENT

Functional ischemic mitral regurgitation is associated with complications and poor prognosis,[1,18] which is independent from ventricular function.[9] Ring annuloplasty is currently used as the method of choice to treat FIMR.[3,10,29] Although short-term studies reported satisfactory outcomes of this technique,[2,5,24] higher than 20% in late recurrence of FIMR and ongoing LV remodeling has been observed.[4,6,11,14,20,22,26] Posterior papillary muscles displacement and continued LV remodeling were the predictors of FIMR recurrence after ring annuloplasty.[11,19] Therefore, to achieve optimal surgical strategies for FIMR treatment, the mechanism of FIMR needed to be thoroughly investigated. Studies in human and animal models have focused on two main components that associated with FIMR including dilatation of mitral annulus and displacement of the PPM.[13,17,27,30]

Augmentation of the interpapillary distances and PPM tethering distances from the anterior mitral annulus have been frequently reported in clinical patient with FIMR or research model of FMR.[15,25,27,28] Those measurements were completed on a two-dimensional (2D) plane. The outward displacement of the PPM would be better evaluated in three-dimensional (3D) plane. Therefore a XYZ coordinated displacement of the PPM would be better understood which could bring some light on the treatment of the FMR.

Three dimensional echocardiography and 3D cardiac MRI were used as non-invasive techniques for clinical studies or research settings to have a better understanding of the tethering

during FIMR or after annuloplasty.[12,15,16] Annular height, commissural width and non-planarity angles have been evaluated in patients with FMR and before and after annuloplasty.[19,21] Those 3D evaluations were limited to the mitral leaflet and were difficult to apply to the entire mitral apparatus in clinical patients and animal models. Piezo-electric crystals for sonomicrometric analysis could provide precise 3D geometric evaluations.[27] These techniques were invasive which made it inappropriate for clinical studies. An *ex vivo* model of FMR allow evaluation of the geometric changes inducing FMR in a 3D plane.

The purposes of this study were to use sonomicrometry in an *ex vivo* heart model to evaluate the tethered distances and tethered angles of the PPM due to regional LV dilatation. We aimed to identify the geometric changes that were associated with the development of FIMR despite normal mitral annulus. The experiments were conducted in *ex vivo* pulsatile model of FIMR with normal mitral annulus seen in recurrence of FIMR after ring annuloplasty cases. We hypothesized that the tethered distances and tethered angles of the PPM increases when FMR is induced.

5.1. Material and methods

5.1.1. Model Preparation

Fresh ovine hearts with no cardiac abnormalities were collected from sheep euthanized for reason unrelated to this study, stored at 4°C and the experiments were carried out within 24 hour. A reversed "U"-shaped incision was made around the PPM without damaging the chordae. The PPM remained intact with a 2 cm strip of myocardium at the apical LV wall. Three sizes of crescent-shaped diaphragmatic patches were chosen to suture close the incision made around the

PPM. The patches were respectively 1 (small), 2 (medium), and 3 (large) centimeters wide at their widest point. The hearts were randomly assigned to one of the following group: small, medium and large group. This created a focal dilatation of the LV and displacement of the PPM.

Six piezo-electric crystals (2 mm round piezo-electric crystal, Sonometrics Corp., London, Canada) were placed within the LV wall. Regional wall motion and distances between piezo-electric crystal pairs were measured continuously with a data acquisition system (SonoSoft, Sonometrics Corp., London, Canada).

The *ex vivo* dynamic hearts were connected to a dynamic pressurization system (Bio-console 520D Centrifugal Blood Pump, Bio Medicus, Minnesota) **(Figure 5.1)**. The dynamic pressurization system generated pulsatile flow with a cannula introduced in the apex of the LV.[22] Pulsatile flow was simulated with a flow of 4 liter per minute and 40 beat per minute with the flow traveling from the apex of the LV into the aorta. The maximum left ventricular pressure (LVP_{max}) was maintained between 85- 120 mmHg. An aortic outflow valve could be adjusted to decrease or increase outflow resistance until LVP_{max} reached desired value. A cannula placed in one of the pulmonary vein was used to measure the volume of MR per minute. The cannula was placed 15 cm above the mitral valve. A high-fidelity pressure transducer (Millar, Inc., Houston, USA) was inserted into the LV in a retrograde fashion via the aorta to measure LVP. Each treatment was observed whether regurgitation occurred or not. The MR volume flow rate was measured in milliliter per minute in heart with MR. The hearts after patch placements were categorized into 2 groups: hearts that produced MR volume (MR+ group) and hearts without MR volume (MR- group).

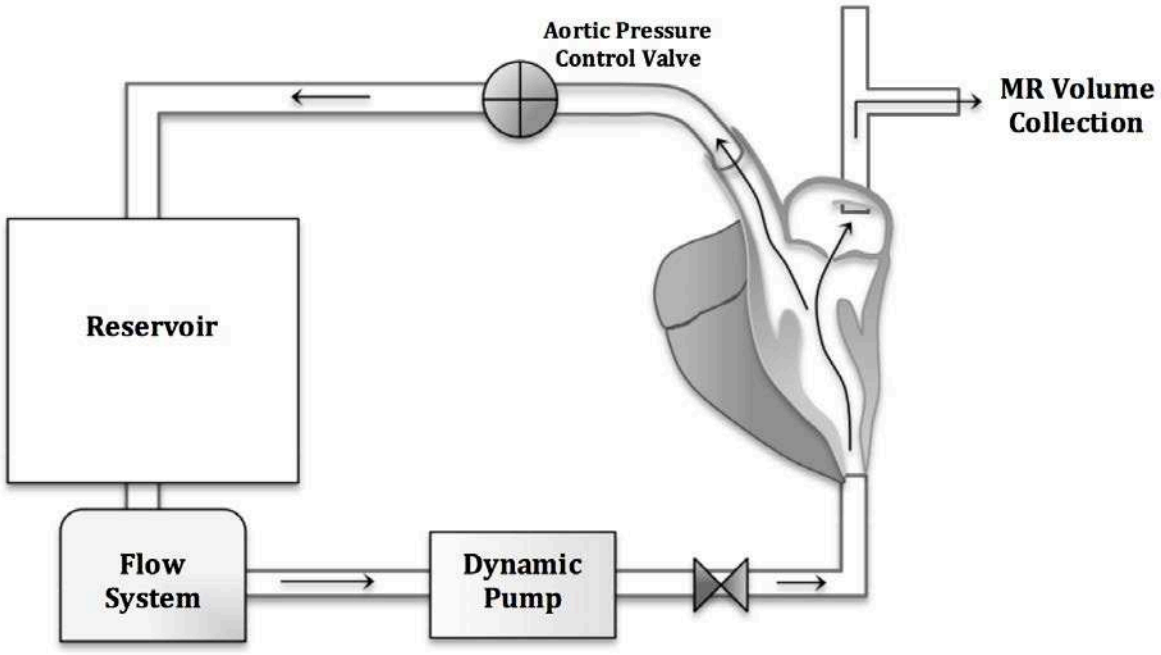

Figure 5.1. Illustration of the heart model connected to the dynamic pressurization system. Black arrows indicated the fluid flow direction.

5.1.2. Measurement of the PPM displacement relative to Cartesian coordinates

Piezo-electric crystals 1, 2, 3 and 4 also served as markers for the best-fitted plane calculation. Data from these piezo-electric crystals were analyzed by a computer software (SonoXYZ, Sonometrics, London, Canada) and used to generate the Cartesian coordinates throughout the time course of an experiment. The piezo-electric crystal at the level of the fibrosa of the annulus was used as the origin for 3 positive (lateral, anterior, and apical) and 3 (medial, posterior, and basal) negative axes. These 6 axes were used for constructing 3 perpendicular planes: annular plane, frontal plane and sagittal plane **(Figure 5.2)**. The positive lateral axis (X axis) passes through piezo-electric crystal #2. The positive apical axis (Y axis), perpendicular

with the X-axis, is directed toward the apical piezo-electric crystal #4. The positive anterior axis (Z axis), perpendicular with the X-axis and Y-axis, was calculated by the computer software (SonoXYZ, Sonometrics, London, Canada) directed toward the annular anterior commissure piezo-electric crystal #3. The 3D PPM positions at LVP_{max} were determined into their X, Y and Z coordinates. Position of the PPM to the fibrosa was recorded in the lateral, anterior, and apical axis. Displacement of PPM in the lateral, anterior and apical axes were calculated with the following formula: (Distance of PPM to Fibrosa after placing patch) – (Distance of PPM to Fibrosa at Baseline).

5.1.3. PPM tethered angle measurements relative to Cartesian coordinates

The PPM tethering angles referred to the mitral annulus were evaluated with the angle α and angle β. The α and β angles at LVP_{max} were measured and calculated referring to the Cartesian coordination planes. Given that α is the angle formed by positive X axial segment and fibrosa-PPM tip segment. The β angle is formed by positive X axial segment and lateral annulus-PPM tip segment **(Figure 5.3)**. The changes of the α and β angles from baseline were evaluated in the annular plane (αa and βa angles) **(Figure 5.3A)** and frontal plane (αf and βf angles) **(Figure 5.3B)**.

5.1.4. Statistical analysis

Analyses were performed with SAS version 9.4 (SAS Institute Inc). Data was report as mean ± SD and statistical significances were considered when $P<0.05$. A paired *t*-test was used to compare continuous data between baseline and after application of the patch. Relative change values were compared between the MR(+) group and MR(-) group with Student's *t*-test. Relative

change values, calculated by the differences between the treatment and baseline value divided by the baseline of each heart model. Multivariate regression analysis based on stepwise model selection was done to determine predictors that associated with MR volume.

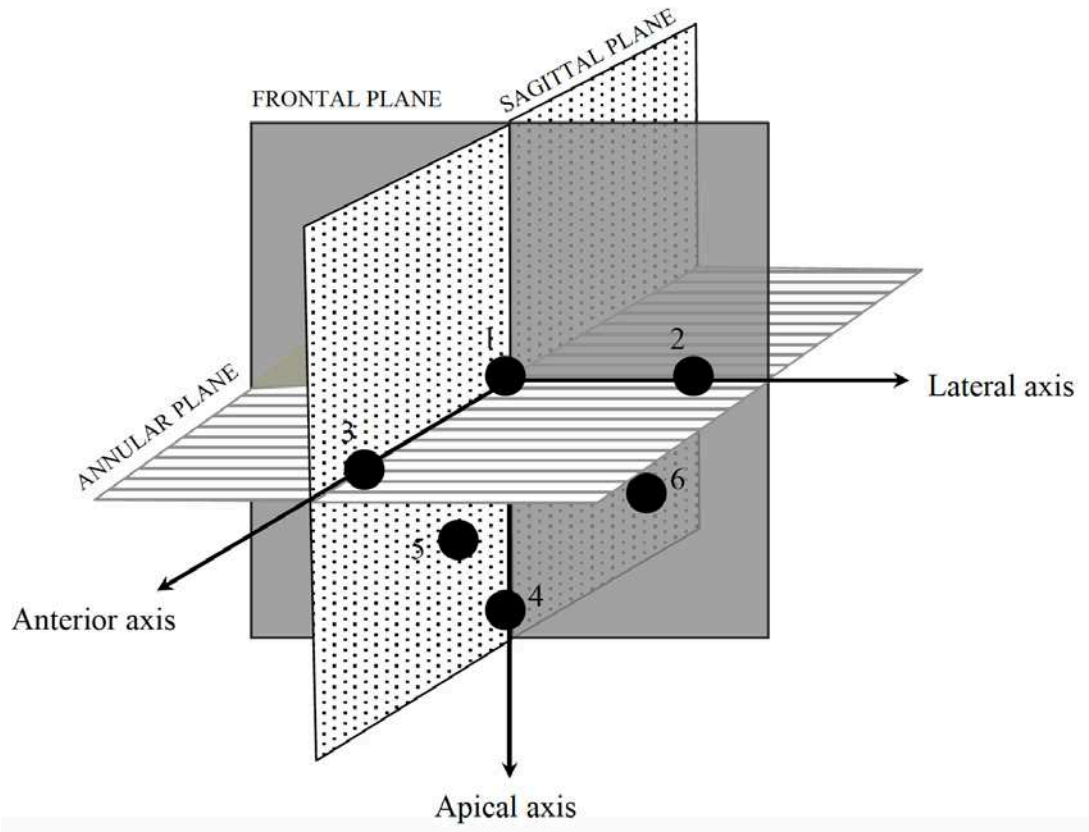

Figure 5.2. Best-fit Cartesian plane calculated from the SonoXYZ software using piezo-electric crystals 1, 2, 3 and 4 as a reference marker. The lateral, anterior and apical axes are labeled as black arrows pointing in the positive direction. Piezo-electric crystals placed in the LV are labeled as black dots.

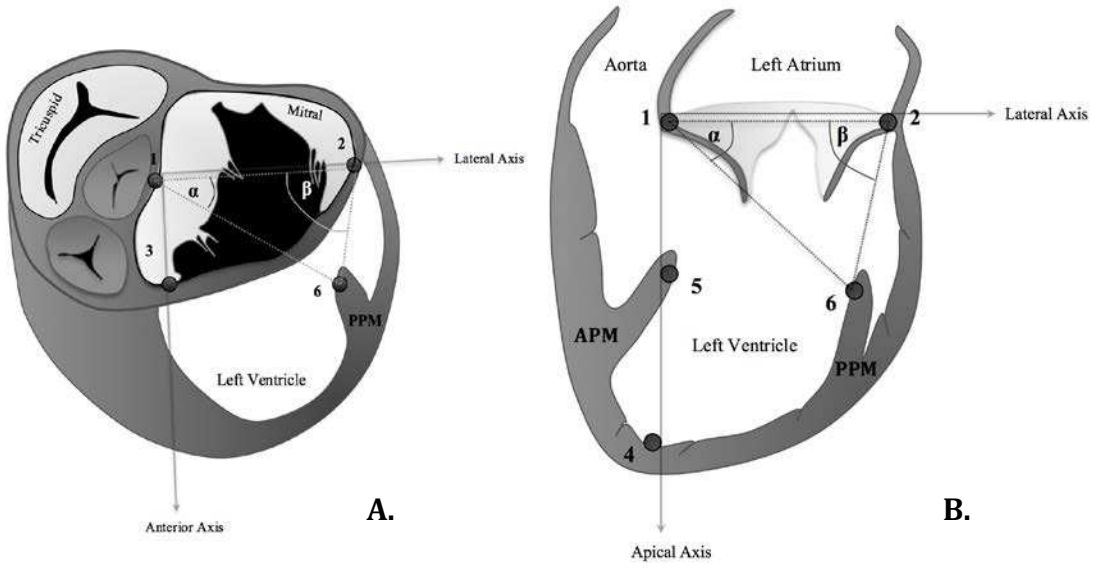

Figure 5.3. Illustrates 6 transducers placement and PPM tethered angles in the annular plane and frontal plane. The numbers marked the landmarks of the transducers. The angles were marked as α and β. Transducer 1, 2, 3 and 4 were used as reference to construct Cartesian planes. (A) Oblique annular plane at the level of the mitral annulus. (B) Frontal plane of the left side of the heart.

5.2. Results

Twenty-two ovine hearts, from the initial pool of 36 hearts, were entered in the study. Fourteen hearts were rejected because of leakage around the sutured patch, failure to generate significant LVP and atrial puncture. Eleven hearts developed MR and were entered in the MR+ group. Two hearts were in the small patch group, 2 were in the medium patch group, and 7 were in the large patch group. Eleven were entered in the MR- group. Five hearts were in the small patch group, 5 were in the medium patch group, and 1 was in the large patch group. Left ventricular volume increased significantly after applying the patches from 25.9±12.0 ml at baseline to 38.3±21.2 ml after applying a patch, (P=0.049) in the MR + group and from

24.1±13.3 ml at baseline to 29.0±14.3 ml (P=0.002) in the MR- group. The LVV after placement of the patch were not significantly different between the MR+ and MR- groups (P=0.207). Mitral annular septo-lateral dimension, commissural-commissural dimension and mitral annular area were not significantly different from baseline and between the two MR groups (P>0.05).

Distances of the PPM tip from different anatomical landmarks measured at baseline and after patch application were reported at LVP_{max} for the MR+ and MR- groups **(Table 5.1)**. In both MR+ and MR- groups, the distances of fibrosa to PPM and interpapillary muscle tips increased significantly compared to baseline. Using the Cartesian planes, lateral displacement of the PPM was significantly greater in both MR+ and MR- groups. Displacement of the PPM in the lateral axis increased from baseline 8.7±7.8 mm (P=0.007) for the MR+ group and 7.5±6.8 mm (P=0.004) for the MR- group **(Figure 5.4)**. No significant changes in the PPM displacement in the apical and anterior direction were noted in both groups.

In MR+ group, the application of the patch significantly reduced the αf angle from 45.3 ±6.6° at baseline to 35.9±8.8° (P<0.05). The angle αa was not significantly changed when compared to baseline (8.5±11.8° *vs* 6.4±8.0°, P>0.05). **Figure 5.5** showed βa and βf angles were not significantly changed when compared to baseline (116.4±64.0° *vs* 136.2±59.8° and 104.9±20.4° *vs* 102.3±14.9, P>0.05 respectively).

In the MR+ group, the amount of MR volume was better determined by a model including the interpapillary muscle distance, lateral axial displacement of the PPM tip, tethering αa angle and the tethering βf angle (P<0.05). Basic descriptive statistics and regression coefficients are shown in **Table 5.2**. The estimated regression equation for the multiple regression of MR volume = 1674.77 + 89.25 (Interpapillary distance) + 69.08 (Lateral axial displacement) – 63.73 (αa angle) + 105.66 (βf angle) (P=0.008, R^2 = 0.83).

Table 5.1. Distance measured from different landmarks to the posterior papillary muscle before and after applying diaphragmatic patch in constructs with MR (MR+) and constructs without MR (MR-)

	MR (+)		MR (-)	
	Baseline (n=11)	**Applied Patch (n=11)**	**Baseline (n=11)**	**Applied Patch (n=11)**
Distance referred to anatomical landmarks				
Fibrosa to PPM, mm	50.41±4.01	56.77±7.28*	50.45±6.85	54.29±6.09*
Lateral to PPM, mm	36.15±3.61	34.91±3.13	36.28±8.62	35.11±7.22
Interpapillary, mm	20.31±7.39	26.36±7.58**	19.11±3.71	25.14±5.00*
Distance referred 3-D axes (using fibrosa as origin)				
Lateral axis, mm	37.83±6.30	46.48±9.52*	30.38±10.98	39.26±11.76*
Anterior axis, mm	4.93±7.44	1.11±13.50	8.38±14.39	2.58±6.62
Apical axis, mm	39.08±8.51	33.11±6.13	35.32±8.63	30.24±12.16

* = *P-value* < 0.05 vs. Baseline
** = *P-value* < 0.001 vs. Baseline

Table 5.2. Multiple regression model with four explanatory variables

Variable	**Coefficient (β)**	**SE**	***P*-Value**	**95% CI**
Intercept	1674.774	1108.64		
Interpapillary distance	89.249	30.09	0.031	11.91-166.59
Lateral axial displacement	69.077	17.43	0.011	24.26-113.89
αa angle	-63.725	10.08	0.002	(-89.64) - (-37.81)
βf angle	105.655	20.80	0.004	52.18-159.13

95% CI; the 95% confidence interval for the partial regression coefficient

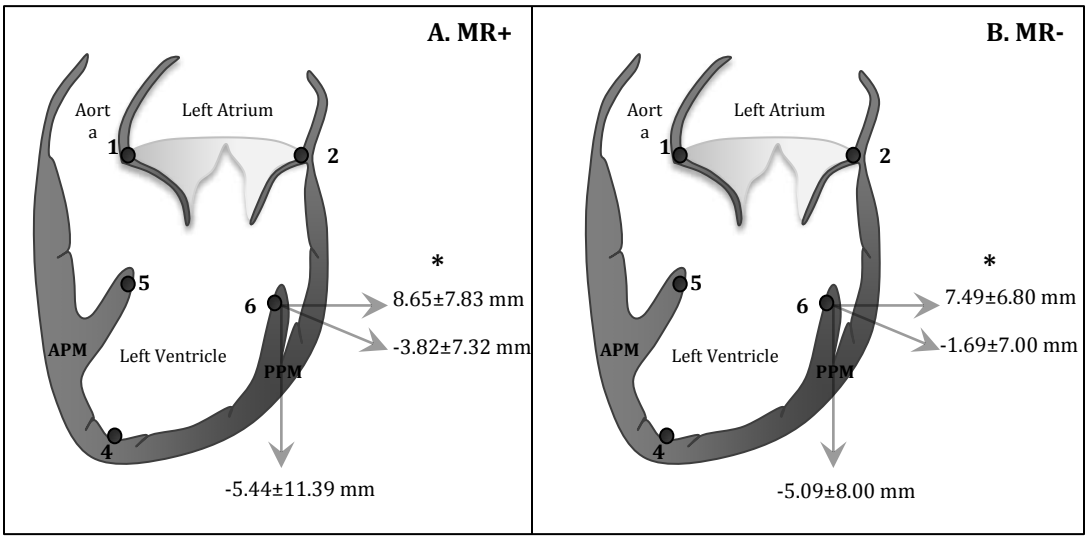

Figure 5.4. Three-dimensional displacement of the ppm within the lateral, apical and anterior axis in (**A**) MR+ and (**B**) MR- heart model groups; * indicates significant PPM displacement after applying patch compared to baseline at maximum LVP (P<0.05).

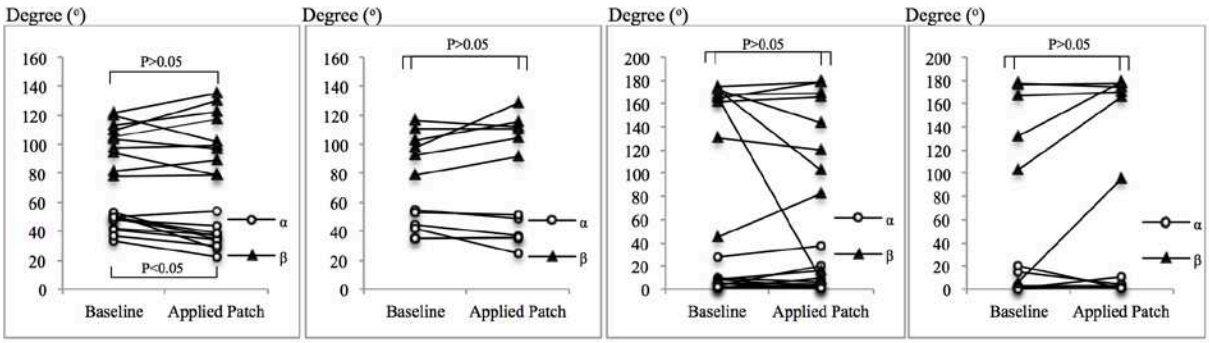

A. Frontal Plane MR (+) | B. Frontal Plane MR (-) | C. Annular Plane MR (+) | D. Annular Plane MR (-)

Figure 5.5. Tethering angles of the PPM tips referred to fibrosa (α) and lateral (β) annular landmarks measured in frontal plane of MR+ group, Frontal Plane of MR- group, Annular plane of MR+ group and annular plane of MR- group.

5.3. Discussions

Three-dimensional evaluation of the geometry of the LV associated to FMR was possible with piezoelectric crystals in an ex-vivo model of FMR. It showed that not only the lateral PPM displacement and the interpapillary muscles were important parameters for the development of FMR but the tethering angle of the PPM was also an important parameters during the development of FMR.

In our model we selectively displaced the PPM to induce an asymmetrical distension on the mitral valve leaflet and annulus. Gorman and colleagues[7] showed a dis-coordination between the anterior and the posterior papillary muscle contributes to FMR. This discoordination result in asymmetrical traction on the mitral valve leaflets.[15]

Most of the studies related to FIMR have looked at interpapillary muscles distance and distance from different points on the mitral annulus to the PPM and documented an increased in tethering as a cause of FIMR following myocardial infarction.[11,12,22,32] We reported similar changes in our *ex vivo* model. Lateral displacement of the PPM in FIMR studies were also reported in animal models.[15,27] Three-dimensional MRI has been used in a porcine model of FIMR to study the remodeling related to FMR.[15] The PPM was displaced posteriorly and the interpapillary muscles distance increased in their porcine model of FIMR.

Using 3D evaluation of the geometry of the LV, the tethering angle of the PPM in the frontal plane was identified as a factor responsible for the development of FMR. The angle in the frontal plane decreased while the PPM was displaced. The reduction of the α angle in the frontal plane in the construct that developed MR was due to upward displacement of the PPM closer to the lateral annulus. This was also found in 3D geometric study of acute and chronic FIMR ovine

model.[7,27] Tethered distance of the PPM tip outside the lateral annulus from both LV remodeling and relative to mitral annuloplasty could restrict the posterior mitral leaflet.[8,12]

In two different studies in an attempt to evaluate PML tethering in FIMR, a similar angle was evaluated before and after annuloplasty and after recurrence.[19,31] However they only used 2D echocardiography which makes the comparison with our study difficult. In their study the tethering angle was reduced after restrictive annuloplasty and increased with recurrence. However the variation of this angle was similar in groups with or without recurrence of mitral regurgitation. Measurement of the angle during 2D echocardiography can be very operator dependent. In our study with evaluation in three different Cartesian planes, the α angle in the frontal plane decreased with development mitral regurgitation.

The tethering α angle of the PPM measured in the annular plane was not significantly increased however it showed a slight increase in the MR(+) group which was not present in the MR(-) group. This may relate to the posterior displacement of the PPM. The tethering α angle of the PPM in the annular plane was a factor for the development of mitral regurgitation in our multivariate regression model. Reduction of this angle was associated with an augmentation of mitral regurgitation. The reduction of the tethering α angle in the annular plane resulted in distortion of the mitral valve apparatus which resulted in FMR. Distortion of the mitral valve has been shown to induce FIMR in an acute situation.[7] Distortion was the result of upward and centroid displacement of the tip of the PPM as reported in this study. Reduction annuloplasty has been shown to alter the geometry of the leaflet apparatus by placing the PPM outside of the annulus in a 3D projection.[12] The displacement of the PPM outside the mitral annulus should further decrease the tethering α angle of the PPM in both the frontal and annular planes. This could be one explanation for a high recurrence rate after reduction annuloplasty.

The tethering β angle in the frontal plane was not significantly affected before and after applying the patch. However it was a significant parameter in multivariate regression model. Augmentation of this angle would result in a more severe mitral regurgitation. Similar results of the tethered angle of PML have been shown in a study evaluating recurrent MR after surgical annuloplasty.[19] Patients that experienced a recurrent FMR had an increased in their tethering angle of the PML. Also, the restrictive annuloplasty by moving the entire mitral annulus toward the fibrosa will increase this angle and more likely contributing to recurrence.[12]

The model developed in this study demonstrated that the development of FMR is multifactorial. The four independent variables included in the model were able to explain 83% of the MR volume. The interpapillary muscle distance, lateral axial displacement of the tip of PPM, and the tethering angle of the β angle in the frontal plane had significantly positive regression effects, indicating that heart with higher values of these measurements were expected to produce higher volume of MR. Meanwhile, the tethering α angle in the annular plane had a significantly negative effect on the MR volume, indicating that after constantly controlling other measurements, hearts with larger tethering α angle in the annular plane was expected to produce lower MR volume.

This study has several limitations. Functional mitral valve regurgitation was induced with only PPM displacement without mitral annular dilatation in *ex vivo* heart models. This study mimicked clinical situations when patients had normal or undersized mitral annulus after mitral annuloplasty yet encountered persistent or recurrent FIMR post-annuloplasty from LV remodeling.[11,12,22,31] This *ex vivo* model even being pulsatile did not reproduced the myocardial contractions during the cardiac cycle that affect the geometry of the LV and the anatomy of the mitral annulus. It mostly reproduced the aneurysmal dilation that occured after myocardial

infarction. Measurements were recorded at maximal pressure in the LV which was equivalent to the systolic pressure at the end of the isovolumetric contraction in the cardiac cycle. The small sample size of this study could have limited the power to detect the significant differences in relative change of the 3D displacement and the PPM tip angles referred to the annulus between the MR(-) and MR(+) groups. However, the purpose of this study was achieved by demonstrating significant tethered angle in the MR(+) group and also strong predictors for MR severity which included the tethered angles of the PPM tip from multivariate analysis.

In conclusion, our study demonstrated that the tethered angle of the PPM tip along with interpapillary muscles tethered distance and lateral displacement of the PPM tip could be used to predict MR severity when measured in 3D Cartesian planes. This could be used to predict MR persistence/recurrence post-annuloplasty. Furthermore, it could be used to evaluate when PPM relocation was needed as an adjunctive treatment. This *ex vivo* study showed the importance of a 3D evaluation of the geometry of the LV and outward displacement of the PPM after myocardial infarction to determine patients at risk of developing FIMR.

REFERENCES

1. Badiwala MV, Verma S, Rao V. 2009. Surgical management of ischemic mitral regurgitation. *Circulation* 120:1287–93.
2. Bolling SF. 2001. Mitral valve reconstruction in the patient with heart failure. *Heart Fail Rev* 6:177–85.
3. Bonow RO, Carabello BA, Chatterjee K, et al. 2008. Focused Update Incorporated Into the ACC/AHA 2006 Guidelines for the Management of Patients With Valvular Heart Disease: A Report of the American College of Cardiology/American Heart Association Task Force on Practice Guidelines (Writing Committee to Revise the 1998 Guidelines for the Management of Patients With Valvular Heart Disease): Endorsed by the Society of Cardiovascular Anesthesiologists, Society for Cardiovascular Angiography and Interventions, and Society of Thoracic Surgeons. *Circulation* 118:523-661.
4. Calafiore AM, Gallina S, Di Mauro M, et al. 2001. Mitral valve procedure in dilated cardiomyopathy: repair or replacement? *Ann Thorac Surg* 71:1146-53.
5. Daneshmand MA, Milano CA, Rankin JS, et al. 2009. Mitral valve repair for degenerative disease: A 20-Year experience. *Ann Thorac Surg* 88:1828–37.
6. Gillinov AM, Wierup PN, Blackstone EH, et al. 2001. Is repair preferable to replacement for ischemic mitral regurgitation?. *Thorac Cardiovasc Surg* 122:1125–41.
7. Gorman III M, Gorman RC, Jackson BM, et al. 1997. Distortions of the mitral valve in acute ischemic mitral regurgitation. *Ann Thorac Surg* 64:1026–1031. https://doi.org/10.1016/S0003-4975(97)00850-3
8. Green GR, Dagum P, Glasson JR, et al. 1999. Restricted posterior leaflet motion after mitral ring annuloplasty. *The Annals of Thoracic Surgery* 68(6):2100–2106. https://doi.org/10.1016/S0003-4975(99)01175-3
9. Grigioni F, Enriquez-Sarano M, Zehr KJ, Bailey KR, Tajik AJ. 2001. Ischemic mitral regurgitation: long-term outcome and prognostic implications with quantitative Doppler assessment. *Circulation* 103:1759–64.
10. Hillis LD, Smith PK, Anderson JL, Bittl JA, Bridges CR, Byrne JG. 2011. ACCF/AHA Guideline for coronary artery bypass graft surgery a report of the American College of Cardiology Foundation/American Heart Association task force on practice guidelines. *Circulation* 124:652–735.
11. Hung J, Papakostas L, Tahta SA, et al. 2004. Mechanism of recurrent ischemic mitral regurgitation after annuloplasty: continued LV remodeling as a moving target. *Circulation* 110(II):II-85–II-90. https://doi.org/10.1161/01.CIR.0000138192.65015.45

12. Hung J, Solis J, Handschumacher MD, Guerrero JL, Levine RA. 2012. Persistence of mitral regurgitation following ring annuloplasty: Is the papillary muscle outside or inside of the ring? *The Journal of Heart Valve Disease* 21(2):218–224.
13. Jensen H, Jensen MO, Ringgaard S, et al. 2008. Geometric determinants of chronic functional ischemic mitral regurgitation: insights from three-dimensional cardiac magnetic resonance imaging. *J Heart Valve Dis* 17:16-22.
14. Jensen H, Jensen MO, Nielsen SL. 2015. Surgical treatment of functional ischemic mitral regurgitation. *J Heart Valve Dis* 24:30-42.
15. Jensen H, Jensen MO, Smerup MH, et al. 2010. Three-dimensional assessment of papillary muscle displacement in a porcine model of ischemic mitral regurgitation. *J Thorac Cardiovasc Surg* 140:1312-8.
16. Khabbaz KR, Mahmood F, Shakil O, et al. 2013. Dynamic 3-dimensional echocardiographic assessment of mitral annular geometry in patients with functional mitral regurgitation. *The Annals of Thoracic Surgery* 95(1):105–110. https://doi.org/10.1016/j.athoracsur.2012.08.078
17. Kono T, Sabbah HN, Rosman H, et al. 1992. Mechanism of functional mitral regurgitation during acute myocardial ischemia. *J Am Coll Cardiol* 19:1101–1105.
18. Kumanohoso T, Otsuji Y, Yoshifuku S, et al. 2003. Mechanism of higher incidence of ischemic mitral regurgitation in patients with inferior myocardial infarction: quantitative analysis of left ventricular and mitral valve geometry in 103 patients with prior myocardial infarction. *J Thorac Cardiovasc Surg* 125:135–43.
19. Kuwahara E, Otsuji Y, Iguro Y, et al. 2006. Mechanism of recurrent/persistent ischemic/functional mitral regurgitation in the chronic phase after surgical annuloplasty: importance of augmented posterior leaflet tethering. *Circulation* 114(I):I-529-I-34. https://doi.org/10.1161/CIRCULATIONAHA.105.000729
20. Lachmann J, Shirani J, Plestis KA, Frater RW, LeJemtel TH. 2001. Mitral ring annuloplasty: An incomplete correction of functional mitral regurgitation associated with left ventricular remodeling. *Curr Cardiol Rep* 3:241-6.
21. Magne J, Pibarot P, Dagenais F, Hachicha Z, Dumesnil JG, Sénéchal M. 2007. Preoperative posterior leaflet angle accurately predicts outcome after restrictive mitral valve annuloplasty for ischemic mitral regurgitation. *Circulation* 115:782–791.
22. McGee J, Edwin C, Gillinov AM, et al. 2004. Recurrent mitral regurgitation after annuloplasty for functional ischemic mitral regurgitation. *J Thorac Cardiovasc Surg* 128:916–24. https://doi.org/10.1016/j.jtcvs.2004.07.037
23. Monnet E, Pouching K. 2013. An ex vivo model of left ventricular dilation and functional mitral regurgitation to facilitate the development of surgical techniques. *The Heart Surgery Forum* 16(6):332-38.
24. Nishimura RA, Otto CM, Bonow RO, et al. 2014. AHA/ACC guideline for the management of patients with valvular heart disease: a report of the American College of Cardiology/American Heart Association Task Force on Practice Guidelines. *Circulation*

129:521–643.
25. Otsuji, Y., Levine, R. A., Takeuchi, M., Sakata, R., & Tei, C. (2008). Mechanism of ischemic mitral regurgitation. *Journal of Cardiology*, *51*(3), 145–156. https://doi.org/10.1016/j.jjcc.2008.03.005
26. Tahta SA, Oury JH, Maxwell JM, Hiro SP, Duran CM. 2002. Outcome after mitral valve repair for functional ischemic mitral regurgitation. *J Heart Valve Dis* 11:11-9.
27. Tibayan FA, Rodriguez F, Zasio MK, et al. 2003. Geometric distortions of the mitral valvular-ventricular complex in chronic ischemic mitral regurgitation. *Circulation* 108(I):II-116-II-21.
28. Uemura T, Otsuji Y, Nakashiki K, et al. 2005. Papillary muscle dysfunction attenuates ischemic mitral regurgitation in patients with localized basal inferior left ventricular remodeling: insights from tissue doppler strain imaging. *Journal of the American College of Cardiology* 46(1):113–119. https://doi.org/10.1016/j.jacc.2005.03.049
29. Vahanian A, Alfieri O, Andreotti F, et al. 2012. Guidelines on the management of valvular heart disease (version 2012). joint task force on the management of valvular heart disease of the European Society of Cardiology (ESC)1; European Association for Cardiothoracic Surgery (EACTS). *Eur Heart J* 33(19):2451-96
30. Yiu SF, Enriquez-Sarano M, Tribouilloy C, Seward JB, Tajik AJ. 2000. Determinants of the degree of functional mitral regurgitation in patients with systolic left ventricular dysfunction: a quantitative clinical study. *Circulation* 102:1400-1406.
31. Zhu F, Otsuji Y, Yotsumoto G, et al. 2005. Mechanism of persistent ischemic mitral regurgitation after annuloplasty importance of augmented posterior mitral leaflet tethering. *Circulation* 112(9):I–396–I–401. https://doi.org/10.1161/CIRCULATIONAHA.104.524561

6. EPICARDIAL PPM REPOSITIONING WITH MITRAL ANNULAR REDUCTION FOR FIMR TREATMENT: INITIAL *EX VIVO* HEART MODEL STUDY

Functional ischemic mitral regurgitation is associated with complications and poor prognosis after cardiac surgery.[3,38] It is characterized by Carpentier type I and type IIIb functional classification.[10] The mortality in coronary artery disease patients is related to the severity of FIMR, which is independently from ventricular function.[24] Twenty-thirty percent, or as high as 59 percent,[43] of the patients with myocardial infarction will encounter FIMR.[7,9,11,16,41] Despite mild mitral regurgitation, the risk of heart failure and mortality significantly increases compared to normal patients and the outcomes worsen with increased severity of FIMR.[6,13,15,24,40,44,61] Regarding to normal mitral leaflet structures, FIMR is related to dilatation of the mitral annulus and restriction of the mitral leaflets during systole due to PMs displacement.

FIMR is widely accepted as a "ventricular" problem.[4] Papillary muscles displacement induced mitral valve tethering, which result in mitral regurgitation from the loss of normal coaptation of the leaflets. In addition to CABG, ring annuloplasty with or without reduction (or *restricted mitral annuloplasty*) is currently used as the method of choice to treat FIMR.[46-48] The concept of ring annuloplasty is to bring the annular dimension closer together so that the mitral leaflets could completely form coaptation. This technique has given high successful rate in short-term studies.[4,11,55] Despite early satisfactory outcomes of this technique, late recurrence of FIMR has been observed in a significant number of cases.[8,17,32,45] Post annuloplasty progression of LV remodeling and mitral valve tethering could impair outcomes from annuloplasty alone.[26] Adjunct

procedures should be used to address the LV remodeling and prevent recurrence of FIMR after surgery.

Since annuloplasty alone could not prevent late recurrent FIMR or improve the survival rate after CABG, therefore we hypothesized that epicardial repositioning of the PPM adjunct with mitral annular reduction would improve leaflet coaptation assessed by reduction of MR. We aimed to show how septo-lateral mitral annular reduction, overall papillary muscle tethering distances, 3D PPM geometry, papillary muscle tethering angle and different methods of treatment influenced MR reduction. This study would demonstrate the feasibility of an epicardial correction to study geometric changes after mitral annular reduction alone compared to PPM repositioning adjunct with mitral annulus reduction in a pulsatile *ex vivo* heart model of FIMR.

6.1. Material and methods

6.1.1. *The ex vivo hearts preparation*

Fresh ovine hearts from 36 adult Dorsett sheep (50±7 kg) with no cardiac abnormalities were collected and stored at 4°C. Experimentation was done within 24 hours. The hearts were prepared and MR was induced by annular dilatation and PPMs displacement as described in previous study from Monnet et al.[52] An incision was made around the PPM without damaging the chordae to allow displacement of the PPM. The PPM remained intact with a 2 cm strip of myocardium at the apical LV wall. LV wall around the PPM was sutured closed with a 3 cm diaphragmatic patch; this creates a focal dilation of the LV wall and cause outward displacement of the PPM. Our previous study on the ex-vivo pulsatile heart model of functional mitral regurgitation had showed that the 3 cm diaphragmatic patch size placement induced the highest

heart models with MR and also produced the highest MR volume. From these data, the 3 cm patch was used to increase the length of the LV wall at the level of the PPM.

In this study, we induced MR by both displacing the PPM away from the anterior mitral leaflet and increasing the septo-lateral annular dimension, mimicking LV remodeling and mitral annular dilatation in FIMR patients.[31,56,65] The left atrium was incised to access the mitral annulus. The septo-lateral annular dimension was measured before inducing annular dilatation. The annular dilatation was achieved by mechanical stretch,[59] without damaging the leaflet and chordae, in the septo-lateral direction until the diameter increased approximately 30 percent of the anterior mitral leaflet height.[36,62,63] Studies have shown that annular dilatation in the septo-lateral direction along with papillary muscle displacement can produce MR.[22,33]

Six intracardiac 2 mm piezo-electric crystals (2 mm round piezo-electric crystals, Sonometrics, London, Canada) were sutured to 6 mitral apparatus landmarks (**Figure 6.1**). Crystal 1 was placed at the level of the fibrosa or septal part of the mitral annulus and Crystal 2 was placed opposite side of Crystal 1 on the mid-lateral or lateral part of mitral annulus. Crystal 3 was placed at the anterior commissure of the mitral annulus and Crystal 4 was placed at the LV apex. These 4 crystals were used for the calculation of the best-fitted plane for further geometry analysis. Crystal 5 was placed on the tip of the APM and Crystal 6 was placed on the tip of the PPM.[12] Nine crystal pairs were of interest and used for the LVV calculation and analysis of the annular and papillary muscles geometry **(Table 6.1)**. Regional wall motion and distances between crystal pairs were measured continuously with sonometric data acquisition system (SonoSoft, Sonometrics Corp., London, Canada). Three-dimensional (3D) coordination of each piezo-electric crystal was recorded at 200 Hz with simultaneous measurement of LVP.[19,30]

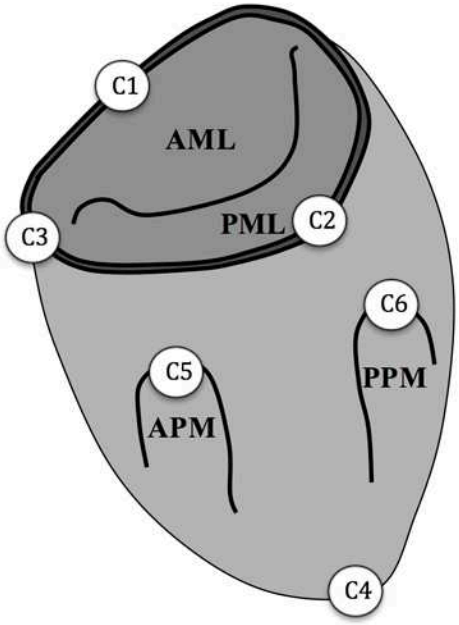

Figure 6.1. Positions of the 6 piezo-electric crystals in the LV and mitral annulus. C1, C2, C3, C4, C5 and C6 represented the piezo-electric crystals 1, 2, 3, 4, 5 and 6 respectively. AML, anterior mitral leaflet; PML, posterior mitral leaflet; APM, anterior papillary muscle; PPM, anterior papillary muscle.

Table 6.1. Piezo-electric crystal pairs used for tethered distance measurements and reference markers for Cartesian plane construction.

Crystal pair	Distance between mitral apparatus landmark
1 and 2	Septo-lateral diameter of the annulus/ Lateral Axis/ Minor Axis I
1 and 3	Anterior axis
1 and 4	Apical Axis
1 and 5	Fibrosa-APM tip distance
1 and 6	Fibrosa-PPM tip distance
2 and 5	Lateral annulus to APM tip distance
2 and 6	Lateral annulus to PPM tip distance
3 and 4	Major Axis
5 and 6	Interpapillary muscle distance/ / Minor Axis II

Abbreviations: APM, anterior papillary muscle; PPM, anterior papillary muscle

Two suture markers were placed on the epicardium to locate APM and PPM bases. After piezo-electric crystals placement, the left atrium and diaphragmatic patch were sutured closed. **Figure 6.2** demonstrates the heart model connected to the pulsatile pressurization system. We used the same settings as in the previous chapter. The heart was mounted on a pulsatile pressurization system (Bio-console 520D Centrifugal Blood Pump, Bio Medicus, Minnesota), which generated pulsatile flow.

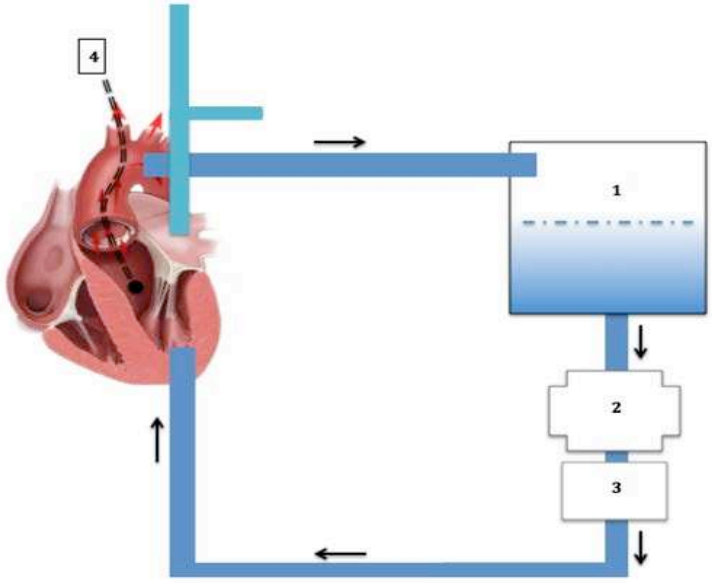

Figure 6.2. FIMR heart model connected to the dynamic pressurization system. The black arrows indicated the flow direction. *1*, reservoir tank; *2*, pump generator; *3*, pulsatile flow generator; *4*, pressure transducer.

The LVP_{max} was maintained at 120±5 mmHg. There was an aortic outflow valve that could be adjusted to decrease or increase outflow resistance until LVP_{max} reached desire value. Pulsatile flow was set at 4 liters per minute, 40 beats per minute with the flow traveling from the

LV apex into the aorta. If MR occurred, the MR flow will be collected and measured from the pulmonary vein cannula. A high-fidelity pressure catheter (Millar, Inc., Houston, USA) was inserted into the LV in a retrograde fashion via the aorta. It was used for LVP measurement throughout the experiment.

The hearts were randomly assigned into 2 groups depending on the method to lower/eliminated MR; Septo-lateral mitral annular reduction (MA) group and PPM repositioning adjunct with septo-lateral mitral annular reduction (MA+PPM) group.

6.1.2. Epicardial correction

In this study, we adapted an epicardial apparatus to alter PMs positions without changing annular dimension. The epicardial apparatus in our study consisted of 4 main parts, 2 cross bars and 2 papillary muscles vertical bars (**Figure 6.3A**). The vertical bars had a retractable pushing pads that were placed on the epicardium at the level of the base of the APM and PPM. In this ex-vivo study, we only adjust the retractable pushing pad at the PPM level. This pad was placed on the epicardium and aimed to push the PPM in a baso-medial direction toward the septal saddle horn of the annulus. Once the PPM vertical bar was placed at the desire position, the proximal of the vertical bar was secured with two mattress sutures apical to the atrioventricular groove and the distal part was secured at the apex. Care must be taken while placing the apparatus to avoid coronary vessels. The first cross bar was used to connect the distal portion of the vertical bars. The second cross bar was connected between the proximal portions (**Figure 6.3B**). The length of the proximal cross bar could be adjusted to reduce the annular septo-lateral dimension.

After application of epicardial apparatus, the *ex vivo* heart was observed whether MR occurred or not. In the MA group, the proximal cross bar length was only adjusted until the maximum reduction, trace or no MR was achieved. In MA+PPM group, the proximal cross bar

length was adjusted until the maximum reduction of MR occurred then the vertical bar pushing pad at the level of PPM was adjusted to gain further maximum MR reduction. Hearts that failed to reproduce MR at baseline or failed to reduce MR after epicardial apparatus placement were excluded from the study.

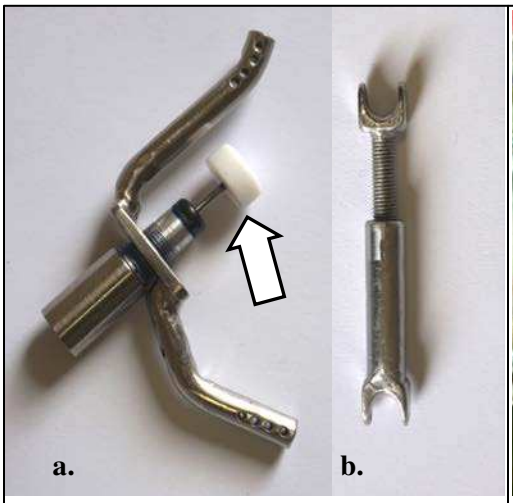

Figure 6.3(A)

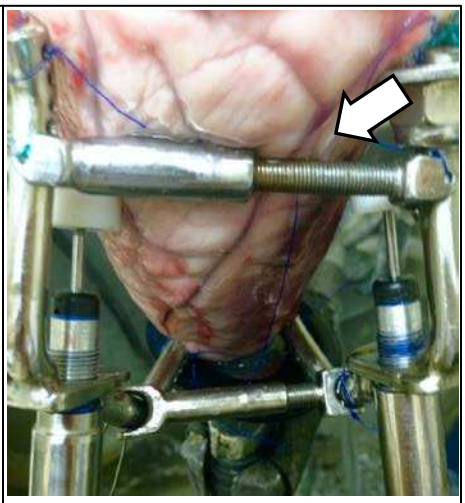

Figure 6.3(B)

Figure 6.3. The epicardial device used for mitral annular dimension reduction and PPM repositioning. **(A)** Papillary muscles vertical bar **(a)** and the cross bar **(b)**. The white arrow indicates retractable pushing pad. **(B)** Mounted epicardial device on the LV. The white arrow indicates the proximal cross bar.

6.1.3. Data acquisition

Figure 6.4 showed the flow chart of the hearts that were included and excluded from the study. Data were collected into 2 groups determined by the treatment method used for MR reduction/elimination.

6.1.3.1. Geometry analysis

Data of the crystal pair distances were collected from each treatment group. Annular and papillary muscles geometry were analyzed at LVP_{max}, which represents the systolic phase when mitral valve closure occurs. Distances between crystal pairs were averaged over 10 pump cycles. Baseline data (Control) for each observation was collected before applying the LV epicardial contouring system and were used as its own control.

Three-dimensional assessments of the papillary muscles tip displacements were evaluated using Cartesian planes at LVP_{max}. The 3D planes were defined by the best-fitted plane using four piezo-electric reference crystals (Crystal 1, 2, 3 and 4). Data from these crystals were analyzed by SonoXYZ software (Sonosoft, Sonometrics, London, Canada) to calculate the Cartesian coordinates throughout the time course of the experiment. We used the same method as in the previous chapter to construct the annular plane (XZ planar), frontal plane (XY) and antero-posterior plane (YZ planar). The XZ, XY and XZ Cartesian coordinate planes were perpendicular to one another. The crystal at the level of the anterior annulus (C1) was use as the origin of 3 perpendicular vector axes.[31] The positive lateral axis (+X) passes through the mid-lateral annular crystal (C2). The positive apical axis (+Y), perpendicular with the lateral axis, was directed toward the apical crystal (C4). The positive anterior axis (+Z), perpendicular with the lateral axis and apical axis, was calculated by SonoXYZ software directed toward the annular anterior commissure crystal (C3). The APM and PPM positions at LVP_{max} were determined into their septo-lateral (X), antero-posterior (Z) and baso-apical (Y) components.

The tethered degree of angle (α or β) of the AMP and PPM tips, reflecting restriction from displaced PPM and annular dilation, were evaluated. The angles were calculated in the annular and frontal planes using the same method as mention in the previous chapter **(Figure**

6.5). The α angle of the PPM was defined as the angle across the PPM tip. It was form by C1-C2 segment and C1-C6 segment. The α angle of the APM was defined as the angle across the APM tip, formed by C1-C2 segment and C2-C5 segment. The β angle of the PPM was form by C1-C2 segment and C2-C6 segment. The β angle of the APM was form by C1-C2 segment and C1-C5 segment. The tethered angles were compared to baseline and between the groups.

6.1.3.2. Quantification of MR, left ventricular volume and mitral annular area analysis

MR stroke volume (milliliters per beat) was quantified by direct measurements of MR volume that exceed from the pulmonary vein port. MR stroke volume above 5 milliliters per beat was considered significant. MR stroke volume was measured and averaged over 10 pump cycles. The percentage of MR reduction from baseline was calculated. In this study, we modified quantification of MR by the measurements of the MR stroke volume from the AHA/ACC guidelines[46] and Zoghbi et al. study.[67] The MR severity was graded on a scale of 0 to 4, in which 0 = no to trace MR (MR <5 ml/beat), 1 = mild (MR 5-20 ml/beat), 2 = moderate (MR 20-30 ml/beat), 3 = moderate to severe (MR 30-40 ml/beat) and 4= severe (MR > 40 ml/beat.

The LVP_{max} resembled the systolic phase in the normal cardiac cycle when the mitral valve was closed. MR should occur in this phase if there were mal-coaptation of the leaflets. Left ventricular volume was obtained and calculated by sonometric data acquisition system (CardioSoft, Sonometrics Corp., London, Canada) at LVP_{max}. The 'Ellipsoid model' equation was used for the LVV calculation. This model used three axes (Major axis, minor axis I and minor axis II). The distance between Crystal 1 and 2 was used as minor axis I. The distance between the anterior commissure of the annulus and the apex was used as major axis. The minor axis II was the axis between the tips of APM-PMM.

EQUATION: $\text{LVV} = \frac{\pi * major\ axis * minor\ axis * minor\ axis\ II}{6}$

Mitral annular area (MAA) before and after treatment was compared. MAA was calculated with the following equation: MAA = π (r_1) (r_2)/4; r_1 is the diameter of the septo-lateral annulus and r_2 is the inter-commissure diameter. After the experiment was completed, the LV was opened for exploration to confirm no damage has been made to the mitral apparatus.

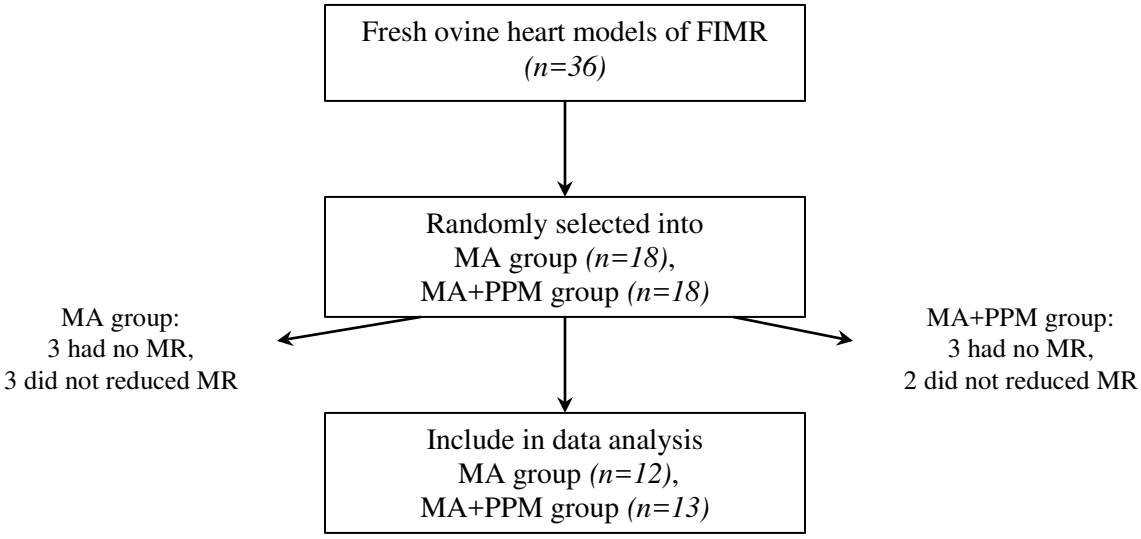

Figure 6.4. Flow chart of the data included in the analysis

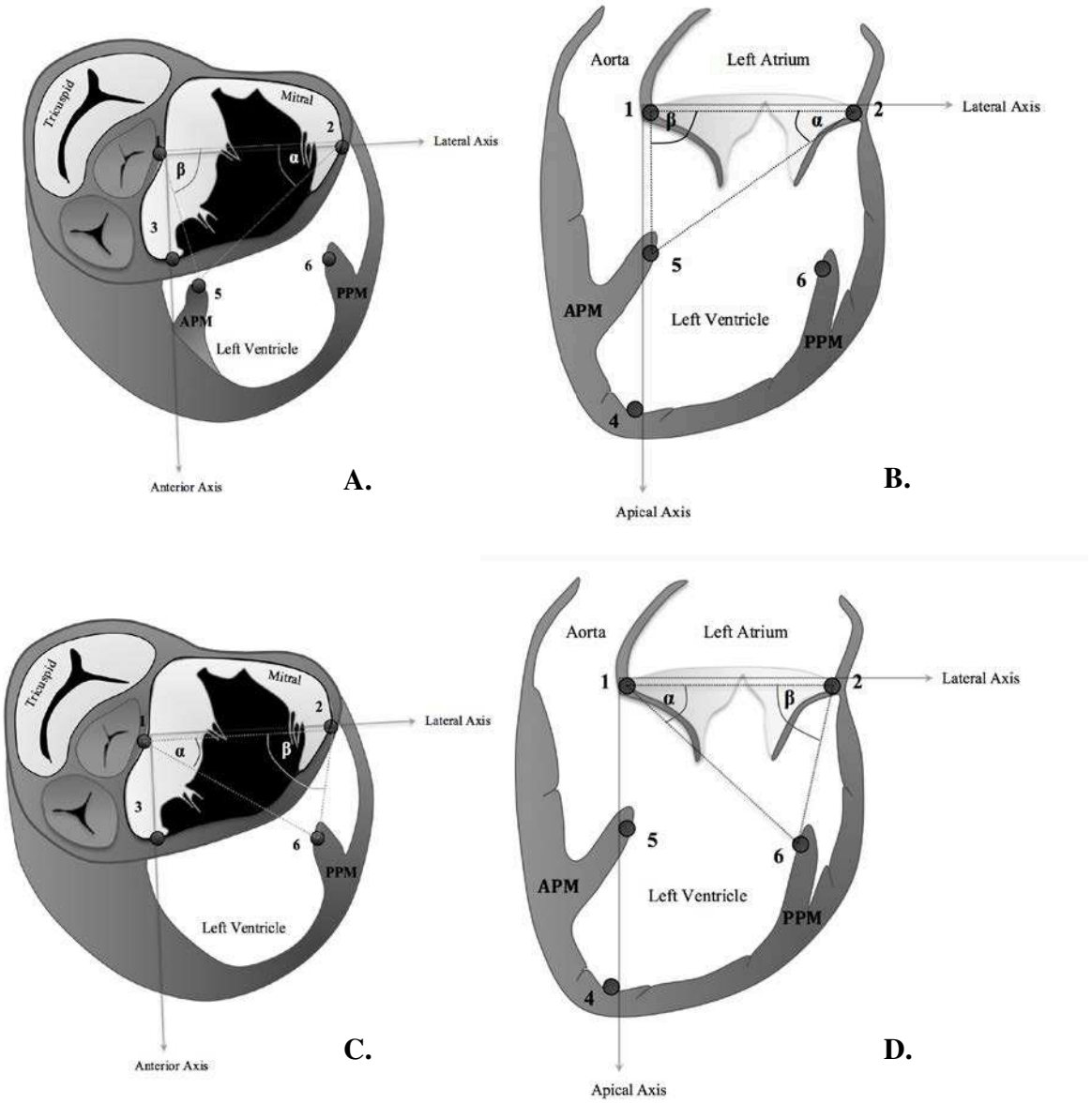

Figure 6.5. Illustrates the APM and PPM tethered angles in the annular plane and frontal plane. The numbers marked the landmarks of the crystal. The angles were marked as α and β. Crystal 1, 2, 3 and 4 were used as reference to construct Cartesian planes. (A, C) Oblique annular plane at the level of the mitral annulus. (B, D) Frontal plane of the left side of the heart.

6.1.4. Statistical analysis

Data were analyzed using SAS version 9.4 (SAS University Edition, Institute Inc., Cary, NC) with significance at $P<0.05$ or stated values. Relative percentage change from baseline was calculated for each variable. Shapiro-Wilk test for normality distribution was tested before analysis. Data with numeric results were presented as median and interquartile range (median [Q1, Q3]), since normality of the data was not achieved. Wilcoxon Sign-ranked test was used for comparison of the variables at baseline and after treatment methods. Percentage relative changes between MA and MA+PPM groups were compared using a Wilcoxon Rank-sum test. Spearman correlation coefficient was used to present association between MR reduction and geometric data variables. Variables that were associated with MR reduction will be further analyzed.

6.2. Results

Left ventricular volume, MAA, and MR are reported in **Table 6.2**. Mitral annular area significantly decreased from baseline in the MA group ($P=0.004$). LVV significantly decreased in MA ($P=0.02$) and MA+PPM ($P=0.01$) groups when compared to its own baseline. MR severity grade significantly decreased from baseline in both MA ($P=0.03$) and MA+PPM groups ($P=0.02$). However, MA+PPM group did not significantly have MR grade and MR reduction lower than MA group **(Table 6.2)**.

The overall tethered distances and 3D displacement of the papillary muscles are reported in **Table 6.3**. The septo-lateral mitral annular distance significantly decreased after applying both methods (MA group $P=0.005$; MA+PPM group $P=0.05$). The tethered distances of the fibrosa to PPM tip and the interpapillary muscles significantly decreased from baseline in MA+PPM

groups (P=0.02 and P=0.047 respectively). The tethered distances of the fibrosa to APM tip significantly increased from baseline in the MA+PPM group (P=0.002). However, there were no statistically significant differences of the septo-lateral mitral annular distances and geometry of the papillary muscles tethered distances found between the 2 groups.

The tethered angles of the papillary muscles referred to the septo-lateral mitral annular segment are reported in **Table 6.3**. The tethering α angle of the APM in the frontal plane significantly increased from baseline in the MA+PPM group (P=0.027). Furthermore, the MA+PPM group had a larger APM and PPM α angle in the frontal plane compared to the MA group after reducing the MR (P=0.04). There were no statistically significant changes in tethering angles found in the MA group compared to baseline.

When including all hearts with MR reduction after applying treatment methods, the percentage of MR reduction correlated with percentage decrease of septo-lateral mitral annular distance (r_s=0.51, P =0.01), the percentage decrease of fibrosa-PPM distance (r_s=0.43, P =0.03) and the percentage increase of the PPM anterior displacement (r_s=-0.41, P =0.04) **(Figure 6.6)**. We further studied how the septo-lateral mitral annular distance, fibrosa-PPM distance and PPM anterior-posterior displacement independently influenced MR reduction. To better understand how these 3 measurements influenced MR reduction, we divided the hearts based on the tertiles of the percentage of septo-lateral mitral annular relative distance reduction, percentage of fibrosa-PPM relative distance reduction and percentage displacement of PPM in the anterior-posterior axis. They were defined by the magnitudes of the septo-lateral mitral annular relative distance reduction; the first (lowest) tertile included septo-lateral mitral annular relative distance reduction lesser than 0.8%, the second (middle) tertile included septo-lateral mitral annular relative distance reduction between 0.8-14.45%, and third (highest) tertile included septo-lateral

mitral annular relative distance reduction greater than 14.45%. The fibrosa-PPM relative distance reduction; the first (lowest) tertile included fibrosa-PPM relative distance reduction lesser than 0%, the second (middle) tertile included fibrosa-PPM relative distance reduction between 0-6.54%, and third (highest) tertile included fibrosa-PPM relative distance reduction greater than 6.54%. Lastly, for the relative displacement of PPM in the anterior-posterior axis; the first (lowest) tertile included relative displacement of PPM in the anterior-posterior axis lesser than -7.75%, the second (middle) tertile included relative displacement of PPM in the anterior-posterior axis between -7.75-225%, and third (highest) tertile included relative displacement of PPM in the anterior-posterior axis greater than 225%. The positive values for the relative displacement of PPM in the anterior-posterior axis indicate anterior displacement and negative values indicate posterior displacement.

Table 6.4 summarized the MR reduction in tertiles of septo-lateral mitral annular reduction, fibrosa-PPM reduction and PPM anterior-posterior displacement. Wilcoxon rank sum test was used for comparison between MA and MA+PPM groups. As a result, MR reduction in the first tertile of septo-lateral mitral annular reduction was significantly higher in the MA+PPM group.

Figure 6.7 suggested that there were thresholds for the influences of septo-lateral mitral annular reduction with MR reduction. Wilcoxon rank sum test showed that the first tertile of hearts within the MA group had a significant lowest MR reduction (28[1.79,37.17] %) when compared with the second and third tertiles median and interquantile range (76.16[47.28,100] % and 100[89.61,100] %, respectively). MR reduction in the MA+PPM group was not significantly different between tertiles. MA+PPM group had significantly higher MR reduction in the first and second tertiles (79.22[64.10,100] % and 87.61[66.91,100] %, respectively) when compared with

the first tertile of the MA group (28[1.79,37.17] %). **Figure 6.8** showed that the fibrosa-PPM reduction in second and third tertiles of both MA and MA+PPM groups have significantly higher MR reduction (47.28[39.71,76.16] %, 100[79.22,100] %, 75.85[64.10,100]% and 81.91[61.91, 100] %, respectively) compared with the MA group first tertile (median and interquantile range, 10[1.79,28] %). No significances were found between the tertiles and treatment groups in PPM anterior-posterior displacement **Figure 6.9**.

Table 6.2. Data of the MR severity, MAA and LVV

	MA Group (n=12)		**MA+PPM Group (n=13)**		**P Value¥**
	Baseline	**Treatment**	**Baseline**	**Treatment**	
PPM tip					
MR grade	1 [1,3]	1* [0.5,1]	1 [1,2]	1* [0,1]	0.75
MR reduction (%)	0	75.61* [39.71,100]	0	70.0* [60.0,100.0]	0.50
MAA (cm^2)	8.47 [5.06,15.66]	6.22* [3.76,9.35]	8.79 [5.51,12.89]	11.24 [6.08,11.68]	0.14
LVV (mL)	42.79 [25.95,59.06]	27.43* [22.65,34.76]	35.61 [33.09,41.7]	32.93* [25.83,38.54]	0.26

Values are in medians and interquartile ranges. MR, mitral regurgitation; MAA, mitral annular area; LVV, left ventricular volume. *Denotes *P-value* <0.05 versus Baseline. ¥ Relative change (%) after epicardial device placement in MA+PPM versus MA group.

Table 6.3. Tethered distances, 3D geometry and papillary muscles tethered angles.

	MA Group (n=12)		MA+PPM Group (n=13)		
	Baseline	**Treatment**	**Baseline**	**Treatment**	**P-Value¥**
Overall tethered distances					
SL Annulus (mm)	26.36 [20.84,35.75]	22.59* [18.5,28.67]	26.5 [23.76,30.45]	24.7* [23.77,28.6]	0.19
Fibrosa-APM tip (mm)	45.47 [40.8,50.19]	45.73 [43.25,52.8]	45.3 [40.3,51.1]	48.75* [42.83,51.1]	0.23
Fibrosa-PPM tip (mm)	54.34 [50.7,56.7]	53.95 [49.35,54.90]	54.39 [48.7,55.8]	52.31* [45.0,54.34]	0.20
Lateral annulus-APM tip (mm)	36.0 [32.5,40.34]	35.17 [32.85,37.85]	36.0 [34.2,38.35]	38.3 [35.64,39.73]	0.07
Lateral annulus-PPM tip (mm)	33.55 [30.76,37.19]	33.7 [31.06,36.9]	32.72 [29.8,34.7]	31.4 [28.2,33.25]	0.11
Interpapillary muscle	30.3 [27.0,32.4]	28.33 [26.7,31.48]	28.5 [25.0,34.3]	28.1* [23.9,30.75]	0.32
3-Dimension of tethered distance					
PPM Lateral (mm)	47.93 [39.07,55.43]	47.49 [40.68,55.45]	44.37 [29.13,55.71]	43.88 [36.86,52.88]	0.10
PPM Apical (mm)	30.49 [24.47,35.79]	26.45 [15.76,30.36]	21.0 [0.75,26.63]	22.99 [18.35,26.36]	0.31
PPM Anterior (mm)	-1.3 [-8.18,2.49]	-1.2 [-9.68,3.91]	-1.3 [-4.46,0.48]	-0.14 [-2.72,3.23]	0.18
APM Lateral (mm)	36.84 [25.9,47.02]	35.61 [21.31,45.14]	34.33 [27.22,46.74]	36.54 [33.04,38.87]	0.47
APM Apical (mm)	26.74 [22.68,32.93]	27.01 [22.59,30.89]	15.36 [5.51,27.45]	26.29 [9.91,30.51]	0.32
APM Anterior (mm)	11.31 [0.49,22.27]	2.73 [-7.31,18.25]	7.95 [2.02,12.31]	8.9 [-2.48,16.20]	0.31
Tethered angles PPM tip					
Fα (º)	33.01 [24.67,44.04]	29.11 [16.15,39.22]	26.24 [15.51,29.17]	27.48 [24.06,40.55]	0.04
Fβ (º)	111.44 [101.68,132.96]	132.10 [111.71,146.05]	124.08 [83.83,133.8]	129.48 [114.5,133.39]	0.16
Aα (º)	6.17 [3.0,10.75]	7.34 [1.67,11.79]	2.22 [1.38,22.42]	5.47 [2.95,7.83]	0.08
Aβ (º)	154.26 [138.71,173.74]	164.11 [149.15,175.94]	167.22 [73.25,175.58]	167.65 [153.59,174.27]	0.08
APM tip					
Fα (º)	39.54 [28.39,48.76]	37.41 [30.41,50.01]	21.09 [13.81,28.57]	34.06* [29.39,44.04]	0.04
Fβ (º)	97.79 [81.35,114.62]	102.71 [81.56,125.7]	112.22 [96.57,132.81]	105.4 [93.09,118.46]	0.22
Aα (º)	20.26 [4.21,37.24]	21.97 [6.9,26.34]	9.65 [3.6,17.97]	29.57 [10.65,32.07]	0.11
Aβ (º)	105.66 [71.33,148.08]	110.38 [63.81,149.53]	118.66 [112.37,154.14]	112.34 [[92.37,143.64]	0.45

Values are in medians and interquartile ranges. *Denotes *P-value* <0.05 versus Baseline. ¥ Relative change (%) after epicardial device placement in MA+PPM versus MA group. APM, anterior papillary muscle; PPM, posterior papillary muscle; SL, septo-lateral; Fα, alpha angle in the frontal plane; Fβ, beta angle in the frontal plane; Aα, alpha angle in the annular plane; Aβ, beta angle in the annular plane.

Table 6.4. Comparison of the MR reduction between MA and MA+PPM groups for each tertiles of septo-lateral mitral annular reduction, fibrosa-PPM reduction and PPM anterior-posterior displacement.

	Tertiles	MA group	MA+PPM group	P Value
		MR reduction (%)	MR reduction (%)	
SL annular relative reduction (%)	1st	28 [1.79,37.17]	79.22 [64.10,100]	0.02*
	2nd	76.16 [47.28,100]	87.61 [66.91,100]	NS
	3rd	100 [89.61,100]	55.14 [34.43,75.85]	NS
Fibrosa-PPM relative reduction (%)	1st	10 [1.79,28]	87.61 [75.22,100]	NS
	2nd	47.28 [39.71,76.16]	75.85 [64.10,100]	NS
	3rd	100 [79.22,100]	81.91 [61.91,100]	NS
PPM anterior-posterior displacement (%)	1st	100 [79.22,100]	100 [79.22,100]	NS
	2nd	52.31 [28,100]	75.85 [63.81,100]	NS
	3rd	26.12 [10,42.24]	70 [64.10,75.22]	NS

Values are in medians and interquartile ranges. MR, mitral regurgitation. NS, no significance found comparing MA+PPM versus MA group. *Denotes *P-value* <0.05 comparing MA+PPM versus MA group.

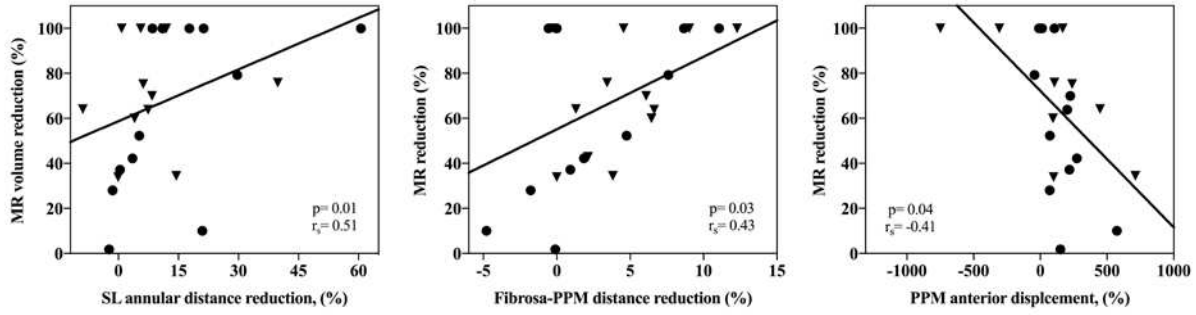

Figure 6.6. Scatter plots and Spearman correlation coefficient of MR volume reduction and *left,* SL annular distance reduction; *middle,* fibrosa-PPM distance reduction; *right,* PPM anterior displacement in percentages. In each subplot, r_s is Spearman correlation coefficient. Scatter plots from MA group are marked as circles and MA+PPM group are marked as triangles.

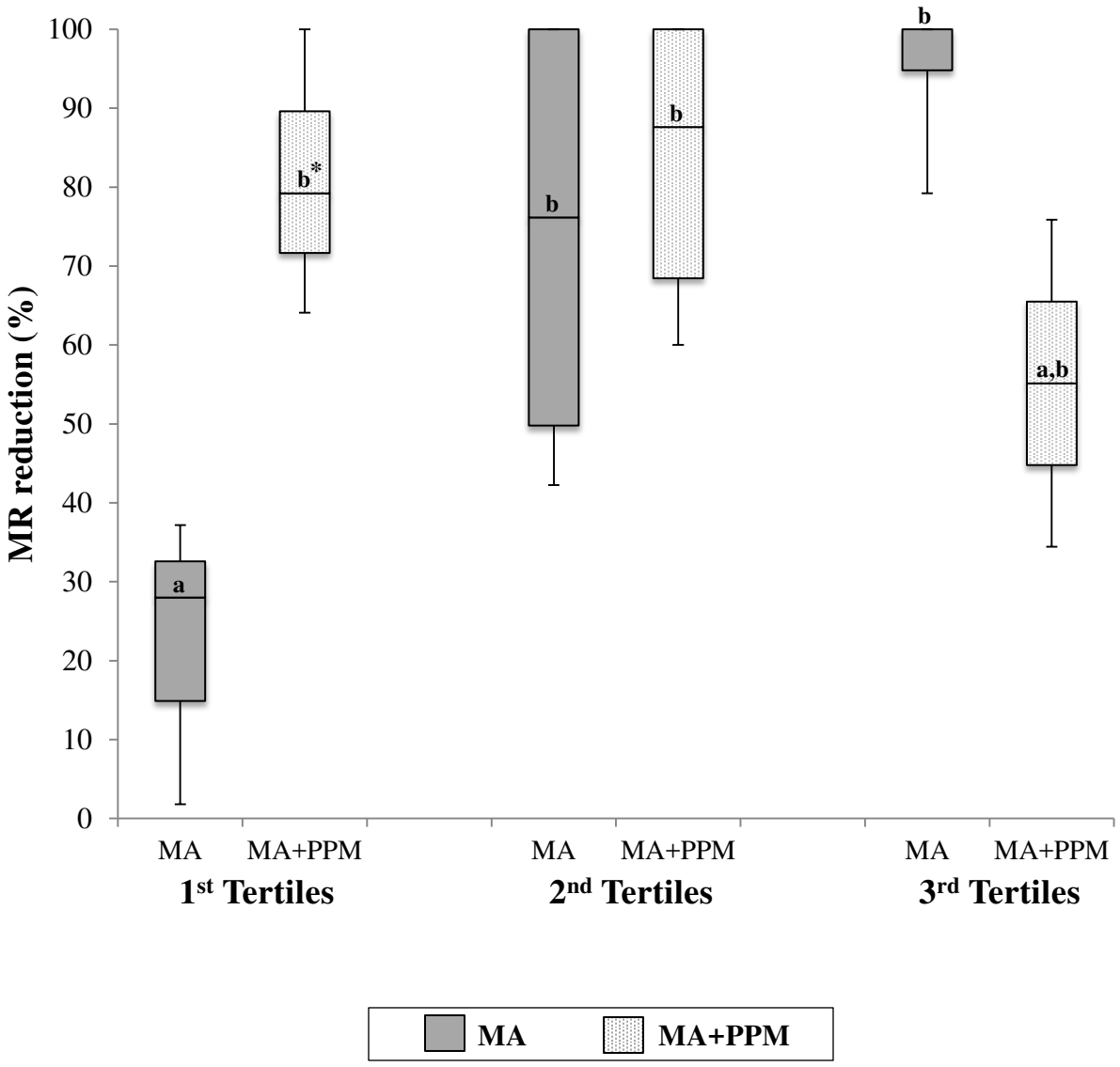

Figure 6.7. Illustration of the severity of MR reduction in tertiles of the septo-lateral mitral annular reduction (relative distance reduction, %). *=*P-value*<0.05 vs MA group within the same tertile. Similar letters indicates no significant difference (*P-value*>0.05)

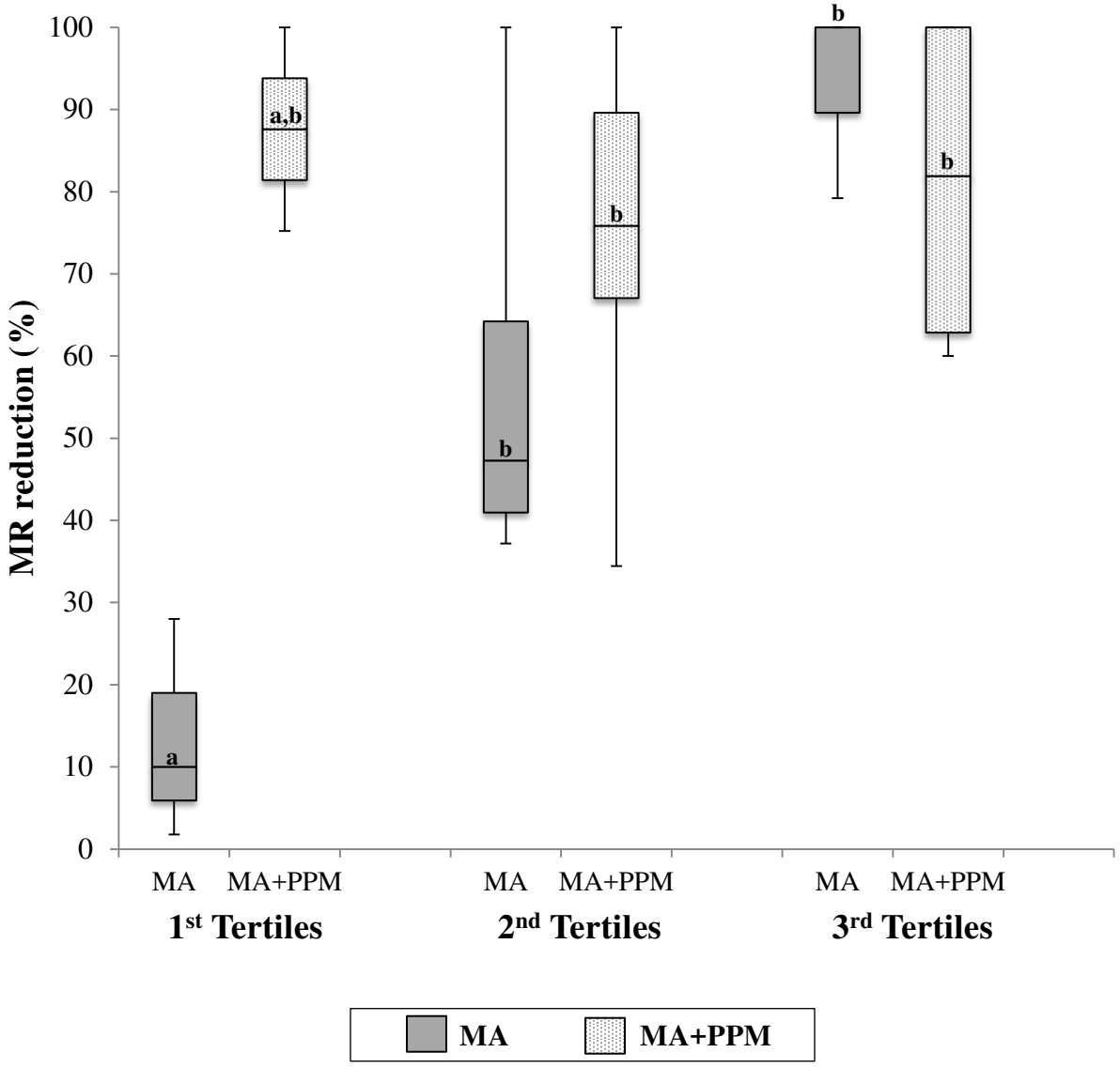

Figure 6.8. Illustration of the severity of MR reduction in tertiles of the fibrosa-PPM reduction (relative distance reduction, %). *=*P-value*<0.05 vs MA group within the same tertile. Similar letters indicates no significant difference (*P-value*>0.05)

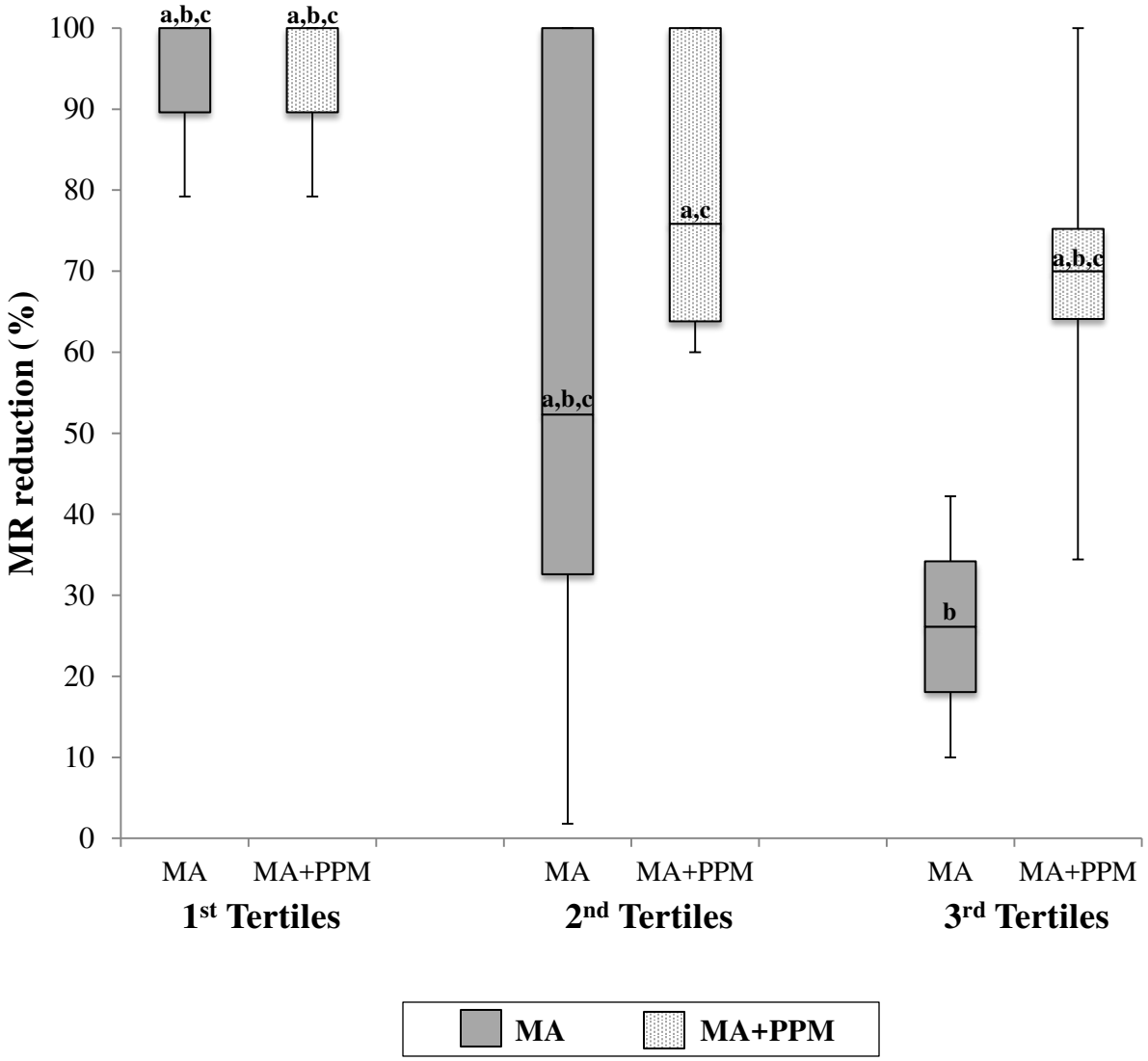

Figure 6.9. Illustration of the severity of MR reduction in tertiles of the PPM anterior-posterior axis displacement (relative distance reduction, %). *=*P-value*<0.05 vs MA group within the same tertile. Similar letters indicates no significant difference (*P-value*>0.05)

6.3. Discussions

Chronic FIMR, typically after posterior-lateral myocardial infarction, caused left ventricle (LV) remodeling.[38] Although LV remodeling displaced both PMs (even the one which is not involved by the infarction) as the entire LV dilated; the APM displacement was minimal compared to the PPM. This event mainly caused asymmetrical PPM displacement at the LV wall where ischemia occurred.[31,53] FIMR patients have restricted leaflet closure due to tethering force influenced by the displaced PMs and concurrent dilated annulus. Miller and colleague have showed that annular reduction in septo-lateral dimension was more significant in reducing MR.[51] Although the concept of ring annuloplasty was to bring the septo-lateral annular dimension closer together so that the mitral leaflets could completely form coaptation, surgical annuloplasty could also potentially increase PML tethering by relatively displacing the PPM outside the mitral annular ring.[23,26,39] Despite excellent long-term results,[25,39] recurrent FIMR and ongoing LV remodeling could be found post-annuloplasty.[5,17]

The concept of reducing PMs tethering by combining subvalvular techniques to normal reduction annuloplasty was adapted by many researchers such as PMs relocation, trans-ventricular suture technique, PMs approximation (PMA), chordal cutting and trans-ventricular devices.[25,37,49,50,54,64] These techniques aimed to eliminate MR by reducing the tethered force on the mitral leaflets. Treatment of moderate to severe FIMR with annuloplasty alone seemed uncertain and the decision to add subvalvular technique depends on each individual case. Szymanski and colleagues[64] showed that in chronic FIMR sheep models second-order mitral chordal cutting improved annuloplasty by reducing papillary muscle tethering. Similar results from a randomized clinical trial (the Papillary Muscle Approximation trial) the PMA in combined with reduction annuloplasty in severe FIMR showed better outcomes of adverse LV

remodeling and recurrent MR than the annuloplasty alone cases.[54] Recent study compared patients with moderate to severe FIMR that had ring annuloplasty only versus patients that have had annuloplasty combined with subvalvular repair (PMs approximation or relocation or chordal cutting). At follow-up, the combined subvalvular repair group had reduced risk of mortality, 56% reduced risk of recurrent MR and significant LV remodeling.[50] There was evidence that non-restrictive annuloplasty adjunct with PPM displacement correction by PPM relocation in severe MR patients showed 97 percent freedom from recurrent MR grade 2 or greater at 5 years post-operatively.[14] PPM relocation and trans-ventricular suture techniques relied on sutures to relocate the PPM tip closer to the annulus. In theory, this created stress on the PPM tip and the annulus and could further lead to avulsion or suture breakage. Subvalvular techniques that reposition the whole body of PMs could help avoid the stress on the PMs tips and some part of the annulus such as PPM approximation[60] and reversing LV remodeling with Dacron patch.[27] LV remodeling with Dacron patch technique eliminated the need of cardiopulmonary bypass and atrial incision which could deteriorate surgical repair. The Dacron patch repositioned the PPM which was persistently effective in reducing moderate chronic IMR, even when LV volume increased. This can reflect structural stabilization by an external patch device of the papillary muscle-LV wall complex that controls mitral valve tethering.[27]

The goal of our study was to evaluate a potential synergistic effect of the association of septo-lateral annular reduction with PPM repositioning. PPM repositioning via epicardial pushing pad at the level of the PPM should give information on how manipulating a single PMs could lower MR. This also introduced a further step in developing epicardial device which lessen the need of open heart surgery. Our study showed that the combined MA+PPM using the

epicardial adjustable apparatus directly repositioned the outwardly displaced PPM and reduced the MR without further compromising the MAA.

The PPM in chronic FIMR was displaced more laterally in chronic FIMR sheep models.[65] They also found that the PML margin was displaced apically in chronic FIMR. Therefore to reduce MR, reversal of these geometric changes should be made. Although we did not see significant changes in the 3D PPM geometry after applying the MA+PPM group, our study revealed decreased of the fibrosa-PPM distance and the interpapillary muscle distance. This could indicate the baso-medial repositioning of the PPM tip. The interpapillary muscle distance was decreased after adjusting the PPM pushing pad to reduce/eliminate MR. Reduction of the interpapillary muscles distance should reduce the tethering force on the leaflets, especially improving the posterior leaflet mobility. Distance between the papillary muscles was a predictor for FIMR severity. Studies in both animal models and human patients have shown that the interpapillary muscle distance was associated with FIMR. Jensen and colleagues[31] used porcine FIMR models and found that the interpapillary muscle distance was the only independent predictor for FIMR severity. A study in patients with chronic FIMR post CABG and reduction ring annuloplasty also showed that the pre-operative interpapillary muscle distance was associated with anterior mitral leaflet tethering, which was associated with recurrent FIMR.[66] Combined PPM reposition with annular reduction lowered PPM tethering which reduced tethering force on the leaflets, especially improving the PML mobility. In our study, the tethered length and angles of the PMs were measured instead of directly measuring from the mitral leaflets. We aim to demonstrate how manipulating the PPM via the epicardial can change the PPM geometry similar to extra-cardiac subvalvular techniques for FIMR treatment. These extra-

cardiac subvalvular techniques have been established to avoid CPB surgery which targeted on reducing the LV dilatation and interpapillary distance.[1,2,57,58]

The reduction of the septo-lateral annular distance and the fibrosa-PPM distance had positive correlations with MR reduction in both treatment groups. The reduction degree of these parameters had different effects. Slight reduction of the septo-lateral annular distance in the combined treatment group significantly reduced MR. The MR reduction was nearly 3 times reduced in the combined group compared to MA alone group, when the SL annular distance was almost at the same size before treatment. This could be the effect of the PPM repositioning inwardly to lower the tethered force on the mitral leaflets. The various degree of septo-lateral annular reduction in the combined treatment group did not differ. They all showed signs of high MR reduction (>50%). On the contrary, aggressively reducing the septo-lateral annulus in the MA group did not show superior effect over combined treatment. Moreover, aggressive reduction of the mitral annulus could induce mitral stenosis.

Tethered angle of the PMs were studied to help give us more information on the changes of the biomechanical mechanisms in heart models that reduced/eliminated MR after treatment. Adjustments of the epicardial pushing pad at the level of the PPM altered both mitral leaflets, since the PPM suspend both mitral leaflets. In **Chapter 5**, we found that the PPM frontal plane α angle decreased 10 degrees in hearts with MR. Therefore, increasing the PPM frontal plane α angle should reduce MR. In this study, the tethered frontal plane α angle of the PPM in the combined treatment group was relatively increased from baseline (15.83±33.34°) compared to MA alone group. This finding along with the decreased of the interpapillary muscles distance suggested that the PPM was repositioned inward and toward the septal annulus by the epicardial pushing pad. Our results demonstrated that combined PPM repositioning via the epicardial

apparatus associated with septo-lateral annular reduction in ovine heart models of FIMR setting improves MR as a result of improved coaptation and reduced interpapillary muscle distance.

Although the *ex vivo* pulsatile heart model of FIMR produces annular dilatation and PPM geometric changes similar to previous studies of FIMR patients,[20,21,42,63] limitations can be found in this study. The primary limitation of this study is that the heart model does not have functional myocardium. LVP and MR were generated by the pressurization of the dynamic pump system. Physiological function of the LV after device placement cannot be assessed such as the ejection fraction, LV elasticity and evaluation of the myocardial blood flow. Further concerns for myocardial blood flow alteration are focal ischemia of the LV myocardium initiate by the contact pressure from the pushing pads. Similar studies of epicardial device that apply pressure on the myocardial wall have not demonstrated focal ischemia from device placement in animal models.[29,34,35]

From this study, we did not know exactly which tethered leaflet resolved after treatment since the PPM that was repositioned had chordae suspended to both leaflets. Leaflet tethering angles using 3D echocardiography with a standard reference system would assist further study on the leaflet 3D geometry. Another limitation of this study is the lack of validation on aggressive annular reduction. In our study we only adjust the proximal cross bar of the epicardial device to reduce the annular dimension until the maximum reduction of MR, trace or no MR was achieved. Although, we have found mitral stenosis in one observation with total MR elimination after MA treatment, but was excluded from the study. Aggressive annular reduction without further causing mitral stenosis along with PPM repositioning may have improved reduction of MR.

REFERENCES

1. Acker MA, Bolling S, Shemin R, et al. 2006. Mitral valve surgery in heart failure: Insights from the Acorn Clinical Trial. *J Thorac Cardiovasc Surg* 132:568–577.e4. https://doi.org/10.1016/j.jtcvs.2006.02.062
2. Acker MA, Jessup M, Bolling SF, et al. 2011. Mitral valve repair in heart failure: Five-year follow-up from the mitral valve replacement stratum of the Acorn randomized trial. *J Thorac Cardiovasc Surg* 142:569–574.e1. https://doi.org/10.1016/j.jtcvs.2010.10.051
3. Badiwala MV, Verma S, Rao V, 2009. Surgical management of ischemic mitral regurgitation. *Circulation* 120:1287–1293. https://doi.org/10.1161/CIRCULATIONAHA.108.836627
4. Bolling SF. 2001. Mitral valve reconstruction in the patient with heart failure. *Heart Fail Rev* 6:177–85.
5. Braun J, van de Veire NR, Klautz RJM, et al. 2008. Restrictive mitral annuloplasty cures ischemic mitral regurgitation and heart failure. *Ann Thorac Surg* 85:430–437. https://doi.org/10.1016/j.athoracsur.2007.08.040
6. Bursi F, Enriquez-Sarano M, Nkomo VT, et al. 2005. Heart failure and death after myocardial infarction in the community the emerging role of mitral regurgitation. *Circulation* 111:295–301. https://doi.org/10.1161/01.CIR.0000151097.30779.04
7. Bursi F, Enriquez-Sarano M, Jacobsen SJ, Roger VL. 2006. Mitral regurgitation after myocardial infarction: A review. *Am J Med* 119:103–112. https://doi.org/10.1016/j.amjmed.2005.08.025
8. Calafiore AM, Gallina S, Di Mauro M, et al. 2001. Mitral valve procedure in dilated cardiomyopathy: repair or replacement? *Ann Thorac Surg* 71:1146–1152. https://doi.org/10.1016/S0003-4975(00)02650-3
9. Carabello BA, 2008. The current therapy for mitral regurgitation. *J Am Coll Cardiol* 52:319–326. https://doi.org/10.1016/j.jacc.2008.02.084
10. Carpentier A. 1983. Cardiac valve surgery - the "French correction." *J Thorac cardiovasc Surg* 86:323–37.
11. Daneshmand MA, Milano CA, Rankin JS, et al. 2009. Mitral valve repair for degenerative disease: a 20-year experience. *Ann Thorac Surg* 88:1828–1837. https://doi.org/10.1016/j.athoracsur.2009.08.008
12. Enriquez-Sarano M, Akins CW, Vahanian A. 2009. Mitral regurgitation. *Lancet* 373:1382–1394. https://doi.org/10.1016/S0140-6736(09)60692-9
13. Fattouch K, Sampognaro R, Speziale G, et al. 2010. Impact of moderate ischemic mitral regurgitation after isolated coronary artery bypass grafting. *Ann Thorac Surg* 90:1187–1194. https://doi.org/10.1016/j.athoracsur.2010.03.103

14. Fattouch K, Castrovinci S, Murana G, et al. 2014. Papillary muscle relocation and mitral annuloplasty in ischemic mitral valve regurgitation: Midterm results. *J Thorac Cardiovasc Surg* 148:1947-50.
15. Feinberg MS, Schwammenthal E, Shlizerman L. 2000. Prognostic significance of mild mitral regurgitation by color Doppler echocardiography in acute myocardial infarction. *Am J Cardiol* 86:903–907. https://doi.org/10.1016/S0002-9149(00)01119-X
16. Foster E. 2010. Mitral regurgitation due to degenerative mitral-valve disease. *N Engl J Med* 363:156–165. https://doi.org/10.1056/NEJMcp0906782
17. Gillinov AM, Wierup PN, Blackstone EH, et al. 2001. Is repair preferable to replacement for ischemic mitral regurgitation? *J Thorac Cardiovasc Surg* 122:1125–1141. https://doi.org/10.1067/mtc.2001.116557
18. Gleyzolle B. Insight into the origins of functional mitral regurgitation and development of a corrective epicardial device: Correction of acute functional mitral regurgitation development of eNew epicardial device. MS [Thesis]. Fort Collins(CO): Colorado State University; 2010.
19. Gorman III JH, Gupta KB, Streicher J., et al. 1996. Dynamic three-dimensional imaging of the mitral valve and left ventricle by rapid sonomicrometry array localization. *J Thorac Cardiovasc Surg* 112:712–724. https://doi.org/10.1016/S0022-5223(96)70056-9
20. Gorman III, JH, Gorman RC, Jackson BM, Enomoto Y, St. John-Sutton MG, Edmunds Jr LH, 2003. Annuloplasty ring selection for chronic ischemic mitral regurgitation: lessons from the ovine model. *Ann Thorac Surg* 76:1556–1563. https://doi.org/10.1016/S0003-4975(03)00891-9
21. Gorman III JH, Jackson BM, Enomoto Y, Gorman RC, 2004. The effect of regional ischemia on mitral valve annular saddle shape. *Ann Thorac Surg* 77:544–548. https://doi.org/10.1016/S0003-4975(03)01354-7
22. Green GR, Dagum P, Glasson JR, et al. 1999a. Mitral annular dilatation and papillary muscle dislocation without mitral regurgitation in sheep. *Circulation* 100, II–95–II–102. https://doi.org/10.1161/01.CIR.100.suppl_2.II-95
23. Green GR, Dagum P, Glasson JR, et al. 1999b. Restricted posterior leaflet motion after mitral ring annuloplasty. *Ann Thorac Surg* 68:2100–2106. https://doi.org/10.1016/S0003-4975(99)01175-3
24. Grigioni F, Enriquez-Sarano M, Zehr KJ, Bailey KR, Tajik AJ, 2001. Ischemic mitral regurgitation long-term outcome and prognostic implications with quantitative doppler assessment. *Circulation* 103:1759–1764. https://doi.org/10.1161/01.CIR.103.13.1759
25. Grossi EA, Patel N, Woo YJ, et al. 2010. Outcomes of the RESTOR-MV Trial (Randomized evaluation of a surgical treatment for off-pump repair of the mitral valve). *J Am Coll Cardiol* 56:1984–1993. https://doi.org/10.1016/j.jacc.2010.06.051

26. Hung J, Papakostas L, Tahta SA, et al. 2004. Mechanism of recurrent ischemic mitral regurgitation after annuloplasty continued lv remodeling as a moving target. *Circulation* 110:II–85–II–90. https://doi.org/10.1161/01.CIR.0000138192.65015.45
27. Hung J, Chaput M, Guerrero JL, et al. 2007. Persistent reduction of ischemic mitral regurgitation by papillary muscle repositioning structural stabilization of the papillary muscle–ventricular wall complex. *Circulation* 116:I–259–I–263. https://doi.org/10.1161/CIRCULATIONAHA.106.679951
28. Hung J, Solis J, Handschumacher MD, Guerrero JL, Levine RA. 2012. Persistence of mitral regurgitation following ring annuloplasty: Is the papillary muscle outside or inside of the ring? *J Heart Valve Dis* 21:218–224.
29. Inoue M, McCarthy PM, Popović ZB, et al. 2004. The Coapsys device to treat functional mitral regurgitation: in vivo long-term canine study. *J Thorac Cardiovasc Surg* 127:1068–1077. https://doi.org/10.1016/j.jtcvs.2003.12.005
30. Jensen H, Jensen MO, Ringgaard S, et al. 2008. Geometric determinants of chronic functional ischemic mitral regurgitation: insights from three-dimensional cardiac magnetic resonance imaging. *J Heart Valve Dis* 17:16–22.
31. Jensen H, Jensen MO, Smerup MH, et al. 2010. Three-dimensional assessment of papillary muscle displacement in a porcine model of ischemic mitral regurgitation. *J Thorac Cardiovasc Surg* 140:1312–1318. https://doi.org/10.1016/j.jtcvs.2009.12.042
32. Jensen H, Jensen MO, Nielsen SL, 2015. Surgical treatment of functional ischemic mitral regurgitation. *J Heart Valve Dis* 24:30–42.
33. Kaplan SR, Bashein G, Sheehan FH, et al. 2000. Three-dimensional echocardiographic assessment of annular shape changes in the normal and regurgitant mitral valve. *Am Heart J* 139:378–387. https://doi.org/10.1016/S0002-8703(00)90077-2
34. Kashem A, Santamore WP, Hassan S, Crabbe DL, Marculies KB, Melvin DB, 2002. CardioClasp: a new passive device to reshape cardiac enlargement. *ASAIO J Am Soc Artif Intern Organs* 48:253–259.
35. Kashem A, Hassan S, Crabbe DL, Melvin DB, Santamore WP. 2013. Left ventricular reshaping: Effects on the pressure-volume relationship. *J Thorac Cardiovasc Surg* 125:391-9.
36. Khabbaz KR, Mahmood F, Shakil O, et al. 2013. Dynamic 3-dimensional echocardiographic assessment of mitral annular geometry in patients with functional mitral regurgitation. *Ann Thorac Surg* 95:105–110. https://doi.org/10.1016/j.athoracsur.2012.08.078
37. Kron IL, Green GR, Cope JT. 2002. Surgical relocation of the posterior papillary muscle in chronic ischemic mitral regurgitation. *Ann Thorac Surg* 74:600–601. https://doi.org/10.1016/S0003-4975(02)03749-9
38. Kumanohoso T, Otsuji Y, Yoshifuku S, et al. 2003. Mechanism of higher incidence of ischemic mitral regurgitation in patients with inferior myocardial infarction: Quantitative

analysis of left ventricular and mitral valve geometry in 103 patients with prior myocardial infarction. *J Thorac Cardiovasc Surg* 125:135–143. https://doi.org/10.1067/mtc.2003.78

39. Kuwahara E, Otsuji Y, Iguro Y, et al. 2006. Mechanism of recurrent/persistent ischemic/functional mitral regurgitation in the chronic phase after surgical annuloplasty importance of augmented posterior leaflet tethering. *Circulation* 114:I–529–I–534. https://doi.org/10.1161/CIRCULATIONAHA.105.000729
40. Lam BK, Blackstone EH, Gillinov AM. 2005. Importance of moderate ischemic mitral regurgitation. *Ann Thorac Surg* 79:462–70.
41. Levine RA, Schwammenthal E, 2005. Ischemic mitral regurgitation on the threshold of a solution from paradoxes to unifying concepts. *Circulation* 112:745–758. https://doi.org/10.1161/CIRCULATIONAHA.104.486720
42. Llaneras MR, Nance ML, Streicher JT, et al. 1994. Large animal model of ischemic mitral regurgitation. *Ann Thorac Surg* 57:432–9.
43. Magne J, Sénéchal M, Dumesnil JG, Pibarot P. 2009. Ischemic mitral regurgitation: a complex multifaceted disease. *Cardiology* 112:244–59.
44. Mallidi HR, Pelletier MP, Lamb J, et al. 2004. Late outcomes in patients with uncorrected mild to moderate mitral regurgitation at the time of isolated coronary artery bypass grafting. *J Thorac Cardiovasc Surg* 127:636–644. https://doi.org/10.1016/j.jtcvs.2003.09.010
45. McGee Jr EC, Gillinov AM, Blackstone EH, et al. 2004. Recurrent mitral regurgitation after annuloplasty for functional ischemic mitral regurgitation. *J Thorac Cardiovasc Surg* 128:916–924. https://doi.org/10.1016/j.jtcvs.2004.07.037
46. Members 2006 Writing Committee. 2008. Focused update incorporated into the ACC/AHA 2006 Guidelines for the management of patients with valvular heart disease a report of the American College of Cardiology/American Heart Association Task Force on Practice Guidelines (Writing Committee to Revise the 1998 Guidelines for the Management of Patients With Valvular Heart Disease): Endorsed by the Society of Cardiovascular Anesthesiologists, Society for Cardiovascular Angiography and Interventions, and Society of Thoracic Surgeons. *Circulation* 118:e523–e661. https://doi.org/10.1161/CIRCULATIONAHA.108.190748
47. Members AF, Vahanian A, Alfieri O, et al. 2012. Guidelines on the management of valvular heart disease (version 2012). *Eur Heart J* 33:2451–2496. https://doi.org/10.1093/eurheartj/ehs109
48. Members WC, Hillis LD, Smith PK, et al. 2011. ACCF/AHA Guideline for coronary artery bypass graft surgery a report of the American College of Cardiology Foundation/American Heart Association task force on practice guidelines. *Circulation* 124:e652–e735. https://doi.org/10.1161/CIR.0b013e31823c074e
49. Messas E, Guerrero JL, Handschumacher MD, et al. 2001. Chordal cutting a new therapeutic approach for ischemic mitral regurgitation. *Circulation* 104:1958–1963. https://doi.org/10.1161/hc4201.097135

50. Mihos CG, Larrauri-Reyes M, Santana O. 2016. A meta-analysis of ring annuloplasty versus combined ring annuloplasty and subvalvular repair for moderate-to-severe functional mitral regurgitation. *J Card Surg* 31:31–37. https://doi.org/10.1111/jocs.12662
51. Miller DC. 2001. Ischemic mitral regurgitation redux—To repair or to replace? *J Thorac Cardiovasc Surg* 122:1059–1062. https://doi.org/10.1067/mtc.2001.120341
52. Monnet E, Pouching K, 2013. An ex vivo model of left ventricular dilation and functional mitral regurgitation to facilitate the development of surgical techniques. *Heart Surg Forum* 16:329–335.
53. Nakai H, Kaku K, Takeuchi M, et al. 2012. Different influences of left ventricular remodeling on anterior and posterior mitral leaflet tethering. *Circulation* 76:2481–2487. https://doi.org/10.1253/circj.CJ-11-1527
54. Nappi F, Spadaccio C, Nenna A, et al. 2017. Is subvalvular repair worthwhile in severe ischemic mitral regurgitation? Subanalysis of the Papillary Muscle Approximation trial. *J Thorac Cardiovasc Surg* 153:286–295.e2. https://doi.org/10.1016/j.jtcvs.2016.09.050
55. Nishimura RA, Otto CM, Bonow RO, et al. 2017. AHA/ACC Focused Update of the 2014 AHA/ACC Guideline for the management of patients with valvular heart disease: a report of the American College of Cardiology/American Heart Association task force on clinical practice guidelines. *Circulation* CIR.0000000000000503. https://doi.org/10.1161/CIR.0000000000000503
56. Otsuji Y, Levine RA, Takeuchi M, Sakata R, Tei C, 2008. Mechanism of ischemic mitral regurgitation. *J Cardiol* 51:145–156. https://doi.org/10.1016/j.jjcc.2008.03.005
57. Power JM, Raman J, Dornom A, et al. 1999. Passive ventricular constraint amends the course of heart failure: a study in an ovine model of dilated cardiomyopathy. *Cardiovasc Res* 44:549–555. https://doi.org/10.1016/S0008-6363(99)00255-2
58. Raman J, Jagannathan R, Chandrashekar P, Sugeng L. 2011. Can we repair the mitral valve from outside the heart? A novel extra-cardiac approach to functional mitral regurgitation. *Heart Lung Circ*. 20:157–162. https://doi.org/10.1016/j.hlc.2010.12.001
59. Richards AL, Cook RC, Bolotin G, Buckner GD. 2009. A dynamic heart system to facilitate the development of mitral valve repair techniques. *Ann Biomed Eng* 37:651–660. https://doi.org/10.1007/s10439-009-9653-x
60. Roshanali F, Vedadian A, Shoar S, et al. 2013. Efficacy of papillary muscle approximation in preventing functional mitral regurgitation recurrence in high-risk patients with ischaemic cardiomyopathy and mitral regurgitation. *Acta Cardiol* 68:271–278.
61. Schroder JN, Williams ML, Hata JA, et al. 2005. Impact of mitral valve regurgitation evaluated by intraoperative transesophageal echocardiography on long-term outcomes after coronary artery bypass grafting. *Circulation* 112:I–293–I–298. https://doi.org/10.1161/CIRCULATIONAHA.104.523472

62. Siefert AW, Jimenez JH, Koomalsingh KJ, et al. 2012. Dynamic assessment of mitral annular force profile in an ovine model. *Ann Thorac Surg* 94:59–65. https://doi.org/10.1016/j.athoracsur.2012.02.074
63. Siefert AW, Rabbah JPM, Koomalsingh KJ, et al. 2013. In vitro mitral valve simulator mimics systolic valvular function of chronic ischemic mitral regurgitation ovine model. *Ann Thorac Surg* 95:825–830. https://doi.org/10.1016/j.athoracsur.2012.11.039
64. Szymanski C, Bel A, Cohen I, et al. 2012. Comprehensive annular and subvalvular repair of chronic ischemic mitral regurgitation improves long-term results with the least ventricular remodeling. *Circulation* 126:2720–2727. https://doi.org/10.1161/CIRCULATIONAHA.111.033472
65. Tibayan FA, Rodriguez F, Zasio MK, et al. 2003. Geometric distortions of the mitral valvular-ventricular complex in chronic ischemic mitral regurgitation. *Circulation* 108:II–116–II–121. https://doi.org/10.1161/01.cir.0000087940.17524.8a
66. van Garsse L, Gelsomino S, Luca F, et al. 2012. Importance of anterior leaflet tethering in predicting recurrence of ischemic mitral regurgitation after restrictive annuloplasty. *J Thoracic CVS Surg* 143(4);S54-9.
67. Zoghbi WA, Enriquez-Sarano M, Foster E, et al. 2003. Recommendations for evaluation of the severity of native valvular regurgitation with two-dimensional and doppler echocardiography. *J Am Soc Echocardiogr* 16:777–802. https://doi.org/10.1016/S0894-7317(03)00335-3

7. CONCLUSIONS

Developing new surgical tools and techniques for FIMR treatment required excessive testing and validation. Animal trials are normally used for standard testing but requires time and expenses. In the early stage of subvalvular adjunctive treatment development, it is best to conduct the experiment in an *ex vivo* pulsatile heart model of FIMR which is cost efficient, requires less time, reduce complexity and lessen the need of laboratory animal usage and sacrifice.

The results of this dissertation have mechanistic and applicable implications. We have managed to develop an *ex vivo* pulsatile heart model for the purpose to study mechanistic of MR from LV dilatation and PPM displacement. The first phase of this study highlights that MR could occur without annular dilatation. MR could be simulated in heart models of LV dilatation and PPM displacement despite normal sized annulus. This could imply to clinical observations in FIMR patients where persistent or recurrent MR often occurred post reduction ring annuloplasty. The propose heart model was comparable to post-annuloplasty recurrent MR of FIMR cases where interpapillary muscle distance played an important part associating with MR severity.

Although displaced distances of the PPM from anatomical landmarks and in 3D coordinate planes from baseline where not different between non-MR and MR occurring heart models, tethering α angle in the frontal plane in heart models with MR showed significant decrease when compared to baseline. This could be an indication that the tethered angles of the PPM tip referred to the annulus should be taken into consideration when treating FIMR, since tethered PPM affects both mitral leaflets.

In the past decades, studies have demonstrated an effective *ex vivo* heart model that mimicked FMR, but none were suitable for studying PMs displacement and validating subvalvular repair that required the continuity of the LV wall and the PMs.[1-4] Most *ex vivo* heart models focused on the dilated annulus or developed the model in a cylinder chamber without the continuity of the PMs and LV wall. In contrast, our study targeted on developing an *ex vivo* heart model of FMR that have PMs attached to the LV. The *ex vivo* pulsatile heart model of FMR that we developed gave us the ability to directly measure the MR and precisely measure the mitral apparatus landmarks via sonomicrometry. The benefits from utilizing this *ex vivo* pulsatile heart model were 1) the ability to make further studies on the PPM repositioning strategies, 2) the procedure could be evaluate on a pseudo-beating heart model with pulsatile fluid flow which would allow us to continuously monitor the MR and mitral geometry. This would help determine how manipulating the mitral apparatus from different surgical repair strategies could change the mitral geometry and reduced MR and 3) the model could be applied for testing and validating the development of future epicardial treatment strategies for FIMR treatment strategies in the early stages of the design before using in animal and clinical trials.

Subvalvular techniques to treat FIMR is a promising path especially in severe FIMR cases when reduction annuloplasty alone causes further LV-mitral valve ring mismatch. The last phase of this research showed that subvalvular epicardial corrections could be done to correct the mitral annulus and the displaced PPM. The study showed that annular reduction and the combined PPM relocation with annular reduction both significantly reduced MR. Lowering the septo-lateral distance, fibrosa to the PPM distance, and PPM posterior displacement after treatment were associated with MR reduction. The combined treatment group had significantly reduced MR even with slightly reduced annular size.

Transcatheter mitral repair and LV devices are being developed to deploy in a beating heart to avoid the requirement of assisted-CPB which lessen the CPB time. These minimally invasive techniques could give profound results especially in some patients that were not good candidates for CABG. In patients with ischemic coronary artery disease, CABG alone usually takes 1-3 hours depending on the number of grafts and the CPB time could increase with complications. CPB procedures that exceed 3 hours are related to increased postoperative complications and mortality.[5] Treatment for FIMR is challenging, since the full mechanisms is not completely understood. Many researches focused on finding the preoperative and post-operative cut-offs for determining the appropriate treatment for FIMR patients. The remaining questions include how to select patients that would benefit from reduction mitral annuloplasty and whether subvalular techniques would add better balanced to the mitral leaflets. This knowledge must be solved to find the best possible treatment tailored for each patient. Further studies on how the tethered PPM angle associated with each mitral leaflet geometry could provide better understanding. Moreover, this could provide further cut-off values when determining patients that would have mitral leaflets tethering after reduction annuloplasty that would need additional subvalvular repair. A standard reference system is important for interpret values between studies. Leaflet tethering angles using 3D echocardiography with a standard reference system would assist further study on the leaflet 3D geometry in the *ex vivo* heart model.

REFERENCES

1. Gleyzolle B. Insight into the origins of functional mitral regurgitation and development of a corrective epicardial device: Correction of acute functional mitral regurgitation development of a new epicardial device. MS [Thesis]. Fort Collins (CO): Colorado State University; 2010.
2. Richards AL, Cook RC, Bolotin G, Buckner GD. 2009. A dynamic heart system to facilitate the development of mitral valve repair techniques. *Ann Biomed Eng* 37:651–60.
3. Katoh T, Ikeda N, Nishi K, Gohra H, Hamano K, Noda H, et al. 1999. A newly designed adapter for testing an ex vivo mitral valve apparatus. *Artificial Organs* 23:920–3.
4. Siefert AW, Rabbah JPM, Koomalsingh KJ, Touchton SA,Jr, Saikrishnan N, McGarvey JR. 2013. In vitro mitral valve simulator mimics systolic valvular function of chronic ischemic mitral regurgitation ovine model. Ann Thorac Surg 95:825–30.
5. Nakasuji M, Matsushita M, Asada A. 2005. Risk factors for prolonged ICU stay in patients following coronary artery bypass grafting with a long duration of cardiopulmonary bypass. J Anesth 19:118-23.

8. LIST OF ABBREVIATIONS

AML	Anterior mitral leaflet
APM	Anterior papillary muscle
CABG	Coronary artery bypass grafting
CPB	Cardiopulmonary bypass
CVS	Cardiovascular
FIMR	Functional mitral regurgitation
FMR	Functional mitral regurgitation
LV	Left ventricle/ventricular
LVP	Left ventricular pressure
LVV	Left ventricular volume
MR	Mitral regurgitation
PMA	Papillary muscle approximation
PML	Posterior mitral leaflet
PMs	Papillary muscles
PPM	Posterior papillary muscle
2D	Two dimensions
3D	Three dimensions